AD_____

Award Number: DAMD17-02-1-0083

TITLE: A Novel Mitochondria-Dependent Apoptotic Pathway (MAP) in Prostate Cancer (Pca) Cells

PRINCIPAL INVESTIGATOR: Dhyan Chandra, Ph.D.

CONTRACTING ORGANIZATION: The University of Texas
M.D. Anderson Cancer Center
Houston, TX 77030

REPORT DATE: January 2004

TYPE OF REPORT: Annual Summary

PREPARED FOR: U.S. Army Medical Research and Materiel Command
Fort Detrick, Maryland 21702-5012

REPORT DOCUMENTATION PAGE

Form Approved
OMB No. 074-0188

1. AGENCY USE ONLY (Leave blank)	2. REPORT DATE	3. REPORT TYPE AND DATES COVERED
	January 2004	Annual Summary (1 Jan 2002 - 31 Dec 2003)

4. TITLE AND SUBTITLE

A Novel Mitochondria-Dependent Apoptotic Pathway (MAP) in Prostate Cancer (Pca) Cells

5. FUNDING NUMBERS

DAMD17-02-1-0083

6. AUTHOR(S)

Dhyan Chandra, Ph.D.

7. PERFORMING ORGANIZATION NAME(S) AND ADDRESS(ES)

The University of Texas
M.D. Anderson Cancer Center
Houston, TX 77030

E-Mail: dchandra@sprdl.mdacc.tmc.edu

8. PERFORMING ORGANIZATION REPORT NUMBER

9. SPONSORING / MONITORING AGENCY NAME(S) AND ADDRESS(ES)

U.S. Army Medical Research and Materiel Command
Fort Detrick, Maryland 21702-5012

10. SPONSORING / MONITORING AGENCY REPORT NUMBER

11. SUPPLEMENTARY NOTES

12a. DISTRIBUTION / AVAILABILITY STATEMENT

Approved for Public Release; Distribution Unlimited

12b. DISTRIBUTION CODE

13. ABSTRACT (Maximum 200 Words)

First, I observed that early during apoptosis induction by a wide spectrum of stimuli, there is a prominent mitochondrial activation, which is characterized by increased mitochondrial respiration, electron transport, and upregulation of multiple respiration-related genes, in particular, cytochrome c. This early mitochondrial activation may represent a defensive mechanism against apoptotic stimulation. In support, many mitochondrially-localized, non-respiration proteins with pro-survival functions including HSP60, Bcl-2, and Bcl-X_L are also up-regulated (Chandra et al., J. Biol. Chem., 277, 50842-54; 2002). Later, when the apoptotic machinery is activated, I notice that there is prominent localization of active caspase-9 and –3 in the mitochondria. The accumulated cytochrome c in the mitochondria early during apoptosis raises a possibility that the mitochondrially-localized caspase-9 might be activated in the organelle in an Apaf-1/cytochrome c-dependent manner. My subsequent biochemical characterizations exclude this possibility and show that the majority of the mitochondrially-localized active caspases, including caspase-9 and caspase-3, result from translocation from the cytosol. The resulting mitochondrial active caspases may function as a positive feedback mechanism to further activate other or residual mitochondrial procaspases, degrade mitochondrial constituents, and disintegrate mitochondrial functions (Chandra and Tang, J. Biol. Chem., 278, 17408-20; 2003). Recently, I observed that active caspase-8 also becomes associated with the mitochondria/ER -enriched membranes and caspase-8 activation plays a critical role in initiating etoposide-induced cell death.

14. SUBJECT TERMS

Prostate Cancer

15. NUMBER OF PAGES

49

16. PRICE CODE

17. SECURITY CLASSIFICATION OF REPORT	18. SECURITY CLASSIFICATION OF THIS PAGE	19. SECURITY CLASSIFICATION OF ABSTRACT	20. LIMITATION OF ABSTRACT
Unclassified	Unclassified	Unclassified	Unlimited

TABLE OF CONTENTS

INTRODUCTION

Apoptosis plays an essential role in animal development and in maintaining the homeostasis of adult tissues (1). The family of caspases (cysteine aspartic acid-specific protease) is the key effectors in the execution of apoptotic cell death (2). Caspases are synthesized as inactive proenzymes, which become proteolytically cleaved during apoptosis to generate active enzymes. The active caspases cleave cellular proteins such as poly(ADP-ribose) polymerase (PARP[1]) to dismantle the apoptotic cells (3). The exact mechanism(s) whereby various caspases become activated are still unclear. Two pathways leading to caspase activation are relatively better understood. In the first, apoptotic stimuli cause the release of cytochrome c (cyt. c) from the intermembrane space (IMS) of the mitochondria to the cytosol. The released cyt. c binds to and activates the adaptor protein Apaf-1, which in turn activates the initiator procaspase-9 in the presence of ATP, leading to the formation of apoptosome and subsequent activation of "executioner" caspases such as caspase-3, -6, or –7 (4). In the second, the FADD/TRADD adaptor proteins recruit the initiator procaspase-8 (or –10) to cell surface death receptors, leading to DISC (Death Receptor-Induced Signaling Complex) formation, caspase-8 activation, and, subsequently, activation of executioner caspases (5).

Most PCa have evolved various mechanisms to subvert apoptotic program and are also resistant to apoptosis induction by most conventional chemotherapeutic drugs. In both cases we know little about the underlying molecular mechanisms. Attenuated apoptotic response and extended cell survival seem to be closely associated with the initiation, progression and metastasis of PCa as well as with their resistance to drugs (4-7). Our novel apoptotic model (MAP, Mitochondria-dependent apoptotic pathway) may partially explain the long-term survivability and drug resistance in PCa cells (8-10). My main objective in proposed grant is to elucidate the following two specific aims:

1) **To determine whether increased cytochrome c translocation to mitochondria during MAP induction is required for apoptosis to occur?**
   In the first year of Statement of work, I addressed the **Specific Aim 1**. We found that variety of apoptotic inducers including certain chemicals and chemotherapeutic drugs seem to kill PCa cells by activating MAP. Apoptosis induced by many stimuli involves an early mitochondrial activation, which is characterized by up-regulation of the mitochondrial respiratory chain (MRC) proteins and many other mitochondrially-localized non-MRC proteins (11). The early up-regulated cyt. c translocates to the mitochondria, which precede its release. Continuous apoptotic response results in release of cyt. c from mitochondria to execute caspase activation and apoptosis.
2) **To determine how mitochondrial procaspase-3 is activated in the organelle.**
   In the second year of Statement of work, I addressed **specific Aim 2.** Now we know that apart from their cytosolic residence, various procaspases are also localized in other subcellular compartments. For example, depending on cell types, procaspase-2 (12), procaspase-3 (13,14), procaspase-8 (15), and procaspase-9 (12,16) have been reported to be present in the IMS of the mitochondria. In all these apoptotic systems, it is generally thought that procaspases "stored" in various subcellular compartments are released, upon apoptosis induction, and become activated in the cytosol, or that the cytosolically activated caspases translocate to various organelles to participate in apoptosis. It is as yet unclear whether the procaspases localized in the organelles (e.g., mitochondria) can *ever* be activated *in situ*. Because procaspase-9 is present in the IMS of the mitochondria (12,16, 17), we hypothesized that the increased mitochondrial cyt. c might lead to the activation of procaspase-9, and subsequently, of procaspase-3, inside the organelle. In this study, we utilized our MAP model to test this hypothesis. Our results show no evidence of cyt. c/Apaf-1-mediated procaspase-9 activation inside the mitochondria. Instead, the results suggest that the mitochondrial active caspase-9 and –3 result mostly from the translocation from the cytosol and partly from caspase-mediated activation in the mitochondria.

BODY

Materials and Methods: Please find details of experimentals in attached manuscript (**Chandra et al., J. Biol. Chem., 2002; Chandra and Tang, J. Biol. Chem, 2003**) in Appendix.

Results and Discussion: Complete findings are illustrated in our published manuscript (**Chandra et al., J. Biol. Chem, 2002; Chandra and Tang, J. Biol. Chem, 2003**) attached in Appendix section.

KEY RESEARCH ACCOMPLISHMENTS

For Specific Aim 1:

1) We found that apoptosis in multiple cell types induced by a variety of stimuli is preceded by an early induction of MRC proteins such as cytochrome c (which is encoded by a nuclear gene) and cytochrome c oxidase subunit II or COX II (which is encoded by the mitochondrial genome). Several non-MRC proteins that are normally localized in the mitochondria, *e.g.*, Smac, Bim, Bak, and Bcl-2, are also rapidly upregulated.
2) The upregulation of many of these proteins (*e.g.*, cytochrome c and COX II) result from transcriptional activation of the respective genes.
3) The upregulated cytosolic cytochrome c rapidly translocates to the mitochondria, resulting in a dramatic accumulation of holocytochrome c in the mitochondria. accompanied by increasing holocytochrome c release into the cytosol.
4) The increased cytochrome c transport from cytosol to the mitochondria does not depend on the mitochondrial protein synthesis or MRC *per se*. In contrast, cytochrome c release from the mitochondria involves dynamic changes in Bcl-2 family proteins (*e.g.*, upregulation of Bak and cytosolic translocation of Bcl-x_L), loss of mitochondrial membrane potential ($D\psi_m$), free radical generation, and opening of permeability transition pore (PTP).
5) Early induction of MRC proteins occurs prior to caspase activation, PARP cleavge and apoptosis induced by various stimuli in multiple cell types.
6) Over-expression of cytochrome c enhances caspase activation and promotes cell death but simple upregulation of cytochrome c using an ecdysone-inducible system is, by itself, insufficient to induce apoptosis.
7) As simple upregulation of cytochrome c using ecdysone inducible system and pCMS-EGFP did not result in increase apoptosis provided evidence that only upregulation of cytochrome c is not sufficient to induce apoptosis. Hence we did not make an attempt to generate ecdysone inducible cells expressing antisense cytochrome c.

For Specific Aim 2:

1) We found that mitochondria possess more significant caspase activity than cytosol in multiple types of cells to execute apoptosis induced by a variety of stimuli.
2) The mitochondrial caspase-9 activation generally appears either after the cytosolic caspase-9 activation or concomitant with the cytosolic caspase-9 activation.
3) Apaf-1 localizes exclusively in the cytosol and translocates to the perinuclear area during apoptosis. Mitochondrial procaspase-9 and –3 also translocated to the cytosol/perinuclear area in multiple cell system with multiple inducers.
4) Biochemical analyses demonstrate that active caspases are located in the IMS of the mitochondria.
5) Cytochrome c and the mitochondrial matrix protein Hsp60 are also rapidly released to the cytosol early during apoptosis. Both the early release of proteins like cytochrome c and Hsp60 from the mitochondria as well as the later translocation of the active caspase-9/-3 are partially inhibited by cyclosporin A, an inhibitor of mitochondrial membrane permeabilization.

6) In-vitro reconstitution and biochemical analyses clearly demonstrates that mitochondrially-localized active caspases result mostly from translocation from cytosol.
7) Utilizing recombinant active caspases in reconstitution experiments we for the first time demonstrates that mitochondrial procaspases can be activated in the organelle itself.
8) Our recent findings also suggest association of active caspase-8 with mitochondria/ER enriched membrane fraction.
9) Mitochondrially localized active caspase-8 can activate cytosolic caspase-3 and ER localized BAP-31 indicating mitochondria-ER crosstalk.
10) The mitochondrial active caspases may function as a positive feedback mechanism to further activate other or residual mitochondrial procaspases, degrade mitochondrial constituents, and disintegrate mitochondrial functions.

REPORTABLE OUTCOMES

Publications:

1) Bhatia, B., Maldonado, C.J., Tang, S., **Chandra, D.,** Klein, R.D. Chopra, D., Shappell, S., Yang, P., Newman, R.A., and Tang, D.G. (2003) Subcellular localization and tumor-suppressive functions of 15-lipoxygenase-2 (15-LOX2) and its splice variants. **Journal of Biological Chemistry,** 278, 25091-100.
2) **Chandra, D.** and Tang, D.G. (2003) Mitochondrially-localized active caspase-9 and caspase-3 results mostly from translocation from cytosol and partly from caspase-mediated activation in the organelle- Lack of evidence for Apaf-1-mediated procaspase-9 activation in the mitochondria. **Journal of Biological Chemistry**, 278, 17408-17420.
3) **Chandra, D.**, Liu, J-W., and Tang, D. G. (2002) Early mitochondria activation and cytochrome c up-regulation during apoptosis. **Journal of Biological Chemistry, 277**, 50842-50854.

Abstract presented in conferences:

1) Choy, G., **Chandra, D.**, Daniel, P., Liu, J., and Tang, D.G. The Role of Bax and Bak in Determining Cancer Cell Sensitivity to Apoptosis Induction. Keystone symposium, Denver, USA, Feb. 3-8, 2004.
2) **Chandra, D.** and Tang D. G. Mitochondrial activation-dependent apoptosis in prostate cancer cells. Prostate Cancer Foundation Tenth Annual Scientific Retreat, New York, USA, Nov. 8-10, 2003.
3) **Chandra, D.,** Deng, X.A., and Tang, D.G. Role of mitochondrially-localized caspase-8 in etoposide-induced breast cancer cell apoptosis. Meeting on Programmed Cell Death, Cold Spring Harbor Laboratory, Cold Spring harbor, New York, USA, Sept. 17-21, 2003.
4) Liu, J., **Chandra, D.**, and Tang, D.G. Transcriptional regulation of BH3-only protein Bim by ROS during mitochondrial activation-dependent apoptosis. Meeting on Programmed Cell Death, Cold Spring Harbor Laboratory, Cold Spring harbor, New York, USA, Sept. 17-21, 2003.
5) **Chandra, D.** and Tang, D. G. Mitochondria activation-dependent apoptotic pathway (MADAP): Transcriptional activation of cytochrome c and increased translocation of cytochrome c to mitochondria preceding apoptosis. 93rd Annual Meeting of American Association for Cancer Research, San Francisco, California, USA, April 6-10, 2002.

CONCLUSIONS

I conclude that early during apoptosis there is prominent mitochondrial activation, characterized by increased mitochondrial respiration, electron transport, and upregulation of multiple respiration-related genes, in particular, cytochrome c. This early mitochondrial activation apparently represents a defensive mechanism (J. Biol. Chem., 277, 50842-54; 2002). Later, when the apoptotic machinery is activated, I notice that there is prominent localization of active caspase-9 and –3 in the mitochondria. Biochemical characterizations revealed that the majority of the mitochondrially-localized active caspases, including caspase-9 and 3, result from translocation from the cytosol (J. Biol. Chem., 278, 17408-20; 2003).

REFERENCES

1. Horvitz, H. R. (1999) Genetic control of programmed cell death in the nematode *Caenorhabditis elegans*. *Cancer Res.* **59**, 1701S-1706S
2. Salvesen, G. S., and Dixit, V. M. (1997) Caspases: intracellular signaling by proteolysis. *Cell* **91**, 443-446
3. Thornberry, N. A., and Lazebnik, Y. (1998) Caspases: enemies within. *Science* **281**, 1312-1316
4. Wang, X. (2001) The expanding role of mitochondria in apoptosis. *Genes & Dev.* **15**, 2922-2933
5. Ashkenazi, A., and Dixit, V. M. (1998) Death receptors: signaling and modulation. *Science* **281**, 1305-1308
6. Guo, Y., Srinivasula, S. M., Druilhe, A., Fernandes-Alnemri, T., and Alnemri, E. S. (2002) Caspase-2 induces apoptosis by releasing proapoptotic proteins from mitochondria. *J. Biol. Chem.* **277**, 13430-13437
7. Paroni, G., Henderson, C., Schneider, C., and Brancolini, C. (2002) Caspase-2 can trigger cytochrome c release and apoptosis from the nucleus. *J. Biol. Chem.* **277**, 15147-15161
8. Robertson, J. D., Enoksson, M., Suomela, M., Zhivotovsky, B., and Orrenius, S. (2002) Caspase-2 acts upstream of mitochondria to promote cytochrome c release during etoposide-induced apoptosis. *J. Biol. Chem.* **277**, 29803-29809
9. Lassus, P., Opitz-Araya, X., and Lazebnik, Y. (2002) Requirement of caspase-2 in stress-induced apoptosis before mitochondrial permeabilization. *Science* **297**, 1352-1354
10. Read, S. H., Baliga, B. C., Ekert, P. G., Vaux, D. L., and Kumar, S. (2002) A novel Apaf-1-independent putative caspase-2 activation complex. *J. Cell Biol.* **159**, 739-745
11. Chandra, D., Liu, J-W., and Tang, D. G. (2002) Early mitochondria activation and cytochrome c up-regulation during apoptosis. *J. Biol. Chem.* **277**, 50842-50854
12. Susin, S. A., Lorenzo, H. K., Zamzami, N., Marzo, I., Brenner, C., Larochette, N., Prevost, M. C., Alzari, P. M., and Kroemer, G. (1999) Mitochondrial release of caspase-2 and –9 during the apoptotic process. *J. Exp. Med.* **189**, 381-394
13. Mancini, M., Nicholson, D. W., Roy, S., Thornberry, N. A., Peterson, E. P., Casiola-Rosen, L. A. and Rosen, A. (1998) The caspase-3 precursor has a cytosolic and mitochondrial distribution: Implications for apoptotic signaling. *J. Cell Biol.* **140**, 1485-1495
14. Samali, A., Zhivotovsky, B., Jones, D. P., and Orrenius, S. (1998) Detection of procaspase-3 in cytosol and mitochondria of various tissues. *FEBS Lett.* **431**, 167-169
15. Quin, Z. H., Wang, Y., Kikly, K. K., Sapp, E., Kegel, K. B., Aronin, N., and DiFiglia, M. (2001) Procaspase-8 is predominantly localized in mitochondria and release into cytoplasm upon apoptotic stimulation. *J. Biol. Chem.* **276**, 8079-8086
16. Krajewski, S., Krajewska, M., Ellerby, L. M., Welsh, K., Xie, Z. H., Deveraux, Q. L., Salvesen, G. S., Bredesen, D. E., Rosenthal, R. E., Fiskum, G., and Reed, J. C. (1999) Release of caspase-9 from mitochondria during neuronal apoptosis and cerebral ischemia. *Proc. Natl. Acad. Sci. U.S.A.* **96**, 5752-5757
17. Zhivotovsky, B., Samali, A., Gahm, A., and Orrenius, S. (1999) Caspases: their intracellular localization and translocation during apoptosis. *Cell Death Differ.* **6**, 644-651

APPENDIX MATERIAL

ABSTRACT

THE ROLE OF BAX AND BAK IN DETERMINING CANCER CELL SENSITIVITY TO APOPTOSIS INDUCTION.

Grace Choy[1], Dhyan Chandra[1], Peter Daniel[2], Junwei Liu[1], and Dean Tang[1]

UT M.D. Anderson Cancer Center[1]. Molecular Hematology and Oncology, Charite - Campus Berlin-Buch, Humboldt University, Germany[2].

The proapoptotic Bcl-2 family proteins, Bax and Bak, have been shown to be essential for initiating the mitochondrial pathway of apoptosis by inducing cytochrome C release. However, the molecular pathway by which this occurs is not completely understood. In cancer cells that have generally sustained numerous mutations in the survival/apoptotic pathways, the effect of Bax and Bak on cell sensitivity to various apoptotic stimuli has not been well studied. In this project, we utilized a prostate cancer cell line, Du145, which lacks the expression of Bax, and first asked whether restoration of Bax expression could sensitize cells to apoptosis induction. We observed that the reconstituted expression of Bax in Du145 resulted in an increased sensitivity to various apoptotic stimuli including etoposide, thapsigargin, staurosporine, γ-irradiation and Fas/cycloheximide. This increased sensitivity was accompanied by increased cytochrome C and Smac release as well as caspase activation. In addition, the role of Bak in cell sensitivity to apoptotic stimuli will be studied using Bak specific siRNA. The results would allow us to determine the importance of Bax and Bak in the induction of apoptosis in cancer cell lines. The outcome of this project has general implications in evaluating the role of Bax and Bak in cancer cell sensitivity to various therapeutics.

ABSTRACT

MITOCHONDRIAL ACTIVATION-DEPENDENT APOPTOSIS IN PROSTATE CANCER CELLS

Dhyan Chandra*, and Dean G. Tang

Department of Carcinogenesis, The University of Texas M.D. Anderson Cancer Center, Science Park Research Division, Smithville, TX 78957.

Most prostate cancer (PCa) have a protracted history of development, suggesting that PCa cells must have evolved various mechanisms to subvert apoptotic program. PCa cells are also resistant to apoptosis induction by most conventional chemotherapeutic drugs. Attenuated apoptotic response and extended cell survival seem to be closely associated with the initiation, progression and metastasis of PCa as well as with their resistance to drugs. Recently, we identified a novel apoptotic pathway, MADAP (mitochondrial activation-dependent apoptotic pathway) that seems to operate in prostate cancer cells as well as many other cancer cells.

MADAP involve an early mitochondrial activation characterized by increased mitochondrial respiration, electron transport, and upregulation of multiple respiration-related genes, in particular, cytochrome c. The upregulated cytochrome c rapidly translocates to and accumulates in the mitochondria, which contributes to entire apoptotic process (Chandra et al., J. Biol. Chem., 277, 50842-54; 2002). The accumulated cytochrome c in the mitochondria early during apoptosis also raises a possibility that the mitochondrially-localized capsase-9 might be activated *In Situ* in an Apaf-1/cytochrome c-dependent manner. Out subsequent biochemical characterizations, however, exclude this possibility and shows that the majority of the mitochondrially-localized active caspases, including caspase-9 and caspase-3, result from translocation from the cytosol (Chandra and Tang, J. Biol. Chem., 278, 17408-20; 2003).

We are currently further studying the role of MADAP in (prostate) cancer cell apoptosis. Elucidation of this pathway, especially the roles of the mitochondrial active caspases and the mechanisms of apoptosome regulation, will lay a foundation for the development of novel apoptosis-based anti-prostate cancer therapeutics.

*D. Chandra gratefully acknowledges the financial support from Department of Defense (DAMD17-02-1-0083) in the form of Postdoctoral Traineeship Awards.

ABSTRACT

ROLE OF MITOCHONDRIALLY-LOCALIZED CASPASE-8 IN ETOPOSIDE-INDUCED BREAST CANCER CELL APOPTOSIS

Dhyan Chandra, Xiaodi A Deng, and Dean G. Tang

Department of Carcinogenesis, the University of Texas M.D. Anderson Cancer Center, Science Park Research Division, Smithville, TX 78957.

We recently reported that active caspase-9 and -3 become associated with the mitochondria in multiple models of chemically-induced apoptosis (Chandra and Tang (2003) J. Biol. Chem. 278, 17408-17420). Here we show that, in MDA-MB-231 cells treated with etoposide (VP16), active caspase-8 was detected, surprisingly, only in the mitochondria-enriched membrane fractions, concomitant with cytochrome c release, PARP cleavage, and apoptotic cell death. Experiments with highly purified mitochondria confirmed the mitochondrial localization of the active caspase-8. Interestingly, caspase-2 was found to be upregulated also only in the mitochondria in response to etoposide treatment. In contrast to caspase-8 and –2, active caspase-9 and -3 were detected in both mitochondrial and cytosolic fractions. These observations raise the possibility that, in response to DNA-damaging signals such as VP16, caspase-8 is either activated in the mitochondria or first activated in the cytosol then translocate to the organelle, which then contributes to apoptotic process. Currently, we are using siRNA and dominant negative mutants to test this possibility.

ABSTRACT

Transcriptional regulation of BH3-only protein Bim by ROS during mitochondrial activation-dependent apoptosis

Jun-Wei Liu, Dhyan Chandra, Dean G. Tang

Department of Carcinogenesis, the University of Texas M.D. Anderson Cancer Center, Science Park Research Division, Smithville, Texas 78957

Bim, a BH3-only apoptotic protein, is upregulated in several models of mitochondrial activation-dependent apoptosis (MADAP, Chandra, JBC, 2002). To elucidate the mechanisms of Bim upregulation in these apoptotic models, we treated several human epithelial cell lines with various stress factors and found that Bim was upregulated in all cell models studied. Accompanying Bim upregulation there were cytochrome c release, caspase-3 activation and apoptotic cell death. In addition to Bim, FoxO3a and several protective factors including p27, MnSOD and Cu/ZnSOD were also upregulated at the transcriptional level. It has been reported that expression of Bim was regulated by FoxO3a in T lymphocytes (Dijkers, Current biol., 2000). In our study, we observed that there were higher ROS (reactive oxygen species) levels in the treated cell lines. The upregulation of FoxO3a, Bim and the protective molecules could all be blocked when the ROS generation was inhibited. ROS generation was independent and proceeding of caspase activation. Based on the above results, we conclude that ROS generation during MADAP induces the upregulation of both pro-apoptotic (e.g., Bim) and anti-apoptotic (e.g., MnSOD) molecules. Persistent apoptotic stimulation then tilts the balance towards cell death.

Keywords: Bim, ROS, FoxO3a

ABSTRACT

Mitochondrial Respiratory Chain (MRC)-Dependent Apoptotic Pathway: Upregulation of MRC Proteins, Accumulation of Cytochrome c in the Mitochondria, and Lack of Release of Mitochondrial Cytochrome c Prior to Caspase Activation and Apoptosis

Dhyan Chandra, and Dean G. Tang

Department of Carcinogenesis, University of Texas MD Anderson Cancer Center, Science Park Research Division, Smithville, TX 78957

Apoptosis induced by many stimuli requires the mitochondrial respiratory chain (MRC), but the molecular mechanisms underlying this MRC-dependent apoptotic pathway, or MAP, remain unclear. We report here that, during MAP, MRC proteins such as cytochrome c, which is encoded by a nuclear gene, and cytochrome c oxidase subunit II (COX II), which is encoded by the mitochondrial genome, are rapidly upregulated. The upregulation of both cytochrome c and COX II results from transcriptional activation of the respective genes. The upregulated cytosolic cytochrome c rapidly translocates to mitochondria, resulting in a dramatic accumulation of cytochrome c in the mitochondria prior to caspase activation and apoptosis. The increased translocation of cytochrome c from cytosol to the mitochondria does not depend on the mitochondrial protein synthesis or MRC *per se*. Surprisingly, no apparent cytochrome c release is observed when caspases are activated and when cells show apoptotic nuclear morphologies, as revealed by several biochemical and biological methods. Over-expression of cytochrome c enhances caspase activation and promotes cell death triggered by MAP inducers, although simple upregulation of cytochrome c using an ecdysone-inducible system is, by itself, insufficient to induce apoptosis. Taken together, these results suggest that early induction of MRC genes, rapid translocation of cytochrome c to and its accumulation in the mitochondria, and absence of cytochrome c release from mitochondria prior to caspase activation are cardinal features of MAP.

THE JOURNAL OF BIOLOGICAL CHEMISTRY
Vol. 277, No. 52, Issue of December 27, pp. 50842–50854, 2002
Printed in U.S.A.

Early Mitochondrial Activation and Cytochrome *c* Up-regulation during Apoptosis*[S]

Received for publication, July 29, 2002, and in revised form, October 22, 2002
Published, JBC Papers in Press, October 28, 2002, DOI 10.1074/jbc.M207622200

Dhyan Chandra‡, Jun-Wei Liu, and Dean G. Tang§

From the Department of Carcinogenesis, University of Texas M. D. Anderson Cancer Center, Science Park Research Division, Smithville, Texas 78957

Apoptosis induced by many stimuli requires the mitochondrial respiratory chain (MRC) function. While studying the molecular mechanisms underlying this MRC-dependent apoptotic pathway, we find that apoptosis in multiple cell types induced by a variety of stimuli is preceded by an early induction of MRC proteins such as cytochrome *c* (which is encoded by a nuclear gene) and cytochrome *c* oxidase subunit II (COX II) (which is encoded by the mitochondrial genome). Several non-MRC proteins localized in the mitochondria, *e.g.* Smac, Bim, Bak, and Bcl-2, are also rapidly up-regulated. The up-regulation of many of these proteins (*e.g.* cytochrome *c*, COX II, and Bim) results from transcriptional activation of the respective genes. The up-regulated cytosolic cytochrome *c* rapidly translocates to the mitochondria, resulting in an accumulation of holocytochrome *c* in the mitochondria accompanied by increasing holocytochrome *c* release into the cytosol. The increased cytochrome *c* transport from cytosol to the mitochondria does not depend on the mitochondrial protein synthesis or MRC *per se*. In contrast, cytochrome *c* release from the mitochondria involves dynamic changes in Bcl-2 family proteins (*e.g.* up-regulation of Bak, Bcl-2, and Bcl-x_L), opening of permeability transition pore, and loss of mitochondrial membrane potential. Overexpression of cytochrome *c* enhances caspase activation and promotes cell death in response to apoptotic stimulation, but simple up-regulation of cytochrome *c* using an ecdysone-inducible system is, by itself, insufficient to induce apoptosis. Taken together, these results suggest that apoptosis induced by many stimuli involves an early mitochondrial activation, which may be responsible for the subsequent disruption of MRC functions, loss of $\Delta\psi_m$, cytochrome *c* release, and ultimately cell death.

Mitochondria generate ATP through the mitochondrial respiratory chain (MRC),[1] which is composed of four multisubunit respiration complexes (I–IV) and two mobile electron carriers (*i.e.* cytochrome *c* and ubiquinone). Electrons from reducing substrates such as NADH and succinate are transferred from complex I (NADH dehydrogenase) or complex II (succinate dehydrogenase), respectively, to ubiquinone, to complex III (cytochrome *c* reductase), to cytochrome *c*, to complex IV (cytochrome *c* oxidase or COX), and finally to O_2. The electron transport through complexes I, III, and IV is accompanied by the pumping of protons from the matrix to the intermembrane space, where the protons establish a mitochondrial membrane potential ($\Delta\psi_m$) by forming a proton and a pH gradient. The reverse flow of the protons from the intermembrane space into the matrix drives another multiprotein complex, F_0F_1-ATPase (or complex V), to produce ATP. The protein subunits in complexes I, III, IV, and V are encoded by both nuclear and mitochondrial genomes, thus necessitating smooth communications between and coordinated gene expressions from two genomes (1). Abnormal MRC functions due to genetic defects or chemical disruption, for example, result in a deficiency in ATP generation, leading to cell necrosis (2–4).

Mitochondria also play a pivotal role in regulating another mode of cell death, *i.e.* apoptosis. Mitochondria generally play a proapoptotic role in most model systems, evoking different mechanisms including ROS production (5–7), Ca^{2+} release (8, 9), $\Delta\psi_m$ collapse (10), opening of the permeability transition pores (PTP) (11, 12), matrix swelling and outer membrane rupture (13), and release of apoptogenic factors including cytochrome *c* (14, 15), apoptosis-inducing factor (16), second mitochondria-derived activator of caspase (Smac/DIABLO; see Refs. 17 and 18), Smac-related serine protease HtrA2 (19–22), endonuclease G (23), and caspases (24, 25). Exactly how these diverse mechanisms converge to activate caspases is still unclear. Two apoptotic pathways are relatively well understood at the molecular level. In the intrinsic (or mitochondrial) pathway, apoptotic signaling somehow impacts mitochondria such that the mitochondrial cytochrome *c* is released into the cytosol, where it binds to the adaptor protein Apaf-1 and procaspase-9, leading to the formation of apoptosome and subse-

* This work was supported in part by the National Institutes of Health NCI Grant CA 90297 and NIEHS Center Grant ES07784, and the University of Texas MD Anderson Cancer Center institutional grants. The costs of publication of this article were defrayed in part by the payment of page charges. This article must therefore be hereby marked "*advertisement*" in accordance with 18 U.S.C. Section 1734 solely to indicate this fact.

[S] The on-line version of this article (available at *http://www.jbc.org*) contains Figs. 1S—3S.

‡ Supported by a Department of Defense Postdoctoral Traineeship Award DAMD17-02-1-0083.

§ To whom correspondence should be addressed: Dept. of Carcinogenesis, University of Texas M. D. Anderson Cancer Center, Science Park Research Division, Park Rd. 1C, Smithville, TX 78957. Tel.: 512-237-9575; Fax: 512-237-2475; E-mail: dtang@sprd1.mdacc.tmc.edu.

[1] The abbreviations used are: MRC, mitochondrial respiratory chain; A/D, actinomycin D; AFC, 7-amino-4-trifluoromethylcoumarin; BMD188, a hydroxamic acid compound; CHX, cycloheximide; COX II, cytochrome *c* oxidase subunit II; CsA, cyclosporin A; DAPI, 4′,6-diamidino-2-phenylindole; GFP, green fluorescence protein; MADAP, mitochondrial activation-dependent apoptotic pathway; PARP, poly(ADP-ribose) polymerase; PTP, permeability transition pore; ROS, reactive oxygen species; RT, reverse transcriptase; VDAC, voltage-dependent anion channel; VP16, etoposide; ρ^0 cells, respiration-deficient cells; TNF-α, tumor necrosis factor-α; AFC, 7-amino-4-trifluoromethylcoumarin; CHAPS, 3-[(3-cholamidopropyl)dimethylammonio]-1-propanesulfonic acid; z, benzyloxycarbonyl; fmk, fluoromethyl ketone; FBS, fetal bovine serum; PBS, phosphate-buffered saline; EGFP, enhanced green fluorescent protein; IMM, inner mitochondrial membrane; OMM, outer mitochondrial membrane; MAC, mitochondria apoptosis-induced channel; NAC, *N*-acetylcysteine.

quent activation of "executioner" caspases such as caspase-3, -6, or -7 (26). In the extrinsic pathway, engagement of the cell surface death receptors (*e.g.* Fas, TNFR1, DR-3, DR-4, and DR-5) results in the activation of initiator caspase-8 through adaptor proteins such as FADD and TRADD (27), which then activates downstream executioner caspases. The death receptor pathway can be amplified by the mitochondrial pathway either through the translocation of tBid, a caspase 8 cleavage product of Bid, to the mitochondria, which induces cytochrome *c* release (28, 29), or through the mitochondrial release of Smac, which neutralizes the inhibitory effect of inhibitor of apoptosis proteins on caspases (17, 18, 30).

Apoptosis induced by many stimuli seems to depend on MRC. For example, MRC function has been reported to be required for apoptosis induced by TNF-α (31–33), lipoxygenase inhibitor nordihydroguaiaretic acid (34), butyrate, and some other short chain fatty acids (35), ceramide (36), hydroxamic acid compound BMD188 (37), manganese (38), synthetic retinoid CD437 (39), O_2 deprivation (40), oxidants such as *tert*-butylhydroperoxide (41) and hydrogen peroxide (42), and Ca^{2+} overloading (43). Thus, in these apoptotic model systems, MRC-deficient ρ^0 cells are more resistant to apoptosis, and MRC inhibitors (such as rotenone and antimycin A) block or inhibit apoptosis. Also in support of the dependence of apoptosis on MRC, complex I deficiency in leukemia cells results in apoptosis resistance (44). Deficiency in complex IV in colon carcinoma cells renders them resistant to apoptosis induction (35). Similarly, F_0F_1-ATPase is required for Bax-induced apoptosis (45).

The molecular mechanisms underlying this MRC-dependent apoptosis remain unclear. Here we report that apoptosis induced by BMD188, a chemical that causes cell death in an MRC-dependent manner (37), involves an early up-regulation of MRC proteins (in particular, cytochrome *c*) prior to caspase activation and cell death. Importantly, this phenomenon seems to represent a general early apoptotic response as it is also observed in multiple cell types induced to die by a variety of stimuli.

MATERIALS AND METHODS

Cells and Reagents

Human osteosarcoma cells 143B(TK$^-$) (143B) and fibroblasts GM701.2-8C (GM701) and their respective mtDNA-less, respiration-deficient ρ^0 derivatives 143B206 and GM701.2–8C (2) cells (46) were kindly provided by Dr. M. King (Thomas Jefferson University). 143B and GM701 cells were cultured in Dulbecco's minimum essential medium (Invitrogen) supplemented with 10% heat-inactivated fetal bovine serum (FBS) and antibiotics. 143B206 and GM701.2–8C (2) cells were cultured in Dulbecco's minimum essential medium with high glucose supplemented with 100 μg/ml pyruvate, 200 ng/ml ethidium bromide, 50 μg/ml uridine, 10% FBS, and antibiotics. Human prostate cancer cells, PC3 and LNCaP, and breast carcinoma cells, MDA-MB231, were purchased from ATCC (Manassas, VA) and cultured in RPMI 1640 supplemented with 5 and 10% FBS, respectively. The ρ^0 PC3 clone 6 cells (37) were cultured as for 143B206 cells.

The primary antibodies used were listed in Table I. Secondary antibodies, *i.e.* goat, donkey, or sheep anti-mouse or rabbit IgG conjugated to horseradish peroxidase, fluorescein isothiocyanate, or rhodamine, together with ECL (enhanced chemiluminescence) reagents were acquired from Amersham Biosciences. Fluorogenic caspase substrates DEVD-AFC and LEHD-AFC, pan-caspase inhibitor z-VAD-fmk, and caspase-3/6/7 inhibitor, z-DEVD-fmk, were bought from Biomol (Plymouth Meeting, PA). Ponasterone and Zeocin were purchased from Invitrogen. Annexin V conjugated to AlexaFluor 568 and mitochondrial dyes were purchased from Molecular Probes (Eugene, OR). Liposome FuGENE 6 was bought from Roche Molecular Biochemicals. All other chemicals were purchased from Sigma unless specified otherwise.

Subcellular Fractionation and Western Blotting

Mitochondria were prepared using differential centrifugation (37, 47, 48) with slight modifications. Briefly, cells were treated with various chemicals or vehicle (ethanol or Me_2SO) control. In some experiments, cells were pretreated with protein synthesis inhibitor cycloheximide (CHX), RNA synthesis inhibitor actinomycin D (A/D), or mitochondrial protein synthesis inhibitor tetracycline before apoptosis induction. At the end of the treatment, cells were harvested by scraping, washed twice in ice-cold PBS, and resuspended in 600 μl of homogenizing buffer (20 mM HEPES-KOH, pH 7.5, 10 mM KCl, 1.5 mM $MgCl_2$, 1 mM sodium EDTA, 1 mM sodium EGTA, and 1 mM dithiothreitol) containing 250 mM sucrose and a mixture of protease inhibitors (1 mM phenylmethylsulfonyl fluoride, 1% aprotinin, 1 mM leupeptin, 1 μg/ml pepstatin A, and 1 μg/ml chymostatin). After 30 min of incubation on ice, cells were homogenized in the same buffer using a glass Pyrex homogenizer (type A pestle, 140 strokes). Unbroken cells, large plasma membrane pieces, and nuclei were removed by centrifuging the homogenates at 500 $\times$ *g* for 5 min at 4 °C. The resulting supernatant was centrifuged at 10,000 $\times$ *g* for 20 min to obtain mitochondria. The remaining supernatant was again subjected to centrifugation at 100,000 $\times$ *g* for 1 h to obtain the cytosolic fraction (*i.e.* S100 fraction). The mitochondrial pellet was washed three times in homogenizing buffer, and then solubilized in TNC buffer (10 mM Tris acetate, pH 8.0, 0.5% Nonidet P-40, 5 mM $CaCl_2$) containing protease inhibitors. Protein concentration was determined by Micro-BCA kit (Pierce).

For Western blotting, 25 μg of proteins (mitochondrial or cytosolic fractions) was loaded in each lane of a 15% SDS-polyacrylamide gel. After gel electrophoresis and protein transfer, the membrane was probed or reprobed, after stripping, with various primary and corresponding secondary antibodies (37, 47). Western blotting was performed using ECL as described previously (37, 47).

Measurement of Apoptosis

Apoptosis was measured using several biochemical and biological approaches.

PARP Cleavage—PARP cleavage assays were performed as described previously (37, 47).

Caspase-3 Activation—Caspase-3 cleavage (activation) was analyzed by Western blotting. Cells were lysed in TNC lysis buffer, and 100 μg of whole cell lysates was separated on 15% SDS-PAGE. After protein transfer, the blot was probed with a monoclonal antibody for caspase-3. The activation of caspase-3 was monitored by a decrease or disappearance of the ~32-kDa procaspase-3 (37).

DEVDase and LEHDase Activity—Cells were washed twice in PBS, and the whole cell lysates were made in the lysis buffer (50 mM HEPES, 1% Triton X-100, 0.1% CHAPS, 1 mM dithiothreitol, and 0.1 mM EDTA). Forty μg of protein was added to a reaction mixture containing 30 μM fluorogenic peptide substrates, DEVD-AFC or LEHD-AFC, 50 mM of HEPES, pH 7.4, 10% glycerol, 0.1% CHAPS, 100 mM NaCl, 1 mM EDTA, and 10 mM dithiothreitol, in a total volume of 1 ml and incubated at 37 °C for 1 h. Production of 7-amino-4-trifluoromethylcoumarin (AFC) was monitored in a spectrofluorimeter (Hitachi F-2000 fluorescence spectrophotometer) using excitation wavelength 400 nm and emission wavelength 505 nm. The fluorescent units were converted into nanomoles of AFC released per h per mg of protein using a standard curve. The results were generally presented as fold activation over the control.

DNA Fragmentation—Fragmented DNA was extracted using SDS/RNase/proteinase K methods (37, 47), and 20 μg of DNA was run on 1.2% agarose gel.

Quantification of Apoptotic Nuclei Using DAPI Staining—Cells were plated on glass coverslips (4×10^4 cells/18-mm^2 coverslip) and the next day treated with vehicle control (*i.e.* ethanol or Me_2SO) or various inducers. Thereafter, cells were incubated live with DAPI (0.5 μg/ml) for 10 min at 37 °C followed by washing. The percentage of cells exhibiting apoptotic nuclei, as judged by chromatin condensation or nuclear fragmentation, was assessed by fluorescence microscopy (49). An average of 600–700 cells was counted for each condition.

Immunofluorescence Analysis of Cytochrome c Distribution, Mitochondrial Membrane Potential, and Apoptosis

Cells grown on glass coverslips were treated for various time intervals. Fifteen min prior to the end of the treatment, cells were incubated live with MitoTracker Orange CMTMRos to label mitochondria (37). Then cells were fixed in 4% paraformaldehyde for 10 min followed by permeabilization in 1% Triton X-100 for 10 min. After washing in PBS, cells were first blocked in 20% goat whole serum for 30 min at 37 °C and then incubated with monoclonal anti-cytochrome *c* antibody (clone 6H2.B4, 1:500) for 1 h at 37 °C. Finally, cells were incubated with fluorescein isothiocyanate-conjugated goat anti-mouse IgG (1:1000) for 1 h at 37 °C. After thorough washing, coverslips were mounted on slides using Vectashield mounting medium (Vector Laboratories, Inc.,

Burlingame, CA) and observed under an Olympus BX40 epifluorescence microscope. Images were captured with MagnaFire software and processed in Adobe Photoshop. In a separate set of samples, following apoptotic treatments, cells were washed once with 1× PBS and then incubated in the Annexin-Binding Buffer containing annexin V-Alexa-Fluor conjugates for 30 min followed by washing. Images were captured on an Olympus IX50 inverted fluorescence microscope.

RT-PCR Analysis of Cytochrome c and COX II mRNA Expression

Total RNA was isolated using Tri-Reagent (Invitrogen). RT was performed using 2 μg of total RNA (at 42 °C for 2 h) in a total 20-μl reaction volume containing random hexamers and Superscript II reverse transcriptase (Invitrogen). PCR primers, designed based on the published cytochrome *c* and COX II cDNA sequences, are 5′-TTTGGATCCAATGGGTGATGTTGAG-3′ (cytochrome *c*, sense), 5′-TTTGAATTCCTCATTAGTAGCTTTTTTGAG-3′ (cytochrome *c*, antisense), 5′-CCATCCCTACGCATCCTTTAC-3′; (COX II, sense), and 5′-GTTTGCTCCACAGATTTCAGAG-3′ (COX II, antisense). For PCR, 1 μl of cDNA was used in a 25-μl reaction containing 0.5 μM primers, dNTPs and *Taq*, using the cycling profile 94 °C × 45 s, 56 °C × 1 min, and 72 °C × 1 min for 14 cycles for COX II and 23 cycles for cytochrome *c* with a final extension at 72 °C for 10 min. PCR products were analyzed on 1% agarose gel. RT-PCR of glyceraldehyde 3-phosphate dehydrogenase (50) was used as a control.

Transient Transfection with pEGFP-Cytochrome c

The pEGFP-cytochrome *c* expression plasmid, in which the full-length rat cytochrome *c* cDNA was cloned into the *Nhe*I and *Xho*I sites of the pEGFP-N1 (Clontech), was kindly provided by Dr. A.-L. Nieminen (Case Western Reserve University; see Ref. 51). GM701 cells, plated 1 day earlier on 10-cm culture dishes to achieve 50–60% confluence, were transfected, using FuGENE 6, with 15 μg of either empty vector alone or pEGFP-cytochrome *c*. Twenty four h after transfection, cells were treated with BMD188 for various times and then harvested and used for subcellular fractionations as described above. To assess apoptosis, GM701 cells grown on coverslips were transfected with 1 μg of plasmids. Twenty four h later, cells were treated with BMD188 followed by DAPI staining as described above. The percentage of GFP-positive and -negative cells with apoptotic nuclear morphology was determined by fluorescence microscopy (49). At least 600–700 cells were counted for each condition.

Up-regulation of Cytochrome c Using the Ecdysone-inducible System

Plasmids pVgRXR and pIND were obtained from Invitrogen. pIND/cyt-c-GFP was prepared by cloning the *Nhe*I/*Not*I fragment of the rat cytochrome *c*-GFP fusion cDNA from pEGFP-cytochrome *c* (51) into pIND/V5-His-B, whereas pIND-GFP was prepared by cloning the EGFP fragment (from pEGFP-N1) between the *Hin*dIII and *Not*I sites of pIND/Hygro (courtesy of Dr. T.-J. Liu, MD Anderson Cancer Center, Houston, TX). Ecdysone-inducible cell lines were generated in two steps. First, GM701 cells were transfected with pVgRXR by electroporation (1025 microfarads, 260 V in a Bio-Rad apparatus). Stable transfectants were selected with Zeocin (500 μg/ml) for 3–4 weeks and stable clones isolated using a cloning ring. The stable clones, named EcR-GM701, were characterized by GFP expression in response to ponasterone (2 μM) after transient transfection with pIND-GFP. EcR-293 cells were kindly provided by Dr. M. Bedford. In the second step, EcR-GM701 and EcR-293 cells were electroporated with pIND/cyt-c-GFP or pIND/GFP followed by G418 (1 mg/ml) selection. Stable clones were picked by ring cloning and screened by immunoblotting using antibody against GFP upon ponasterone (2 μM) induction. GM701-pIND/cyt-c-GFP, GM701-pIND/GFP, 293-pIND/cyt-c-GFP, and 293-pIND/GFP cells were maintained in Zeocin (500 μg/ml) and G418 (1 mg/ml)-containing medium. These cells were used in subcellular fractionation and apoptosis studies upon treatment with ponasterone for various times.

Up-regulation of Cytochrome c Using the pCMS-EGFP Expression System

Full-length cDNA sequence of human cytochrome *c* was synthesized by PCR amplification using *Taq* polymerase (Eppendorf, Germany) and cloned between the EcoRI and *Xba*I sites of pCMS-EGFP vector (Clontech). The Kozak sequence was introduced in sense primer. The resultant plasmid was sequenced and designated as pCMS-EGFP/cyt-c, in which cytochrome *c* and EGFP are synthesized from two separate promoters. GM701 fibroblasts were either untransfected or transfected with the empty vector (pCMS-EGFP) or pCMS-EGFP/cyt-c. Twenty-four h after transfection, cells were harvested, and mitochondrial and cytosolic fractions were prepared, and 25 μg/lane of protein from each sample was separated by 15% SDS-PAGE. Following protein transfer, the membranes were probed and reprobed with antibodies against cytochrome *c*, GFP, actin, or HSP60, as indicated under "Results." Apoptosis was quantified using the DAPI staining 24 h after transfection.

Statistical Analysis

The statistical significance between experimental groups was determined by Student's *t* test using the SPSS-10 software. Differences at $p < 0.05$ were considered statistically significant.

RESULTS

Multiple Apoptotic Stimuli Induce an Increase of MRC Proteins Such as COX II and Cytochrome c Early during Apoptosis Induction—We demonstrated previously (37) that apoptosis of epithelial cancer cells induced by chemical BMD188 requires the MRC function. Thus, ρ^0 PC3 (prostate cancer) cells or PC3 cells whose MRC had been blocked by various respiration complex-specific inhibitors were more resistant to BMD188-induced apoptosis (37). Further experiments demonstrate that BMD188 induces apoptosis in many other cell types, *e.g.* 143B osteosarcoma cells (Supplemental Material Fig. 1S) and GM701 fibroblasts (not shown) also in an MRC-dependent manner. To explore the molecular mechanisms of this MRC-dependent apoptotic pathway, we purified mitochondrial and S100 cytosolic fractions and used them in quantitative Western blotting to examine the protein levels of two essential MRC components, cytochrome *c*, which is encoded by the nuclear gene, and COX II, which is encoded by the mitochondrial genome. The protein levels were then correlated with caspase activation, which is measured by DEVDase activity, caspase-3 activation, or PARP cleavage, and with apoptosis, which is quantitated by counting apoptotic nuclei (see details under "Materials and Methods").

By using the above approach, we found that treatment of 143B cells with BMD188 induced a rapid (within 5 min) increase in the protein level of COX II (Fig. 1*A*). COX II protein was never detected in the cytosolic fractions in all of our experiments (Fig. 1*A* and not shown), suggesting that there was no substantial mitochondrial damage during subcellular fractionations and that the cytosolic fractions were not contaminated with the mitochondrial proteins. The reciprocal experiments measuring the lactate dehydrogenase (a cytosolic protein) activity also indicated that there was minimal contamination of the mitochondrial fractions with the cytosolic proteins (not shown). The COX II protein level plateaued at 30 min to 1 h after BMD188 treatment and slightly declined thereafter (Fig. 1*A*). Interestingly, 15 min post-BMD188 treatment, the total cytochrome *c* protein level also increased, in both cytosol and mitochondria (Fig. 1*A*), as revealed by monoclonal antibody against cytochrome *c* clone 7H8.2C12, which recognizes both apocytochrome *c* (*i.e.* cytochrome *c* in the cytosol without heme attached) and holocytochrome *c* (*i.e.* cytochrome *c* in the mitochondria with heme attached). (Note that, depending on the respiration status, a small amount of cytochrome *c* is often detected in the cytosol of untreated cells.) The cytochrome *c* levels continued to increase until ~1 h when an ~4-fold increase of cytochrome *c* was detected in both cytosol and mitochondria, and 22% of the cells were apoptotic (Fig. 1*A*). When ~50% 143B cells were apoptotic and prominent PARP cleavage (an indication of caspase activation) was observed at 2 h, cytochrome *c* levels in both compartments slightly decreased (Fig. 1*A*). Note that PARP cleavage becomes detectable only after sufficient numbers of cells have undergone apoptosis (*e.g.* see Fig. 1, *A–E*). By 4 h when most PARP was cleaved and ~90% of

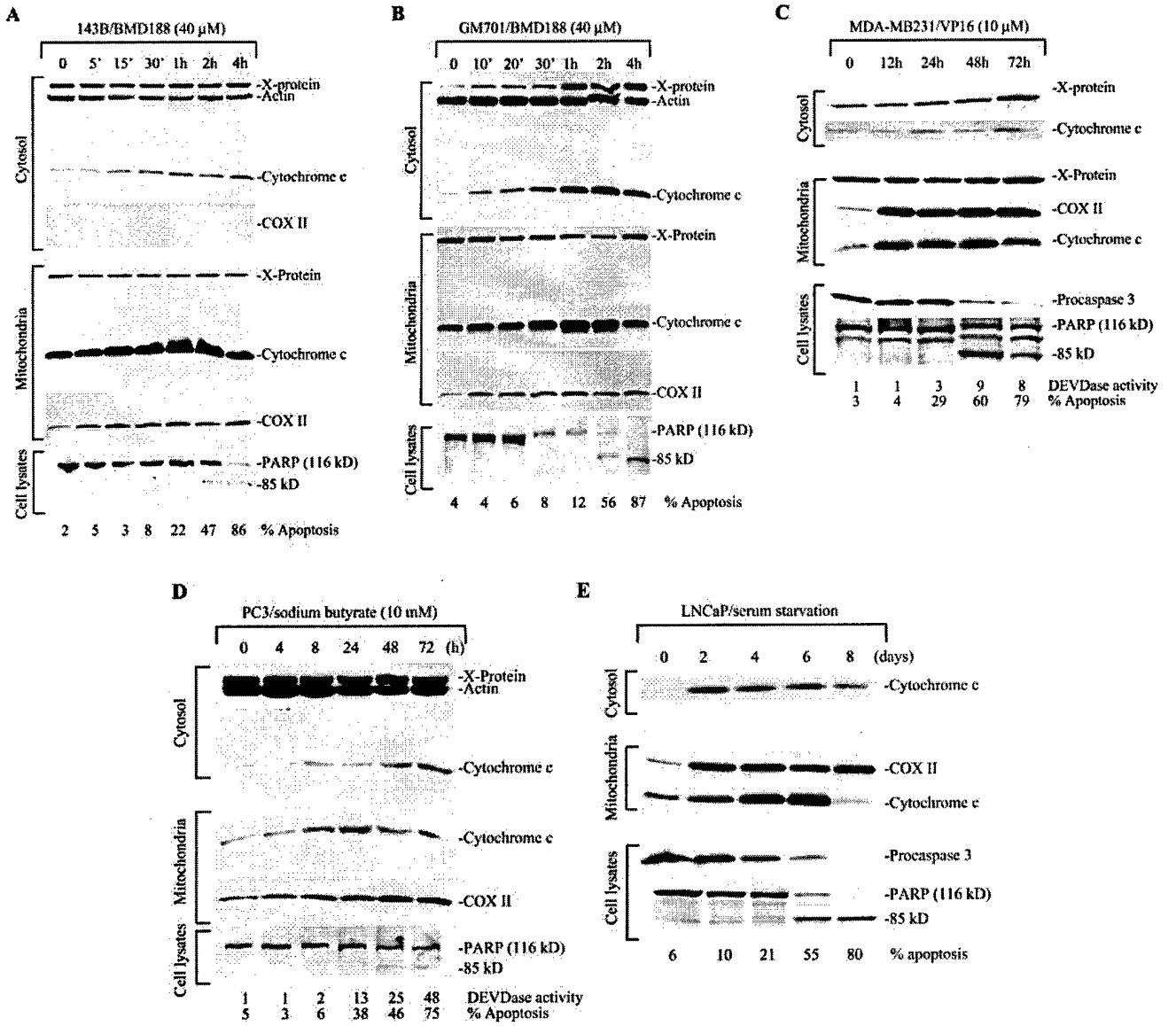

FIG. 1. **Up-regulation of MRC proteins early during apoptosis induction.** Western blot analysis of cytosolic and mitochondrial fractions from 143B cells treated with BMD188 (*A*), GM701 cells treated with BMD188 (*B*), MDA-MB-231 cells treated with VP16 (*C*), PC3 cells treated with sodium butyrate (*D*), and LNCaP cells treated with serum starvation (*E*). Mitochondrial and cytosolic fractions were prepared, and 25 μg of proteins (cytosolic or mitochondrial fractions) from each sample was used in Western blotting for cytochrome *c*, COX II, and actin. Several different biochemical (PARP cleavage, caspase-3 activation, and DEVDase activity) and biological (*i.e.* apoptotic nuclear morphology upon DAPI labeling of live cells) methods were used, in different combinations, to assess apoptosis (see "Materials and Methods"). In some samples (*e.g. A, B,* and *D*), the cytosol blots were incubated with a mixture of antibodies to both cytochrome *c* and actin. Data shown are representative of 3–5 independent experiments.

the cells were apoptotic, significant amounts of mitochondrial cytochrome *c* similar to the basal level and of cytosolic cytochrome *c* higher than the basal level were still observed (Fig. 1*A*). Note that 7H8.2C12 also detected an ~50-kDa protein labeled as *X*-protein, whose identity remains unclear (37, 47, 52).

Similarly, treatment of GM701 fibroblasts with BMD188 rapidly up-regulated COX II as well as cytochrome *c* (Fig. 1*B*). Increased COX II was detected at 10 min and plateaued by 1 h after drug treatment (Fig. 1*B*). Increased cytochrome *c* was observed in both cytosol (~3-fold) and mitochondria (~1.5-fold) in the first 10–20 min, and by 30 min the increase became more obvious (5-fold in cytosol and 2.5-fold in mitochondria) (Fig. 1*B*). By 1 h, when ~12% cells were apoptotic, peak levels of cytochrome *c* in both cytosol (10-fold increase) and mitochondria (4-fold increase) were observed (Fig. 1*B*). By 2 h when ~60% of the cells was apoptotic and PARP was cleaved, mitochondrial cytochrome *c* began to decrease, whereas the cytosolic cytochrome *c* level remained about the same (Fig. 1*B*). By 4 h when ~90% of cells were apoptotic and PARP was nearly completely cleaved, cytochrome *c* levels in both cytosol and mitochondria decreased (Fig. 1*B*). As observed previously (37) in PC3 cells, in both 143B and GM701 cells treated with BMD188, apoptosis could be dose-dependently inhibited by z-VAD-fmk, a pan-caspase inhibitor, as well as by z-DEVD-fmk, a caspase-3/6/7 inhibitor (not shown), suggesting that the cell death is caspase-dependent. Collectively, data presented in Fig. 1, *A* and *B*, together with our previous observations showing early induction of COX I (encoded by mitochondrial genome) and COX IV (encoded by the nuclear genome) (37), suggest that there is an early induction of MRC proteins during apoptosis induced by BMD188, an agent whose pro-apoptotic effect depends on MRC (37).

To determine whether this early induction of MRC proteins

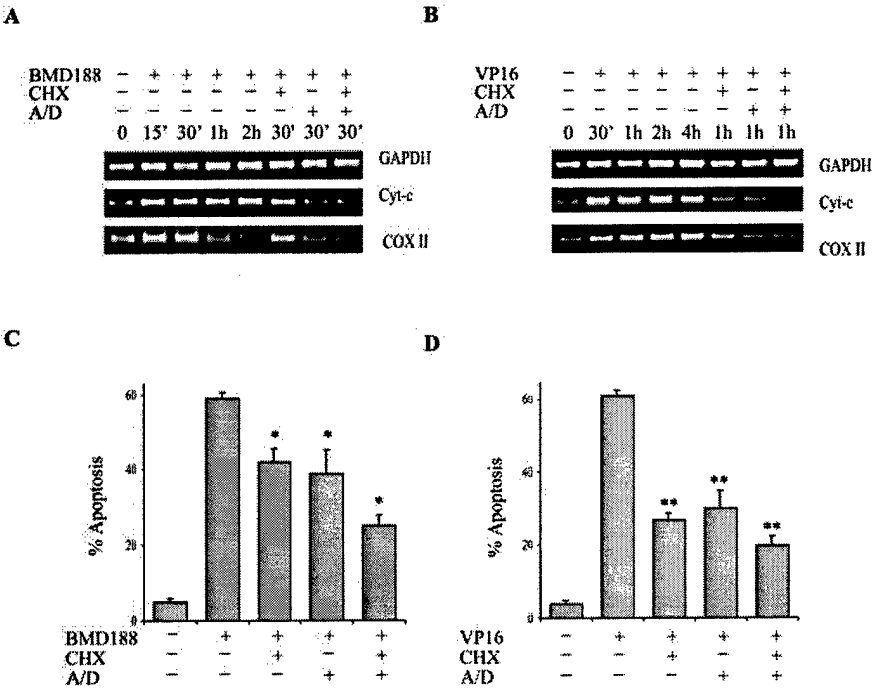

FIG. 2. **Transcriptional activation of cytochrome *c* and COX II genes and inhibition of apoptosis by transcription and translation inhibitors.** *A* and *B*, transcriptional up-regulation of cytochrome *c* (Cyt-*c*) and COX II. *A*, GM701 fibroblast cells were treated with BMD188 (40 μM); or *B*, MDA-MB-231 cells were treated with VP16 (10 μM) for the time intervals indicated. Some samples were pretreated with cycloheximide (CHX, 1 μM), actinomycin D (A/D, 1 nM), or both for 1 h before apoptotic stimulation. RT-PCR was performed as detailed under "Materials and Methods." Data are representative of at least five separate experiments. *C* and *D*, inhibition of apoptosis by protein and RNA synthesis inhibitors. GM701 (*C*) or MDA-MB-231 (*D*) cells grown on glass coverslips were treated with BMD188 (40 μM, 2 h) or VP16 (10 μM, 48 h), respectively, either alone or in the presence of CHX, A/D, or both as indicated. The percentages of apoptotic cells upon DAPI staining were enumerated under a fluorescent microscope. Values represent the mean ± S.D. from five separate experiments. *, $p < 0.05$; **, $p < 0.01$ (Student *t* test) compared with cells treated BMD188 (*C*) or VP16 (*D*) alone.

is restricted only to MRC-dependent apoptotic stimuli, we carried out similar experiments in multiple cell types with a variety of apoptotic inducers of different mechanisms of action. First, we treated MDA-MB231 breast cancer cells with VP16 (etoposide), a commonly used chemotherapeutic drug that inhibits DNA topoisomerase II. As shown in Fig. 1*C*, maximum up-regulations of COX II and cytochrome *c* occurred as early as 12 h after drug treatment. Nearly all up-regulated cytochrome *c* was present in the mitochondria in MDA-MB231 cells treated with VP16 (Fig. 1*C*), which is different from 143B or GM701 cells treated with BMD188 (Fig. 1, *A* and *B*). By 12 h no caspase activation and significant death were detected (Fig. 1*C*). By 24 h caspases (*i.e.* DEVDase) were activated ~3-fold, and ~30% of the cells were apoptotic (Fig. 1*C*). By 48 h after the drug treatment when obvious caspase-3 cleavage and DEVDase activity were detected, PARP was cleaved, and 60% of the cells were apoptotic, maximum levels of cytochrome *c* and COX II were still observed in the mitochondria (Fig. 1*C*). By 72 h when nearly 80% of the cells were apoptotic and prominent caspase-3 cleavage occurred, cytochrome *c* in the mitochondria decreased but the COX II protein level remained about the same (Fig. 1*C*). There was a slight increase of cytochrome *c* in the cytosol 24–72 h after VP16 treatment (Fig. 1*C*). Apoptosis in MDA-MB-231 cells was dose-dependently inhibited by z-VAD-fmk or z-DEVD-fmk (not shown), suggesting that the VP16-induced cell death is also caspase-dependent.

Likewise, treatment of PC3 cells with butyrate, a short chain fatty acid inhibitor of histone deacetylase (35), resulted in a time-dependent up-regulation of COX II and cytochrome *c* in both cytosolic and mitochondrial compartments (Fig. 1*D*). By 24 h post-treatment when caspase activity increased by 13-fold, PARP was cleaved, and ~40% of the cells were apoptotic, the maximum amount of cytochrome *c* accumulated in the mitochondria (Fig. 1*D*). Starting from 48 h on, the mitochondrial cytochrome *c* began to decrease accompanied by an increase in the cytosolic cytochrome *c* (Fig. 1*D*). Similarly, in LNCaP cells subjected to serum starvation, maximum induction of COX II was observed by day 2, after which the COX II protein remained at a similar level up to day 10 (Fig. 1*E* and data not shown). By contrast, a time-dependent up-regulation of cytochrome *c* in the mitochondria was observed (Fig. 1*E*). Two days after withdrawal of serum, increased cytochrome *c* in the mitochondria and maximum level of cytochrome *c* in the cytosol were observed (Fig. 1*E*). There was slightly increased procaspase-3 cleavage and cell death at this time point (Fig. 1*E*). By 4 days when further increased caspase-3 activation and cell death were observed, the mitochondrial cytochrome *c* continued to increase while the cytosolic cytochrome *c* slightly decreased. By 6 days when obvious caspase-3 activation, PARP cleavage, and apoptosis were observed, the mitochondrial cytochrome *c* reached peak level, whereas the cytosolic cytochrome *c* level remained unchanged (Fig. 1*E*). By 8 days when caspase-3 and PARP were completely cleaved and 80% of the cells apoptotic, the mitochondrial cytochrome *c* was almost completely lost, and the cytosolic cytochrome *c* also decreased (Fig. 1*E*).

Similar studies in PC3 cells treated with camptothecin and DLD-1 (colon cancer) cells treated with herbimycin also revealed rapid up-regulations of cytochrome *c* and COX II (not shown). Altogether, these data demonstrate that early up-regulation of MRC proteins such as COX II and cytochrome *c* represents a common early event in apoptosis induced by diverse stimuli.

Increased Cytochrome c and COX II Proteins Result from Transcriptional Activation—Cytochrome *c* is a cytosolic protein encoded by a nuclear gene. Upon synthesis, depending on the metabolic status of the cells, the majority or a fraction of the apocytochrome *c* rapidly translocates to the mitochondria to participate in the electron transport (1). Within mitochondria, apocytochrome *c* is "anchored" to cytochrome *c* heme lyase and turns into holocytochrome *c* upon heme binding (1, 53). Therefore, the increased cytochrome *c* protein levels in both cytosol and mitochondria (Fig. 1, *A–E*) suggest an increased transcription and/or translation. To test this possibility, we used semiquantitative RT-PCR to analyze the mRNA levels of cytochrome *c* and COX II during the early phase of apoptosis induction by some of the inducers used in Fig. 1. As shown in Fig. 2*A*, treatment of GM701 cells with BMD188 resulted in a maximum increase in cytochrome *c* mRNA as early as 15 min, which remained elevated at similar levels until 2 h. Similarly, maximum induction of COX II mRNA was also observed at 15 min post-BMD188 treatment, which decreased by 1 h (Fig. 2*A*).

TABLE I
Primary antibodies used in this study

Ab[a]	Type	Source (catalog no.)	Remarks
Actin	Mouse mAb	ICN (69100)	
Bad	Mouse mAb	Santa Cruz Biotechnology (sc-8044)	
Bak	Rb pAb	Santa Cruz Biotechnology (sc-832)	
Bak	Rb pAb	Upstate Biotechnology (06–536)	Recognizes activated Bak
Bax	Rb pAb	Santa Cruz Biotechnology (554104)	
Bax	Rb pAb	Upstate Biotechnology (06–499)	Recognizes activated Bax
Bcl-2	Mouse mAb	Pharmingen (14831A)	
Bcl-x	Rb pAb	Pharmingen (610211)	
Bid	Rb pAb	Dr. X Wang	Recognizes both t Bid and uncleaved Bid
Bim	Rb pAb	Calbiochem (202000)	
COX I	Mouse mAb	Molecular Probes (A-6403)	
COX II	Mouse mAb	Molecular Probes (A-6404)	
COX IV	Mouse mAb	Molecular Probes (A-6431)	
Cyt-c	Mouse mAb (clone 6H2.B4)	Pharmingen (556432)	Recognizes holocytochrome *c* on immunofluorescence
Cyt-c	Mouse mAb (clone 7H8.2C12)	Pharmingen (65981A)	Recognizes apo- and holo-cyt-*c* on Western blot
Cyt-c	Mouse mAb	R & D Systems (6380-MC-100)	Recognizes holocytochrome *c* only on Western blot
Caspase-3	Mouse mAb	Transduction Laboratories (C31720)	Recognizes the proform only
Caspase-9	Rb pAb	Chemicon (AB16970)	
GFP	Mouse mAb	Clontech (8362–1)	
PARP	Rb pAb	Roche Molecular Biochemicals (1 835 238)	
Smac	Rb pAb	Dr. X. Wang	
HSP60	Mouse mAb	Chemicon (mAb3514)	

[a] The abbreviations used are: Ab, antibodies; COX I/II/IV, cytochrome *c* oxidase subunit I/II/IV; cyt-*c*, cytochrome *c*; GFP, green fluorescence protein; PARP, poly-(ADP-ribose); polymerase; mAb, monoclonal antibody; pAb, polyclonal antibody; Rb, rabbit; HSP60, heat shock protein 60.

The induction of both cytochrome *c* and COX II mRNAs was inhibited by A/D, which inhibits RNA transcription. CHX, a protein synthesis inhibitor, did not significantly affect cytochrome *c* mRNA level but significantly inhibited the mRNA of mitochondria-encoded COX II (Fig. 2*A*). The combination of A/D and CHX resulted in slightly greater inhibition of the cytochrome *c* and COX II mRNAs than either inhibitor alone (Fig. 2*A*). As expected, CHX and A/D, either individually or in combination, inhibited BMD188 up-regulated COX II and cytochrome *c* proteins in GM701 cells (not shown). Similar RT-PCR analysis was carried out in MDA-MB231 cells treated with VP16. As shown in Fig. 2*B*, the cytochrome *c* mRNA was maximally induced as early as 30 min post-treatment, which stayed up-regulated at similar levels up to 4 h, the longest time interval examined. In contrast, COX II mRNA was up-regulated in a time-dependent manner, and the peak-level induction was observed at 4 h (Fig. 2*B*). CHX significantly inhibited both cytochrome *c* and COX II mRNA expression, and A/D demonstrated a more prominent inhibitory effect (Fig. 2*B*), which is different from BMD188-treated GM701 cells. The combination of CHX and A/D inhibited their mRNA up-regulations more significantly than either treatment alone (Fig. 2*B*). Together, these results suggest that the up-regulated COX II and cytochrome *c* proteins early during apoptosis induction (Fig. 1, *B* and *C*) resulted from an increased mRNA transcription. That CHX also inhibited the mRNA expression of COX II and/or cytochrome *c* (Fig. 2, *A* and *B*) is probably due to inhibition of the transcriptional machinery by CHX.

To assess the potential importance of *de novo* RNA and/or protein synthesis in the above apoptotic models, GM701 (Fig. 2*C*) and MDA-MB-231 (Fig. 2*D*) cells were pretreated with A/D, CHX, or both 1 h before treating with BMD188 and VP16, respectively. The results indicate that pretreatment of cells with these inhibitors significantly inhibited apoptosis, and the inhibition was more pronounced in VP16-treated MDA-MB231 cells. In both cases, the combination of A/D and CHX resulted in greater inhibition of apoptosis than either inhibitor alone (Fig. 2, *C* and *D*).

Cytochrome c Up-regulation in Relation to Cytochrome c Release and Caspase Activation—The preceding experiments demonstrate that multiple apoptotic stimuli, perhaps through transcriptional activation, up-regulate cytochrome *c*, leading to increased cytochrome *c* protein levels in both mitochondria and cytosol. In the intrinsic apoptotic pathway, mitochondrial holocytochrome *c* is released into the cytosol to trigger caspase activation, and only the holo- but not apocytochrome *c* has the apoptogenic effect (14). The anti-cytochrome *c* antibody (*i.e.* 7H8.2C12) utilized in the experiments of Fig. 1 recognizes both apo- and holocytochrome *c* (Table I). Consequently, we could not determine whether the increased cytochrome *c* in the cytosol (Fig. 1, *A–E*) represents the newly synthesized apocytochrome *c*, mitochondrially released holocytochrome *c*, or a mixture of both. R & D Systems has recently developed an antibody that specifically recognizes holocytochrome *c* (Table I). We thus took advantage of this antibody and utilized BMD188 as the primary apoptotic inducer to address the relationships among cytochrome *c* up-regulation, cytochrome *c* release, and caspase activation.

In untreated GM701 cells holocytochrome *c* existed only in the mitochondria (Fig. 3*A*). Fifteen min post-BMD188 treatment, slightly increased holocytochrome *c* was observed in the mitochondria, but no holocytochrome *c* could be detected in the cytosol (not shown). By 30 min, there was a substantial increase in the mitochondrial holocytochrome *c* accompanied by a small amount of holocytochrome *c* release into the cytosol. By 1 h, the mitochondrial holocytochrome *c* level remained about the same as at 30 min, but the holocytochrome *c* level in the cytosol dramatically increased (Fig. 3*A*). By 2 h, the majority of holocytochrome *c* was released from the mitochondria, whereas the holocytochrome *c* level in the cytosol remain about the same as at 1 h (Fig. 3*A*). By 4 h, the holocytochrome *c* in both mitochondria and cytosol could hardly be detected. These changes in holocytochrome *c* were confirmed by fluorescence microscopy (see Fig. 4). Combined with the data presented in Fig. 1*B* and 2*A*, the following scenario can be presented to explain the cytochrome *c* movement. Early (*i.e.* within 10–15

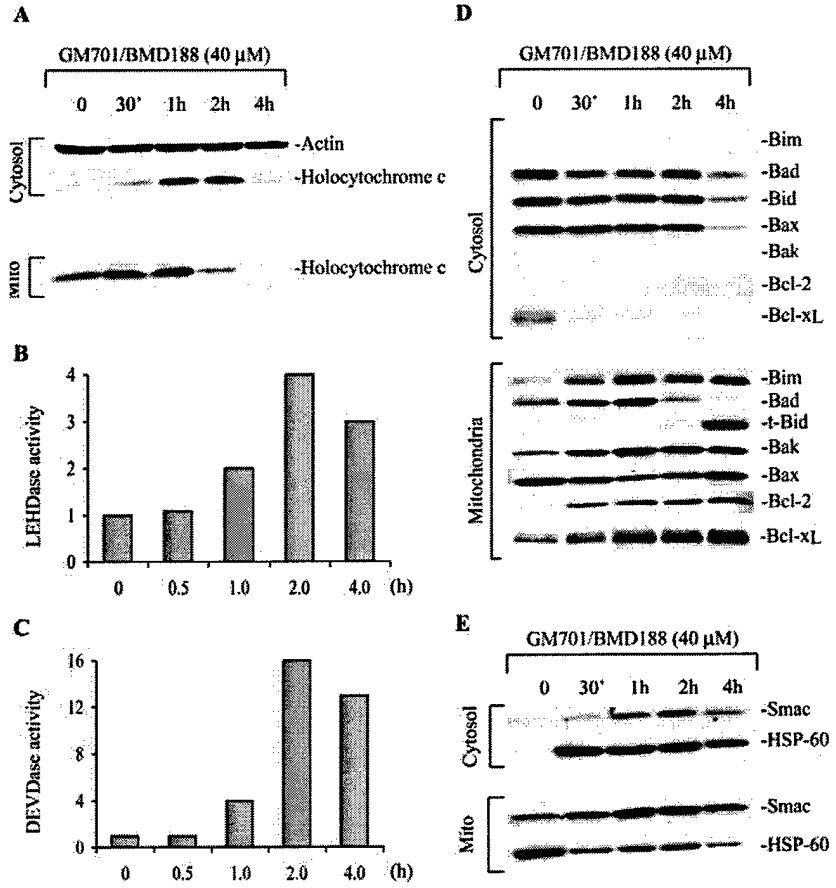

FIG. 3. **Cytochrome *c* alterations in relation to caspase activation (*A–C*), changes in Bcl-2 family proteins (*D*), and release of mitochondrial proteins larger than cytochrome *c* (*E*).** *A*, GM701 cells were treated with BMD188, and mitochondrial (*Mito*) and cytosolic fractions were prepared as described under "Materials and Methods." Forty μg of cytosolic or mitochondrial proteins from each sample was used in Western blotting for holocytochrome *c* together with actin. *B* and *C*, whole cell lysates (40 μg) were used to measure LEHDase activity (*B*) and DEVDase activity (*C*), respectively. *D* and *E*, the same blot as shown in *A* was stripped and sequentially reprobed for various Bcl-2 family proteins (*D*) or for Smac and HSP60 (*E*). Note that essentially identical results were obtained for Bak and Bax when using antibodies that recognize the conformationally active proteins (Table I; data not shown). Data shown are representative of 3–5 independent experiments.

min) post-BMD188 treatment, cytochrome *c* is transcriptionally up-regulated resulting in increased cytochrome *c* protein, part of which is transported into the mitochondria and part of which is retained in the cytosol. By 30 min, continued cytochrome *c* up-regulation leads to further increased holocytochrome *c* enrichment in the mitochondria and, at the same time, a low level of mitochondrial holocytochrome *c* begins to be released. By 1 h, the total cytochrome *c* level (as detected by 7H8.2C12) reaches a maximum in the mitochondria (Fig. 1*B*), whereas the holocytochrome *c* level in the mitochondria remains about the same as at 30 min (Fig. 3*A*), suggesting that at this time point either significant cytochrome *c* release is taking place or mitochondria are no longer able to convert apocytochrome *c* to holocytochrome *c*. The high level of holocytochrome *c* in the cytosol at 1 h (Fig. 3*A*) supports the former possibility. By 2 h, 7H8.2C12 still detects a high level of cytochrome *c* in the mitochondria (Fig. 1*B*), but the mitochondrial holocytochrome *c* is nearly completely released into the cytosol (Fig. 3*A*; also see Fig. 4*I*), suggesting that mitochondria can no longer convert the newly synthesized and transported apocytochrome *c* to holocytochrome *c* at this time point. By 4 h, 7H8.2C12 still detects a significant amount of cytochrome *c* in both mitochondria and cytosol (Fig. 1*B*), but the holocytochrome *c* in both compartments is barely detectable (Fig. 3*A*), suggesting that most of the cytochrome *c* detected by 7H8.2C12 at this time point is apocytochrome *c*. The nearly complete disappearance of holocytochrome *c* in both mitochondria and cytosol probably results from either its preferential release outside of the cells (54) or preferential degradation.

Next, we correlated cytochrome *c* alterations with the activation of the initiator caspase, caspase-9, and the executioner caspase, caspase-3. As shown in Fig. 3, *B* and *C*, caspase-9 (*i.e.* LEHDase activity) and caspase-3 (*i.e.* DEVDase activity) activation was observed at 1 h and reached the maximum levels by 2 h. In all apoptotic systems examined (Fig. 1 and data not shown), caspase activation (as judged by procaspase cleavage and/or substrate cleavage) was observed concomitant with or downstream of cytochrome *c* release.

Together, these results (Fig. 1, Fig. 2, *A* and *B*, and Fig. 3, *A–C*) suggest early cytochrome *c* up-regulation and translocation to the mitochondria preceding holocytochrome *c* release and caspase activation in BMD188-induced apoptosis of GM701 fibroblasts. Similarly, VP16-treated MDA-MB231 cells showed up-regulated cytochrome *c* mRNA as early as 30 min (Fig. 2*B*) and maximally induced cytochrome *c* protein, most of which accumulated in the mitochondria by 12 h (Fig. 1*C*). However, cytochrome *c* release from the mitochondria (not shown), caspase activation, and cell death (Fig. 1*C*) were not observed until ~24 h, again suggesting early cytochrome *c* up-regulation and translocation to the mitochondria preceding cell death. Similar sequence of alterations was also observed in serum-starved LNCaP cells.[2]

Cytochrome c Release Involves Dynamic Changes in Bcl-2 Family Proteins, Loss of $\Delta\psi_m$, and Opening of PTP—Next, we carried out four sets of experiments in BMD188-treated GM701 cells to investigate the potential mechanisms of cytochrome *c* release. In the first, we examined the involvement of Bcl-2 family proteins as they play an essential role in regulating mitochondrial integrity and cytochrome *c* release (26, 55). Specifically, we examined three BH3-only proteins (*i.e.* Bim, Bad, and Bid), two multidomain proapoptotic proteins (*i.e.* Bax and Bak), and two multidomain anti-apoptotic proteins (*i.e.* Bcl-2 and Bcl-x_L). As shown in Fig. 3*D*, dynamic changes were observed with these proteins. Bim, detected only in the mitochondria, was up-regulated (Fig. 3*D*), resulting from transcriptional

[2] J.-W. Liu, D. Chandra, and D. G. Tang, manuscript in preparation.

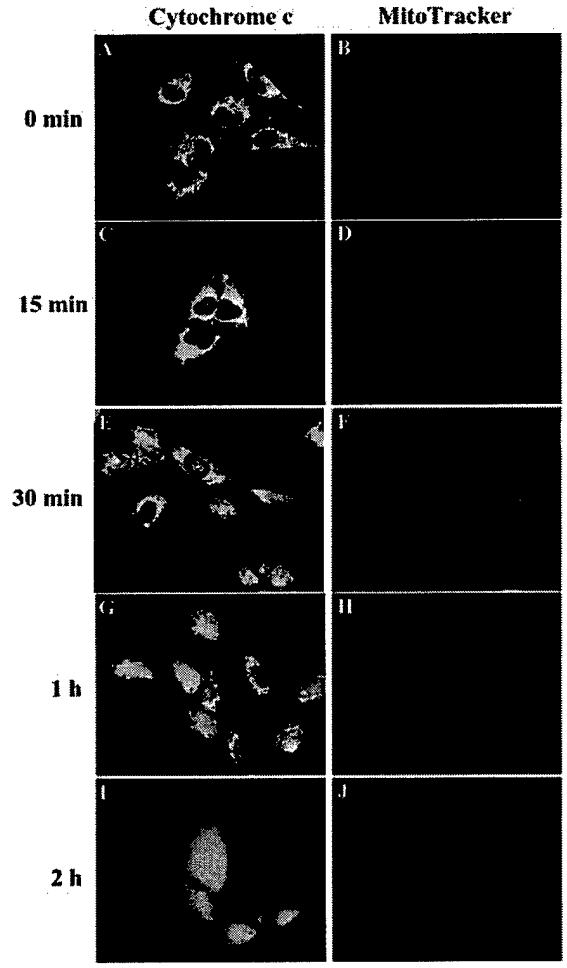

FIG. 4. **Loss of $\Delta\psi_m$ precedes cytochrome *c* release during BMD188-induced GM701 cell apoptosis.** Shown are representative microphotographs of cytochrome *c* (*A*, *C*, *E*, *G*, and *I*) and MitoTracker labeling of mitochondria (*B*, *D*, *F*, *H*, and *J*) in GM701 cells treated with BMD188 (40 μM) for 0 (*A* and *B*), 15 (*C* and *D*), and 30 min (*E* and *F*), and 1 (*G* and *H*), and 2 h (*I* and *J*). Another set of experiments with identical time points was performed to identify apoptotic cells using annexin V (see Supplemental Material Fig. 2S). See text for detailed discussions. Consistent with the Western blotting data and our previous observations (37), increased cytochrome *c* labeling was observed between 15 min and 1 h under the microscope, which was not well reproduced on micrographs. Original magnifications. ×200.

activation (not shown). Bad, detected mainly in the cytosol, showed a time-dependent translocation to the mitochondria until 2 h, when the mitochondria-associated Bad could hardly be detected. By 4 h, the mitochondria-associated Bad was undetectable, and the cytosolic Bad was mostly gone (Fig. 3*D*). Bid cleavage and activation, evidenced by the appearance of tBid in the mitochondria, was observed at 2 h and completed at 4 h (Fig. 3*D*), suggesting that this is a relatively late event, consistent with caspase-8 cleavage and activation starting from 2 h (not shown). Bax, detected equally in cytosol and mitochondria, showed somewhat complex alterations. Between 30 min and 2 h, Bax in both compartments was decreased. By 4 h, however, the cytosolic Bax was significantly decreased with a concomitant increase in the mitochondria (Fig. 3*D*). Bak, detected only in the mitochondria, on the other hand, showed a time-dependent increase that plateaued at 1 h (Fig. 3*D*). Interestingly, antibodies recognizing conformationally active Bax and Bak (Table I) revealed essentially identical changes in the two proteins (not shown). Bcl-2 and Bcl-x_L showed very similar changes; both proteins showed a time-dependent increase exclusively in the mitochondria (Fig. 3*D*). The early increase in the mitochondrial Bcl-x_L may also involve its translocation from the cytosol as a decreased cytosolic Bcl-x_L protein level was observed at 30 min post-treatment (Fig. 3*D*). These data suggest that dynamic changes in the Bcl-2 family proteins may be involved in cytochrome *c* release in BMD188-induced GM701 cell death.

In the second set of experiments, we examined the release of two other mitochondrial proteins that are significantly larger than cytochrome *c*: Smac, an ~25-kDa intermembrane protein (17, 18), and HSP60, a 60-kDa heat-shock protein localized in the matrix (56). As shown in Fig. 3*E*, Smac release, similar to holocytochrome *c* release (Fig. 3*A*), was observed 30 min after BMD188 treatment and plateaued by 2 h. Also similar to cytochrome *c*, the mitochondrial Smac protein level demonstrated a steady increase (Fig. 3*E*), suggesting an up-regulated transcription and/or translation. Interestingly, significant amounts of Smac still existed at 2 and 4 h when the majority of holocytochrome *c* had been released into the cytosol (compare Fig. 3, *E* and *A*), perhaps reflecting continuously up-regulated Smac synthesis just as significant amounts of cytochrome *c* in the mitochondria detected by 7H8.2C12 at these time points (see Fig. 1*B*). In contrast to holocytochrome *c* and Smac, HSP60 was maximally released as early as 30 min, and its levels in the mitochondria and cytosol remained relatively constant after 30 min until 4 h (Fig. 3*E*). Together, these data suggest that proteins significantly bigger than cytochrome *c* are also released during BMD188-induced apoptosis of GM701 cells.

In the third set of experiments, we used immunofluorescence microscopy and 6H2.B4, an antibody that recognizes only holocytochrome *c* in immunostaining (Table I), to examine the relationship between $\Delta\psi_m$ and mitochondrial cytochrome *c* release. As shown in Fig. 4*A*, holocytochrome *c* in untreated GM701 fibroblasts was distributed in the mitochondria, which colocalized with MitoTracker labeling (Fig. 4*B*). No significant changes were observed in the staining patterns of cytochrome *c* and mitochondria by 15 min (Fig. 4, *C* and *D*). By 30 min, most cytochrome *c* was clearly localized in the mitochondria (Fig. 4*E*), consistent with only very low levels of holocytochrome *c* release detected on Western blotting (see Fig. 3*A*). However, most mitochondria had lost the $\Delta\psi_m$ as indicated by the loss of MitoTracker labeling (Fig. 4*F*). Interestingly, nuclei were labeled by the MitoTracker dye starting from 30 min (compare Fig. 3*F* with *B* and *D*). Labeling with AlexaFluor-annexin V revealed similar degrees of low basal level apoptosis before and at 30 min (see Supplemental Material Fig. 2S, *A–F*). Consistent with Western blotting data (Fig. 3*A*), cytochrome *c* release became prominent by 1 h (Fig. 4*G*), when all mitochondria had lost the $\Delta\psi_m$ (Fig. 4*H*). Meanwhile, apoptosis significantly increased (Supplemental Material Fig. 2S, *G–H*). By 2 h, cytochrome *c* was completely released from mitochondria (Fig. 4*I*), fully consistent with the Western blotting data (Fig. 3*A*). MitoTracker labeling was barely detectable (Fig. 4*J*), and apoptosis became widespread (Supplemental Material Fig. 2S, *I* and *J*). By 4 h neither cytochrome *c* nor MitoTracker labeling could be seen (not shown). These fluorescence microscopy results provide direct confirmation of the Western blotting data and also indicate that loss of $\Delta\psi_m$ precedes holocytochrome *c* release from mitochondria. Similar changes in $\Delta\psi_m$ and holocytochrome *c* release were also observed in MDA-MB-231 cells treated with VP16 (not shown).

Loss of $\Delta\psi_m$ may result from opening of PTP, which in turn may be involved in cytochrome *c* release (10–12). To test this possibility, in the final set of experiments, we pretreated GM701 cells with cyclosporin A (CsA), which directly inhibits PTP (10–12), and NAC which indirectly inhibits PTP by blocking ROS generation (11, 12, 34), before apoptotic stimulation

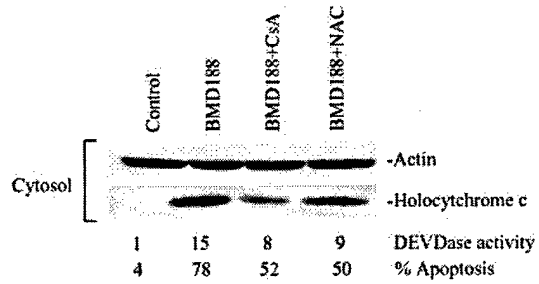

FIG. 5. **Inhibitors of PTP and ROS generation inhibits cytochrome *c* release, caspase activation, and apoptosis in GM701 cells treated with BMD188.** Cells were pretreated with CsA (5 μM) or NAC (1 μM) for 1 h, followed by addition of BMD188 (40 μM) for 2 h. Cytosolic fractions were prepared as described under "Materials and Methods," and 40 μg of proteins was used in Western blotting for holocytochrome *c* together with actin. The percentage of apoptotic cells was determined under a fluorescent microscope upon DAPI staining. DEVDase activity was measured using 40 μg of whole cell lysates. Data shown are representative of at least three independent experiments.

with BMD188. As shown in Fig. 5, both CsA and NAC partially inhibited holocytochrome *c* release, caspase activation, and apoptosis in GM701 cells.

Increased Transport of Cytosolic Cytochrome c into the Mitochondria Is Independent of MRC—The preceding experiments demonstrate that apoptosis induced by multiple stimuli is preceded by an up-regulation of cytochrome *c* synthesis and transport into the mitochondria. Normal cytochrome *c* transport into the mitochondria has been shown to be mediated by a unique mechanism that does not depend on mitochondrial respiration or $\Delta\psi_m$ (1, 53). To determine whether or not the continuously enhanced cytochrome *c* transport into the mitochondria during apoptosis depends on MRC or $\Delta\psi_m$, we employed two experimental strategies. In the first, we pretreated PC3 cells with tetracycline, which inhibits the mitochondrial protein synthesis and the MRC activity (1), prior to BMD188 treatment. As shown in Fig. 6*A*, inhibition of MRC function by tetracycline significantly delayed caspase activation, consistent with the previous observations (37) that BMD188-induced PC3 cell apoptosis requires MRC. Treatment with tetracycline also resulted in, as expected, the retention of most cytochrome *c* in the cytosol (Fig. 6*B*, *0 lane*), because the protein is not needed for the electron transport (1). Upon BMD188 treatment, a time-dependent translocation of cytosolic cytochrome *c* to mitochondria was still observed (Fig. 6*B*), suggesting that the BMD188-induced increase of cytochrome *c* transport to the mitochondria does not depend on MRC *per se*.

In the second strategy, we treated MRC-deficient ρ^0 PC3 cells (clone 6) (37) with BMD188. As in tetracycline-pretreated PC3 cells, the majority of cytochrome *c* in untreated ρ^0 PC3 cells was retained in the cytosol (Fig. 6*C*, *0 lane*). BMD188 treatment again induced a rapid translocation of cytosolic cytochrome *c* to the mitochondria (Fig. 6*C*). The accumulation of cytochrome *c* in the mitochondria reached peak level at ~4 h after BMD188 treatment, at which time increased caspase activation and apoptosis were observed (Fig. 6*C*). In wild-type, respiration-competent PC3 cells, 40 μM BMD188 induced maximum caspase activation and killed ~90% of the cells within 4 h (37). In contrast, BMD188 at the same dose induced similar levels of caspase activation and apoptosis in ρ^0 PC3 cells only after ~24 h treatment (Fig. 6*C*). Together with the tetracycline experiments, these observations suggest that the BMD188-induced cell death but not cytochrome *c* translocation to the mitochondria depends on the MRC function.

Up-regulation of Cytochrome c Alone Is Insufficient to Induce Apoptosis but Potentiates Cell Death by BMD188—To test whether increased cytochrome *c* synthesis and enrichment in

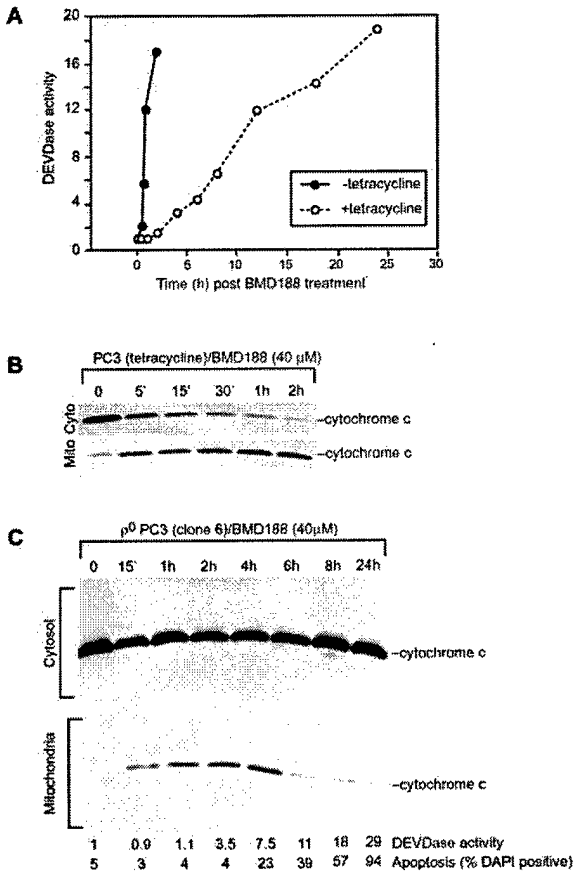

FIG. 6. **BMD188-induced PC3 cell apoptosis, but not BMD188-stimulated cytochrome *c* translocation to the mitochondria, depends on MRC.** *A*, tetracycline inhibits BMD188-induced caspase activation in PC3 cells. PC3 cells were pretreated with tetracycline (1 μg/ml) for 1 h and then treated with BMD188 (40 μM) in the presence of tetracycline. Whole cell lysates were prepared at the time points indicated and used to measure DEVDase activity. *B*, MRC-inhibited PC3 cells treated with tetracycline still show a time-dependent translocation of cytochrome *c* from cytosol to the mitochondria upon BMD188 treatment. Thirty μg/lane of the fractionated cytosolic or mitochondrial proteins (see "Materials and Methods") was used in Western blotting for cytochrome *c*. *C*, respiration-deficient ρ^0 PC3 (clone 6) cells (37) still show cytochrome *c* translocation to the mitochondria in response to BMD188 treatment. Thirty μg/lane of the fractionated cytosolic or mitochondrial proteins was used in Western blotting for cytochrome *c*. In the meantime, ρ^0 PC3 cells treated with BMD188 for the same time intervals were also used to measure DEVDase activity and apoptosis.

the mitochondria contribute to apoptosis induction, we transiently transfected GM701 cells with an expression plasmid encoding cytochrome *c*-GFP (cyt-c-GFP) fusion protein, which has been shown previously (51) to localize effectively to the mitochondria and to be released from the mitochondria during staurosporine-induced apoptosis. Twenty-four h after transfection, cells were treated with BMD188 for various lengths of time, followed by quantification of apoptotic nuclei in both GFP-positive as well as GFP-negative cells. As shown in Fig. 7*A*, GM701 cells transfected with the GFP alone (control vector) showed similar levels of apoptosis in both GFP^+ and GFP^- populations. In contrast, in GM701 cells transfected with the cyt-c-GFP, the BMD188-induced apoptosis was significantly enhanced (Fig. 7*A*). For example, 3 h after BMD188 treatment, >90% of the GFP^+ cells was apoptotic compared with ~60% of apoptosis in GFP^- cells (Fig. 7*A*).

The above results suggest that up-regulation of cytochrome *c* by enforced expression potentiated apoptosis induced by BMD188. To address whether up-regulation of cytochrome *c* is by itself sufficient to induce apoptosis, we used an ecdysone-

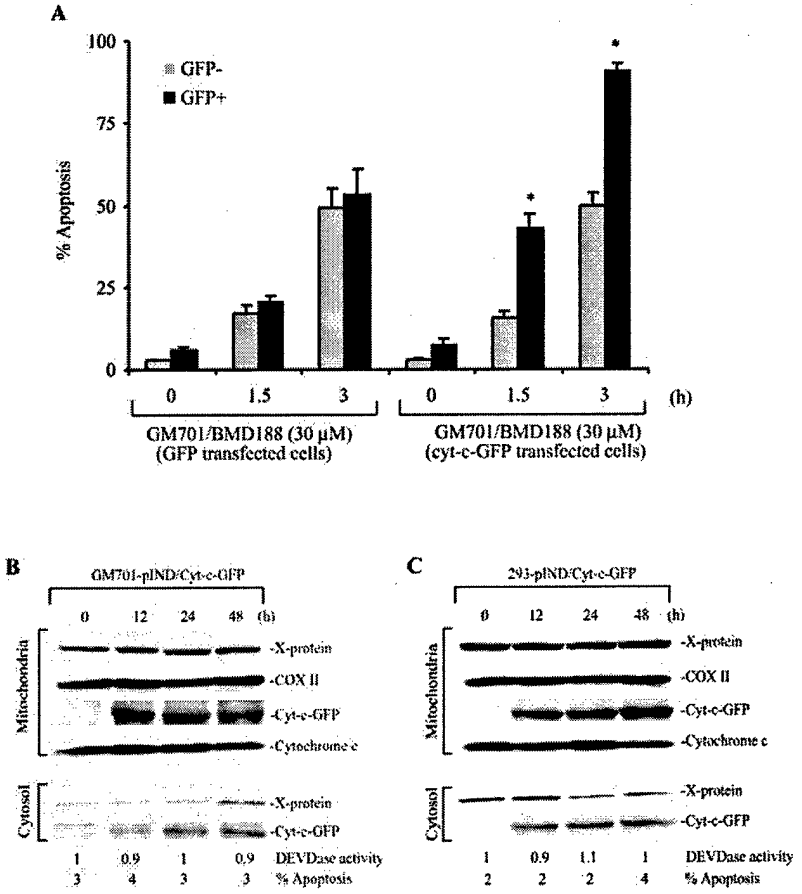

FIG. 7. Overexpression of cytochrome *c* enhanced BMD188 induced apoptosis (*A*) but cytochrome *c* overexpression by itself (*i.e.* without stimulation) is insufficient to trigger apoptosis (*B*). *A*, GM701 fibroblast cells were transfected with plasmids encoding GFP or cyt-c-GFP. Twenty four h later, cells were treated with BMD188 (30 μM) for the times indicated. Cells were labeled live with DAPI 15 min before the end of the treatment followed by fixation in 4% paraformaldehyde. Apoptosis was quantified by nuclear morphology. The results are presented as % of apoptosis in both GFP^+ or GFP^- cell populations. Values represent the mean ± S.D. from three separate experiments. *, significantly different ($p < 0.01$, Student's *t* test) compared with GFP^- cells. *B* and *C*, Western blot analysis of cytosolic and mitochondrial fractions from GM701-pIND/cyt-c-GFP (*B*) and 293-pIND/cyt-c-GFP (*C*) cells induced by ponasterone (2 μM) for the time intervals indicated. Twenty five μg/lane of proteins from each sample was separated by 15% SDS-PAGE. Following protein transfer, membranes were probed and reprobed with antibodies against COX II, cytochrome *c* (which recognizes only endogenous cytochrome *c* but not cyt-c-GFP), or GFP (which recognizes GFP or cyt-c-GFP). Apoptosis and DEVDase activity were determined as described under "Materials and Methods." Data presented are representative of three separate experiments.

inducible system to establish transcriptionally inducible cytochrome *c* in GM701 and 293 cells. Double stable clones of each cell type expressing inducible GFP or cyt-c-GFP in response to a ligand such as ponasterone were generated in two steps as detailed under "Materials and Methods." The resultant cells, *i.e.* GM701-pIND/GFP, GM701-pIND/cyt-c-GFP, 293-pIND/GFP, and 293-pIND/cyt-c-GFP cells, were treated with 2 μM ponasterone for various time intervals to induce the expression of GFP or cyt-c-GFP. As shown in Fig. 7, *B* and *C*, ponasterone induced a rapid induction of cyt-c-GFP, the majority of which, like endogenous cytochrome *c*, was localized in the mitochondria, whereas ponasterone-induced GFP alone was mainly localized in the cytosol (not shown). Ponasterone treatment did not affect the expression of endogenous cytochrome *c* or COX II (Fig. 7, *B* and *C*). Up-regulation of cyt-c-GFP in both GM701 (Fig. 7*B*) and 293 (Fig. 7*C*) cells did not lead to increased caspase activation or apoptosis.

In the above experiments, we utilized the cyt-c-GFP fusion protein, which, although being able to correctly target to the mitochondria (see Ref. 51; data not shown), might not be fully functional as an electron carrier in the MRC because of the presence of the GFP tag. To exclude this possibility, we made a new expression construct, pCMS-EGFP/cyt-c, in which the human cytochrome *c* (without any tag) and the EGFP are independently synthesized from two separate promoters (see "Materials and Methods"). In this way, cytochrome *c* and GFP are made as two separate proteins. By using this vector, we carried out experiments similar to those in Fig. 7, *B* and *C*. As shown in Supplemental Material Fig. 3S, as early as 24 h after transient transfection of pCMS-EGFP/cyt-c, the cytochrome *c* level was significantly up-regulated (~4-fold) only in the mitochondria, compared with untransfected cells or cells transfected with the empty vector. As expected, GFP was detected

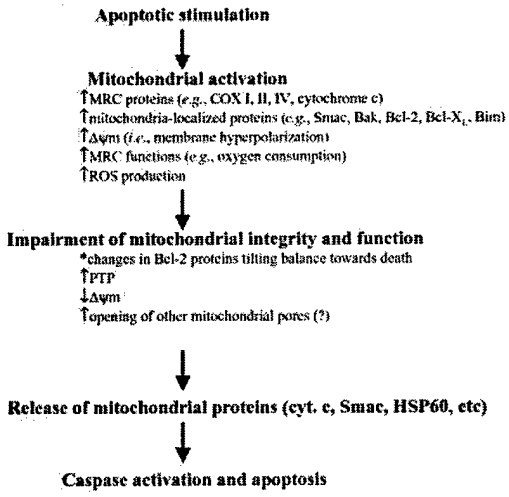

FIG. 8. **A scheme illustrating the sequence of events in MADAP, highlighting the potentially critical role of early mitochondrial activation in causing subsequent mitochondrial dysfunction and cytochrome *c* release.**

only in the cytosol of the transfected cells (Fig. 3S). Because the up-regulated cytochrome *c* was detected only in the mitochondria, it is reasonable to think that this exogenous cytochrome *c*, just like the endogenous protein, should be functional in participating in MRC electron relays. Nevertheless, there was no significantly increased cell death at 24 (Fig. 3S) to 72 h (not shown) after the transfection. Together, this set of experiments provides independent supporting evidence that up-regulation of cytochrome *c* alone is insufficient in inducing apoptosis.

DISCUSSION

Up-regulation of MRC Proteins and Mitochondrial Activation Early during Apoptosis Induction—Our previous studies (37) and the present work show that apoptosis induced by multiple stimuli is temporally preceded by an early induction of MRC proteins such as cytochrome *c* and COX II. For example, induction of cytochrome *c* and COX II mRNAs and proteins in GM701 cells treated with BMD188 occurs within 10 min (Fig. 1*B* and 2*A*), preceding caspase activation and death, which becomes detectable at 30 min to 1 h (Figs. 1*B* and 3; Supplemental Material Fig. 2S). Similarly, up-regulated cytochrome *c* and COX II mRNAs and proteins in MDA-MB231 cells treated with VP16 occur much earlier than caspase activation and apoptosis (Figs. 1*C* and 2). Recent work by others has also revealed increased expressions of cytochrome *c* and COX II preceding cell death in Jurkat cells treated with camptothecin (57) or breast cancer cells treated with teniposide (58). The increased cytochrome *c* and COX II proteins in these apoptotic model systems appear to result from the transcriptional activation of the respective genes, as illustrated in BMD188-treated GM701 cells (Fig. 2*A*) and VP16-treated MDA-MB231 cells (Fig. 2*B*). Because COX II is encoded by the mitochondrial genome and cytochrome *c* the nuclear genome, these observations suggest that the MRC components encoded by both genomes are coordinately induced early in apoptotic signal transduction by these stimuli. In support, two other MRC proteins, COX I and COX IV, also encoded by the mitochondrial and nuclear genomes, respectively (1), are similarly up-regulated during apoptosis induced by BMD188 (37), camptothecin (57), and teniposide (58).

Why should cells up-regulate these MRC proteins in response to apoptotic stimuli of diverse mechanisms of action (see Refs. 37, 57, and 58; this study)? Multiple pieces of evidence suggest that the up-regulation of MRC proteins may represent one aspect of a more global mitochondrial activation response (Fig. 8). First, not only MRC proteins but also many mitochondrially localized, non-MRC proteins are up-regulated. For example, in BMD188-induced GM701 cell death, Bcl-2 family proteins Bim, Bak, and Bcl-2 as well as Smac, all encoded by the nuclear genes and normally localized exclusively in the mitochondria, are up-regulated (Fig. 3, *D* and *E*). Similarly, both Bim and Bcl-2 are also induced in serum-starved LNCaP cells and VP16-treated MDA-MB231 cells.[2] Second, apoptosis induced by many of these apoptotic stimuli exemplified by BMD188 (37), camptothecin (57), staurosporine (13), Fas (59), and Mn(II) (38) is preceded by an early hyperpolarization of the $\Delta\psi_m$ (Fig. 8), thus indicative of enhanced electron transport and MRC activity. Third, these inducers rapidly up-regulate the oxygen consumption capacity of the cells (*e.g.* 37, 57, 58) or COX activity (35), suggesting that the up-regulated MRC components are functionally participating in the electron transport. Finally, mitochondria represent the primary site of ROS generation in the cells, and enhanced MRC activity is generally accompanied by increased ROS production (5–7). Indeed, increased ROS generation has been observed early in apoptosis induced by most of these stimuli including TNF-α, Fas, BMD188, nordihydroguaiaretic acid, camptothecin, Fas, Mn(II), retinoid CD437, ceramide, short chain fatty acids, hypoxia, and deprivation (31–43, 57–59). Altogether, these observations suggest that one of the common events in apoptosis induced by a wide spectrum of stimuli is early mitochondrial activation manifested as increased synthesis of mitochondrially localized (both MRC and non-MRC) proteins and increased $\Delta\psi_m$, oxygen consumption, and ROS production (Fig. 8).

This early mitochondrial activation could represent a defensive response of cells to various stresses. However, the fact that cells lacking a functional MRC (*i.e.* ρ^0 cells) or cells with deficient MRC function due to either chemical blocking or genetic mutation/deletion of individual respiratory proteins are often resistant to apoptosis induction (31–43) (Supplemental Material Fig. 1S; see discussion in Introduction) strongly suggests that the MRC and early mitochondrial activation are also causally involved in apoptosis induction (see below). In this sense, apoptosis triggered by the stimuli that cause early mitochondrial activation and require the mitochondrial activation for the apoptotic effect can be called mitochondrial activation-dependent apoptotic pathway or MADAP.

Importance of Early Mitochondrial Activation and Cytochrome c Up-regulation in MADAP—How might early mitochondrial activation contribute to apoptosis induction? We shall address this question later in the context of cytochrome *c* release. However, a detailed look at the potential role of cytochrome *c* movement in BMD188-induced GM701 cell death may shed some light on this question. Early upon stimulation the apoptotic signals rapidly up-regulate cytochrome *c*, some of which translocates to the mitochondria. As the increased cytochrome *c* synthesis in the cytosol and transport into the mitochondria continue and intensify, holocytochrome *c* is gradually released from the mitochondria into the cytosol to initiate apoptosome formation. Remarkably, increased cytochrome *c* synthesis and transport are still observed even when holocytochrome *c* is nearly completely released from the mitochondria (Figs. 1*B*, 2*A*, and 3*A*). Therefore, cytochrome *c* undergoes cyclic changes in this apoptotic model, *i.e.* increased apocytochrome *c* synthesis in the cytosol → increased apocytochrome *c* transport into the mitochondria → increased holocytochrome *c* accumulation in the mitochondria → increased holocytochrome *c* release into the cytosol → the whole cycle continues until all holocytochrome *c* is released from the mitochondria and until mitochondria no longer have the ability to convert up-regulated apocytochrome *c* to holocytochrome c.

Several pieces of evidence suggest that the increased cytochrome *c* translocation to and its accumulation in the mitochondria might contribute to apoptosis induction. First, in all the cases studied, the translocation of cytochrome *c* to and its accumulation in the mitochondria occur prior to caspase activation and cell death (Fig. 1, *A–E* and data not shown). Second, in ρ^0 and tetracycline-treated PC3 cells, although cytochrome *c* translocation still occurs, its peak accumulation in the mitochondria is delayed, *i.e.* from ~1 to 2–4 h (37) (Fig. 6, *B* and *C* of this work). In the meantime, caspase activation as well as cell death are also delayed (Fig. 6; 37). Third, inhibition of *de novo* mRNA synthesis by A/D or protein synthesis by CHX inhibits BMD188 and VP16-induced up-regulation in COX II and cytochrome *c* as well as apoptosis (Fig. 2). Although A/D and CHX may likely affect many other gene and protein targets, it is reasonable to think that their inhibitory effects on cytochrome *c* up-regulation, at least partially, contribute to their inhibition of apoptosis. Finally, enforced overexpression of exogenous cytochrome *c*, which also rapidly translocates to the mitochondria (not shown), significantly potentiates apoptosis (Fig. 7*A*). Interestingly, simply up-regulating cytochrome *c* expression is insufficient to trigger apoptosis; in the absence of an apoptotic inducer, up-regulated cytochrome *c* does not increase spontaneous cell death (Fig. 7, *B* and *C*; Supplemental Material Fig. 3S). These observations suggest that the accumulation of cytochrome *c* in the mitochondria may represent only one of the apoptosis-initiating factors and that it is the combination of many factors during mitochondrial activation that eventually leads to mitochondrial dysfunction, cytochrome *c* release, and caspase activation (see below).

How is the newly synthesized cytochrome *c* transported into

the mitochondria during MADAP? Normally, most cytochrome *c*, upon synthesis, is immediately transported to the mitochondria in which the protein turns into holocytochrome *c* as the result of binding to the heme group, and this transport process utilizes a unique import pathway that does not depend on the MRC or $\Delta\psi_m$ (1, 53). Likewise, the increased transport of cytochrome *c* to the mitochondria in BMD188-induced PC3 cell death does not depend on the MRC or $\Delta\psi_m$, as it also occurs in ρ^0 cells or when MRC is inhibited by tetracycline (Fig. 6). In support of this conclusion, increased cytochrome *c* accumulation in the mitochondria is still observed long after the mitochondria have lost the $\Delta\psi_m$ (compare Figs. 1*B*, 3*A*, and 4).

Our observation that cytochrome *c* can be transcriptionally up-regulated leading to increased apocytochrome *c* proteins in the cytosol has a practical implication. In the literature, frequently only the increased cytosolic cytochrome *c* levels are shown, and this is used as evidence of cytochrome *c* release from the mitochondria. Without using an antibody that specifically recognizes the holocytochrome *c* (Table I) and without demonstrating correspondingly decreased mitochondrial cytochrome *c*, however, it will be unable to distinguish whether the increased cytochrome *c* in the cytosol results from mitochondrial release or from the transcriptional up-regulation of the gene.

How Might Cytochrome c Be Released during MADAP?—The apoptogenic holocytochrome *c* is normally sequestered in the mitochondrial intermembrane space. The outer mitochondrial membrane (OMM) has a limited permeability allowing the passage of molecules <1.5 kDa, and the inner mitochondrial membrane (IMM) is essentially impermeable. Although still highly debatable, three major models have been proposed to explain how cytochrome *c* might be released from the mitochondria during apoptosis (60). In the first, proapoptotic Bcl-2 family proteins, Bax and Bak in particular, directly form pores on OMM to release selectively cytochrome *c* without major effects on mitochondrial function (61–63). In the second model, apoptotic signals open the PTP resulting in the loss of $\Delta\psi_m$ and swelling of the mitochondrial matrix, which causes eventual OMM rupture, nonselective OMM permeabilization, and cytochrome *c* release (63–65). In the third model, apoptotic signaling evokes the opening of a voltage-independent megapore termed MAC (mitochondria apoptosis-induced channel) (66). MAC is distinct from PTP in that it does not have voltage-dependent anion channel (VDAC, located in OMM) as a component, and it displays multiple conductance levels, with a peak single channel opening of ~2.5 nS, corresponding to a pore diameter of ~4.5 nm (66). Therefore, MAC is significantly bigger than the Bax/Bak channel or PTP (66).

None of these models alone seems to be able to explain completely how cytochrome *c* might be released during MADAP. Instead, dynamic changes in Bcl-2 family proteins, opening of PTP and loss of $\Delta\psi_m$, and opening of much larger pores (that can allow the release of HSP60 from the matrix) all seem to be involved. For example, in BMD188-induced GM701 cell death, all three BH3 domain-only proteins, *i.e.* Bim, Bad, and Bid, are activated; Bim is up-regulated transcriptionally (Fig. 3*D* and data not shown); Bad rapidly translocates to the mitochondria, and Bid is cleaved late during apoptosis (Fig. 3*D*). In contrast, the multidomain Bcl-2 proteins show complex alterations; both Bcl-x_L and Bcl-2 are induced and concentrated in the mitochondria, and Bak is induced whereas Bax is reduced early during apoptosis induction (Fig. 3*D*). Similar alterations such as rapid induction of Bim mRNA and protein have also been observed in MDA-MB231 cells treated with VP16 and LNCaP cells subjected to serum starvation.[2] Because the Bcl-2 proteins normally function in the mitochondria to maintain the organelle integrity and functional homeostasis (26, 55, 63, 64, 67), these dynamic changes may reflect the life-and-death "battle" among these proteins. Thus, it is possible that, as Bim and Bad are activated and Bak is induced, Bax is down-regulated, and prosurvival Bcl-2 and Bcl-x_L are up-regulated in order to prolong the cell survival. As apoptotic stimulation continues, more Bim and Bak are induced, and more Bad is translocated to the mitochondria, tilting the balance toward cell death. In this scenario, cytochrome *c* might be released through the Bax/Bak channel (as a significant amount of Bax is always present in the mitochondria) or through Bak alone, which has been shown recently (68) to play a critical role in mediating cytochrome *c* release in anticancer drug-induced apoptosis.

The Bax/Bak pores are small (0.5 nS; 66) and are thought to release selectively cytochrome *c* without significantly affecting mitochondrial parameters such as membrane permeability and matrix volume (61–63). In apoptosis induced by BMD188 (37) and many other stimuli (*e.g.* see Refs. 13, 38, 57, and 59), there is an early IMM hyperpolarization and increased $\Delta\psi_m$ followed by subsequent loss of $\Delta\psi_m$. Furthermore, at least in the case of BMD188-induced GM701 cell death, proteins much larger than cytochrome *c* (*i.e.* 25-kDa Smac and 60-kDa HSP60) are also released from mitochondria. Together, these observations suggest that cytochrome *c* release in these apoptotic systems may involve opening of PTP or MAC or some other pores in addition to Bcl-2 family proteins (Fig. 8). The supporting evidence comes from the loss of the $\Delta\psi_m$ at 30 min when the majority of cytochrome *c* in most cells is still in the organelle (Fig. 4), suggesting PTP opening prior to cytochrome *c* release. More importantly, BMD188-induced cytochrome *c* release and subsequent caspase activation and cell death in GM701 cells can be inhibited by CsA, which inhibits cyclophilin D, an important component of the PTP, as well as by NAC, which indirectly inhibits PTP (11, 12). The inhibitory effect of NAC also suggests ROS production by BMD188, as observed previously (37). It is interesting to note that the patterns of cytochrome *c* release and Smac are very similar (Fig. 3, *A* and *D*), suggesting that these two intermembrane proteins may utilize the same (or similar) channel or pore for their exodus. Surprisingly and intriguingly, the matrix protein HSP60 is maximally released into the cytosol much earlier, at a time when cytochrome *c*/Smac release has just started (see Fig. 3, *A* and *D*). These differential release kinetics suggest the following: 1) the release of these individual proteins is specific, which cannot be accounted for by nonspecific rupture of OMM; and 2) different channels or pores are probably utilized to release different proteins.

It is noteworthy that Bim is rapidly and commonly induced in the three MADAP systems we examined in detail, *i.e.* BMD188-treated GM701 cells (this study), serum-deprived LNCaP cells,[2] and VP16-treated MDA-MB231 cells,[3] suggesting that this may be the key BH3-only molecule in initiating MADAP. Interestingly, Bim has been shown recently to induce both Bax/Bak-dependent and Bax/Bak-independent cytochrome *c* release (69). In the latter mechanism, Bim directly interacts with VDAC and triggers VDAC-dependent cytochrome *c* release (69). Because VDAC is an integral component of PTP and also forms pores with Bax (63–65), which in turn seems to be part of the MAC (66), it is possible that all these proteins together form very dynamic pores/channels of different sizes and selectivity at the contact sites of IMM and OMM, which are opened by BH3-only proteins such as Bim and closed by anti-apoptotic proteins such as Bcl-2 and Bcl-x_L.

In summary, our data presented herein, together with other

[3] D. Chandra, J.-W. Liu, and D. G. Tang, unpublished observations.

data (31–45, 57, 58) suggest the apoptotic model presented in Fig. 8. In response to a wide diversity of apoptotic stimuli, cells immediately wage a defensive response characterized by mitochondrial activation, manifested by rapid up-regulations of multiple MRC proteins and enhanced MRC activities such as oxygen consumption. In the meantime, Bcl-2 proteins undergo dynamic alterations in attempt to keep the cells alive. In the persistent apoptotic stimulation, the increasing ROS production as a result of continuously increased MRC activation and cytochrome *c* accumulation in the mitochondria results in the opening of PTP and/or other pores and loss of $\Delta\psi_m$, which, together with more pro-apoptotic changes in the Bcl-2 family proteins, leads to the release of holocytochrome *c* and, subsequently, activation of caspases.

Acknowledgments—We thank Dr. A.-L. Nieminen for providing pEGFP-cytochrome *c*; Dr. T.-J. Liu for pIND-GFP; Dr. M. Bedford for EcR-293 cells; Dr. M. King for 143B, 143B206, and GM701.2-8C cells; Dr. A. Porter at Biomide Corp., for BMD188; Drs. K. Kiguchi and K. Klaypool for help in fluorescence microscopy; T. Higgins and Y. Yonekawa for technical assistance; and members of the Tang laboratory for helpful discussions. We are also grateful to Dr. X. Wang for antibodies against Smac and tBid.

REFERENCES

1. Poyton R. O., and McEwen, J. E. (1996) *Annu. Rev. Biochem.* **65,** 563–607
2. Eguchi, Y., Shimizu, S., and Tsujimoto, Y. (1997) *Cancer Res.* **57,** 1835–1840
3. Leist, M., Single, B., Castoldi, A. F., Kuhnle, S., and Nicotera, P. (1997) *J. Exp. Med.* **185,** 1481–1486
4. Formigli, L., Papucci, L., Tani, A., Schiavone, N., Tempestini, A., Orlandini, G. E., Capaccioli, S., and Orlandini, S. Z. (2000) *J. Cell. Physiol.* **182,** 41–49
5. Lotem, J., Peled-Kamar, M., Groner, Y., and Sachs, L. (1996) *Proc. Natl. Acad. Sci. U. S. A.* **93,** 9166–9171
6. Um, H.-D., Orensteine, J. M., and Wahl, S. M. (1996) *J. Immunol.* **156,** 3469–3477
7. Tan, S., Sagara, Y., Liu, Y., Maher, P., and Schubert, D. (1998) *J. Cell Biol.* **141,** 1423–1432
8. Richter, C. (1993) *FEBS Lett.* **325,** 104–107
9. Gunter, T. E., Gunter, K. K., Sheu, S. S., and Gavin, C. E. (1994) *Am. J. Physiol.* **267,** C313–C339
10. Zamzami, N., Marchetti, P., Castedo, M., Zanin, C., Vayssiere, J.-L., Petit, P. X., and Kroemer, G. (1995) *J. Exp. Med.* **181,** 1661–1672
11. Zarotti, M., and Szabo, I. (1995) *Biochim. Biophys. Acta* **1241,** 139–179
12. Marzo, I., Brenner, C., Zamzami, N., Susin, S. A., Beutner, G., Brdiczka, D., Remy, R., Xie, Z.-H., Reed, J. C., and Kroemer, G. (1998) *J. Exp. Med.* **187,** 1261–1271
13. Vander-Heiden, M. G., Chandel, N. S., Williamson, E. K., Schumacker, P. T., and Thompson, C. B. (1997) *Cell* **91,** 627–637
14. Liu, X., Kim, C. N., Yang, J., Jemmerson, R., and Wang, X. (1996) *Cell* **86,** 147–157
15. Kluck, R. M., Martin, S. J., Hoffman, B. M., Zhou, J. S., Green, D. R., and Newmeyer, D. D. (1997) *EMBO J.* **16,** 4639–4649
16. Susin, S. A., Lorenzo, H. K., Zamzami, N., Marzo, I., Snow, B. E., Brothers, G. M., Mangion, J., Jacotot, E., Costantini, P., Loeffler, M., Larochette, N., Goodlett, D. R., Aebersold, R., Siderovski, D. P., Penninger, J. M., and Kroemer, G. (1999) *Nature* **397,** 441–446
17. Du, C., Fang, M., Li, Y., Li, L., and Wang, X. (2000) *Cell* **102,** 33–42
18. Verhagen, A. M., Ekert, P. G., Pakusch, M., Silke, J., Connolly, L. M., Reid, G. E., Moritz, R. L., Simpson, R. J., and Vaux, D. L. (2000) *Cell* **102,** 43–53
19. Suzuki, Y., Imai, Y., Nakayama, H., Takahashi, K., Takio, K., and Takahashi, R. (2001) *Mol. Cell* **8,** 613–621
20. Verhagen, A. M., Silke, J., Ekert, P. G., Pakusch, M., Kaufmann, H., Connolly, L. M., Day, C. L., Tikoo, A., Burke, R., Wrobel, C., Moritz, R. L., Simpson, R. J., and Vaux, D. L. (2002) *J. Biol. Chem.* **277,** 445–454
21. Hegde, R., Srinivasula, S. M., Zhang, Z., Wassell, R., Mukattash, R., Cilenti, L., DuBois, G., Lazebnik, Y., Zervos, A. S., Fernandes-Alnemri, T., and Alnemri, T. (2002) *J. Biol. Chem.* **277,** 432–438
22. Martins, L. M., Iaccarino, I., Tenev, T., Gschmeissner, S., Totty, N. F., Lemoine, N. R., Savopoulos, J., Gray, C. W., Creasy, C L.,. Dingwall, C., and Downward, J. (2002) *J. Biol. Chem.* **277,** 439–444
23. Li, L. Y., Luo, X., and Wang, X. (2001) *Nature* **412,** 95–99
24. Mancini, M., Nicholson, D. W., Roy, S., Thornberry, N. A., Peterson, E. P., Casciola-Rosen, L. A., and Rosen, A. (1998) *J. Cell Biol.* **140,** 1485–1495
25. Susin, S. A., Lorenzo, H. K., Zamzami, N. Marzo, I., Brenner, C., Larochette, N., Prevost, M. C., Alzari, P. M., and Kroemer, G. (1998) *J. Exp. Med.* **189,** 381–394
26. Wang, X. (2001) *Genes Dev.* **15,** 2922–2933
27. Ashkenazi, A., and Dixit, V. M. (1998) *Science* **281,** 1305–1308
28. Li, H., Zhu, H., Xu, C.-J., and Yuan, J. (1998) *Cell* **94,** 491–501
29. Luo, X., Budihardjo, I. Zou, H., Slaughter, C., and Wang, X. (1998) *Cell* **94,** 481–490
30. Deng, Y., Lin, Y., and Wu, X. (2002) *Genes Dev.* **16,** 33–45
31. Schultze-Osthoff, K., Beyaert, R., Vandevoorde, V., Haegeman, G., and Fiers, W. (1993) *EMBO J.* **12,** 3095–3104
32. Higuchi, M., Aggarwal, B. B., and Yeh, E. T. H. (1997) *J. Clin. Invest.* **99,** 1751–1758
33. Deshpande, S. S., AngKeow, P., Huang, J., Ozaki, M., and Iran, K. (2000) *FASEB J.* **14,** 1705–1714
34. Tang, D. G., and Honn, K. V. (1997) *J. Cell. Physiol.* **172,** 155–170
35. Heerdt, B. G., Houston, M. A., and Augenlicht, L. H. (1997) *Cell Growth Differ.* **8,** 523–532
36. Quillet-Mary, A., Jaffrezou, J.-P., Mansat, V., Bordier, C., Naval, J., and Laurent, G. (1997) *J. Biol. Chem.* **272,** 21388–21395
37. Joshi, B., Li, L., Taffe, B. G., Zhu. Z., Wahl, S., Tian, H., Ben-Josef, E., Taylor, J. D., Porter, A. T., and Tang, D. G. (1999) *Cancer Res.* **59,** 4343–4355
38. Oubrahim, H., Stadtman, E. R., and Chock, P. B. (2001) *Proc. Natl. Acad. Sci. U. S. A.* **98,** 9505–9510
39. Hail, N. Jr., Youssef, E. M., and Lotan, R. (2001) *Cancer Res.* **61,** 6698–6702
40. McClintock, D. S., Santore, M. T., Lee, V. Y., Brunelle, J., Budinger, G. R., Zong, W. X., Thompson, C. B., Hay, N., and Chandel, N. S. (2002) *Mol. Cell. Biol.* **22,** 94–104
41. Sestili, P., Brambilla, L., and Cantoni, O. (1999) *FEBS Lett.* **457,** 139–143
42. Dumont, A., Hehner, S. P., Hofmann, T. G., Ueffing, M., Droge, W., and Schmitz, M. L. (1999) *Oncogene* **18,** 747–757
43. Chauvin, C., De Oliveira, F., Ronot, X., Mousseau, M., Leverve, X., and Fontaine, E. (2001) *J. Biol. Chem.* **276,** 41394–41398
44. Kataoka, A., Kubota, M., Watanabe, K., Sawada, M., Koishi, S., Lin, W. W., Usami, I., Akiyama, V., Kitoh, T., and Furusho, K. (1997) *Cancer Res.* **57,** 5243–5245
45. Matsuyama, S., Xu, Q., Velours, J., and Reed, J. C. (1998) *Mol. Cell* **1,** 327–336
46. King, M. P., and Attardi, G. (1989) *Science* **246,** 500–503
47. Tang, D. G., Li, L., Zhu, Z., and Joshi, B. (1998) *Biochem. Biophys. Res. Commun.* **242,** 380–384
48. Liu, J.-W., Chandra, D., Tang, S.-H., Chopra, D., and Tang, D. G. (2002) *Cancer Res.* **62,** 2976–2981
49. Tang, D. G., Li, L., Chopra, D. P., and Porter, A. T. (1998) *Cancer Res.* **58,** 3466–3479
50. Tang, D. G., Tokumoto, Y. M., and Raff, M. C. (2000) *J. Cell Biol.* **148,** 971–984
51. Heiskanen, K. M., Bhat, M. B., Wang, H.W., Ma, J., and Nieminen, A.-L. (1999) *J. Biol. Chem.* **274,** 5654–5658
52. Yang, J., Liu, X., Bhalla, K., Kim, C. N., Ibrado, A. M., Cai, J., Peng, T.-I., Jones, D. P., and Wang, X. (1997) *Science* **275,** 1129–1132
53. Stuart, R. A., and Neupert, W. (1990) *Biochimie (Paris)* **72,** 115–121
54. Jemmerson, R., LaPlante, B., and Treeful, A. (2002) *Cell Death Differ.* **9,** 538–548
55. Ranger, A. M., Malynn, B. A., and Korsmeyer, S. J. (2001) *Nat. Genet.* **28,** 113–118
56. Xanthoudakis, S., Roy, S., Rasper, D., Hennessey, T., Aubin, Y., Cassady, R., Tawa, P., Ruel, R., Rosen, A., and Nicholson, D. W. (1999) *EMBO J.* **18,** 2049–2056
57. Sanchez-Alcazar, J., Ault, J. G., Khodjakov, A., and Schneider, E. (2000) *Cell Death Differ.* **7,** 1090–1100
58. Sanchez-Alcazar, J., Khodjakov, A., and Schneider, E. (2001) *Cancer Res.* **61,** 1038–1044
59. Banki, K., Hutter, E., Gonchoroff, N. J., and Perl, A. (2000) *J. Immunol.* **162,** 1466–1479
60. Degterev, A., Boyce, M., and Yuan, J. (2001) *J. Cell Biol.* **155,** 695–697
61. Wei, M. C., Zong, W. X., Cheng, E. H., Lindsten, T., Panoutsakopoulou, V., Ross, A. J., Roth, K. A., MacGregor, G. R., Thompson, C. B., and Korsmeyer, S. J. (2001) *Science* **292,** 727–730
62. Waterhouse, N. J., Goldstein, J. C., von Ahsen, O., Schuler, M., Newmeyer, D. D., and Green, D. R. (2001) *J. Cell Biol.* **153,** 319–328
63. Harris, M. H., and Thompson, C. B. (2000) *Cell Death Differ.* **7,** 1182–1191
64. Zamzami, N., and Kroemer, G. (2001) *Nat. Rev. Mol. Cell. Biol.* **2,** 67–71
65. Shimizu, S., Ide, T., Yanagida, T., and Tsujimoto, Y. (2000) *J. Biol. Chem.* **275,** 12321–12325
66. Pavlov, E. V., Priault, M., Pierkiewicz, D., Cheng, E. H.-Y., Antonsson, B., Manon, S., Korsmeyer, S. J., Mannella, C. A., and Kinnally, K. W. (2001) *J. Cell Biol.* **155,** 719–724
67. Cheng, E. H., Wei, M. C., Weiler, S., Flavell, R. A., Mak, T. W., Lindsten, T., and Korsmeyer, S. J. (2001) *Mol. Cell* **8,** 705–711
68. Wang, G.-Q., Gastman, B. R., Wieckoski, E., Goldstein, L. A., Gambotto, A., Kim, T.-H., Fang, B., Rabinovitz, A., Yin, X.-M., and Rabinowich, H. (2001) *J. Biol. Chem.* **276,** 34307–34317
69. Sugiyama, T., Shimizu, S., Matsuoka, Y., Yoneda, Y., and Tsujimoto, Y. (2002) *Oncogene* **21,** 4944–4956

THE JOURNAL OF BIOLOGICAL CHEMISTRY
Vol. 278, No. 19, Issue of May 9, pp. 17408–17420, 2003
Printed in U.S.A.

Mitochondrially Localized Active Caspase-9 and Caspase-3 Result Mostly from Translocation from the Cytosol and Partly from Caspase-mediated Activation in the Organelle

LACK OF EVIDENCE FOR Apaf-1-MEDIATED PROCASPASE-9 ACTIVATION IN THE MITOCHONDRIA*

Received for publication, January 22, 2003
Published, JBC Papers in Press, February 28, 2003, DOI 10.1074/jbc.M300750200

Dhyan Chandra‡ and Dean G. Tang§

From the Department of Carcinogenesis, University of Texas MD Anderson Cancer Center, Science Park Research Division, Smithville, Texas 78957

Active caspase-9 and caspase-3 have been observed in the mitochondria, but their origins are unclear. Theoretically, procaspase-9 might be activated in the mitochondria in a cytochrome *c*/Apaf-1-dependent manner, or activated caspase-9 and -3 may translocate to the mitochondria, or the mitochondrially localized procaspases may be activated by the translocated active caspases. Here we present evidence that the mitochondrially localized active caspase-9 and -3 result mostly from translocation from the cytosol (into the intermembrane space) and partly from caspase-mediated activation in the organelle rather than from the Apaf-1-mediated activation. Apaf-1 localizes exclusively in the cytosol and, upon apoptotic stimulation, translocates to the perinuclear area but not to the mitochondria. In most cases, the mitochondrially localized procaspase-9 and -3 are released early during apoptosis and translocate to the cytosol and/or perinuclear area. Cytochrome *c* and the mitochondrial matrix protein Hsp60 are also rapidly released to the cytosol early during apoptosis. Both the early release of proteins like cytochrome *c* and Hsp60 from the mitochondria as well as the later translocation of the active caspase-9/-3 are partially inhibited by cyclosporin A, an inhibitor of mitochondrial membrane permeabilization. The mitochondrial active caspases may function as a positive feedback mechanism to further activate other or residual mitochondrial procaspases, degrade mitochondrial constituents, and disintegrate mitochondrial functions.

Apoptosis plays an essential role in animal development and in maintaining the homeostasis of adult tissues (1). The family of caspases (cysteine aspartic acid-specific protease) is the key effector in the execution of apoptotic cell death (2). Caspases are synthesized as inactive proenzymes, which become proteolytically cleaved during apoptosis to generate active enzymes. The active caspases cleave cellular proteins such as poly(ADP-ribose) polymerase (PARP)[1] to dismantle the apoptotic cells (3). The exact mechanism(s) whereby various caspases become activated are still unclear. Two pathways leading to caspase activation are relatively better understood. In the first pathway, apoptotic stimuli cause the release of cytochrome *c* (cyt. c) from the intermembrane space (IMS) of the mitochondria to the cytosol. The released cyt. c binds to and activates the adaptor protein Apaf-1, which in turn activates the initiator procaspase-9 in the presence of ATP, leading to the formation of apoptosome and subsequent activation of "executioner" caspases such as caspase-3, -6, or -7 (4). In the second pathway, the FADD/TRADD adaptor proteins recruit the initiator procaspase-8 (or -10) to cell surface death receptors, leading to death receptor-induced signaling complex formation, caspase-8 activation, and, subsequently, activation of executioner caspases (5). Recent evidence also implicates caspase-2 activation upstream of the cyt. c/Apaf-1 apoptosome-initiated apoptosis (6–10) or cyt. c/Apaf-1-independent apoptotic pathways (11–13).

Apart from their cytosolic residence, procaspases are also localized in other subcellular compartments. For example, procaspase-2 has been found in the Golgi apparatus and nucleus (14, 15). Procaspase-12 is mainly expressed in the endoplasmic reticulum where it serves as a major sensor of local stress (16). Depending on cell types, procaspase-2 (17), procaspase-3 (18, 19), procaspase-8 (20), and procaspase-9 (17, 21) have been reported to be present in the IMS of the mitochondria. Active caspases have also been found in different subcellular compartments. For example, in response to tumor necrosis factor-α, procaspase-1 translocates to the nucleus where it is proteolytically activated (22, 23). Upon treatment with tunicamycin, some activated caspase-12 translocates to or around the nuclei of apoptotic cells (24). In some experimental systems, the mitochondrially localized procaspase-2 and -3, upon activation, translocate to the nucleus (14, 15, 17). Activated caspase-7 has been shown to be associated exclusively with the mitochondrial/microsomal fractions (25). Activated forms of caspase-2 and caspase-9 have been detected in the mitochondria (17). Acti-

* This work was supported in part by NCI Grant CA 90297 and NIEHS Center Grant ES07784 from the National Institutes of Health and by institutional grants from the University of Texas MD Anderson Cancer Center. The costs of publication of this article were defrayed in part by the payment of page charges. This article must therefore be hereby marked "*advertisement*" in accordance with 18 U.S.C. Section 1734 solely to indicate this fact.

‡ Supported by Department of Defense Postdoctoral Traineeship Award DAMD17-02-1-0083.

§ To whom correspondence should be addressed: Dept. of Carcinogenesis, University of Texas MD Anderson Cancer Center, Science Park Research Division, Park Rd. 1C, Smithville, TX 78957. Tel.: 512-237-9575; Fax: 512-237-2475; E-mail: dtang@sprd1.mdacc.tmc.edu.

[1] The abbreviations used are: PARP, poly(ADP-ribose) polymerase; AFC, 7-amino-4-trifluoromethylcoumarin; Apaf-1, apoptotic protease-activating factor-1; BMD188, a hydroxamic acid compound; cyt. c, cytochrome *c*; CsA, cyclosporin A; DAPI, 4′,6-diamidino-2-phenylindole; IMS, intermembrane space; MADAP, mitochondrial activation-dependent apoptotic pathway; MMP, mitochondrial membrane permeabilization; MRC, mitochondrial respiratory chain; OMM, outer mitochondrial membrane; VDAC, voltage-dependent anion channel; CHAPS, 3-[(3-cholamidopropyl)dimethylammonio]-1-propanesulfonic acid; Z, benzyloxycarbonyl; PBS, phosphate-buffered saline; MOPS, 4-morpholinepropanesulfonic acid; fmk, fluoromethyl ketone; *Pan*, pantothenate.

TABLE I
Primary antibodies used in this study

Ab[a]	Type	Source (catalog no.)	Remarks
Actin	Mouse mAb	ICN (69100)	
Apaf-1	Rb pAb	Pharmingen (559683)	Recognizes Apaf-1 on Western
Apaf-1	Rat mAb	Chemicon (90001740)	Recognizes Apaf-1 on immunofluorescence
COX II	Mouse mAb	Molecular Probes (A-6404)	
Cyt. c	Mouse mAb	R & D Systems (6380-MC-100)	Recognizes holocytochrome *c* only on Western
Caspase-3	Rb pAb	Biomol (SA-320)	Recognizes the proform and cleaved fragments on Western; also used for fluorescence
Caspase-9	Rb pAb	Chemicon (Ab 16970)	Recognizes the proform and cleaved fragments on Western; also used for fluorescence
PARP	Rb pAb	Roche Applied Science (1 835 238)	
Hsp60	Mouse mAb	Chemicon (mAb 3514)	
Smac	Rb pAb	Dr. X. Wang	
VDAC	Rb pAb	Calbiochem (PC no. 548)	

[a] The abbreviations used are as follows: Ab, antibodies; COX II, cytochrome *c* oxidase subunit II; mAb, monoclonal antibody; pAb, polyclonal antibody; Rb, rabbit; Hsp60, heat shock protein 60.

vated caspase-2 has also been detected in apoptotic nuclei (26). Upon induction of apoptosis, mitochondrial procaspase-9 translocates to the cytosol and nucleus in both cell culture and animal model systems (17, 21). Similarly, activated caspase-3 has been detected in normal and apoptotic nuclei (27–29). In all these apoptotic systems, it is generally thought that procaspases "stored" in various subcellular compartments are released, upon apoptosis induction, and become activated in the cytosol or that the cytosolically activated caspases translocate to various organelles to participate in apoptosis. It is still unclear whether the procaspases localized in the organelles (*e.g.* mitochondria) can *ever* be activated *in situ*. A pertinent philosophical question is why these procaspases have to be "imported" into these organelles if they can only be activated in the cytosol?

Recently, we have found that apoptosis induced by many stimuli involves an early mitochondrial activation, which is characterized by up-regulation of the mitochondrial respiratory chain (MRC) proteins and many other mitochondrially localized non-MRC proteins (30). A cardinal feature of this mitochondrial activation-dependent apoptotic pathway (or MADAP) is the early up-regulation and enrichment of cyt. c in the mitochondria, which precede its release. Because procaspase-9 is present in the IMS of the mitochondria (14, 17, 21), we hypothesized that the increased mitochondrial cyt. c might lead to the activation of procaspase-9 and, subsequently, of procaspase-3 inside the organelle. In this study, we utilized our MADAP model to test this hypothesis. Our results show no evidence of cyt. c/Apaf-1-mediated procaspase-9 activation inside the mitochondria. Instead, the results suggest that the mitochondrial active caspase-9 and -3 result mostly from the translocation from the cytosol and partly from caspase-mediated activation in the mitochondria.

MATERIALS AND METHODS

Cells and Reagents—GM701.2-8C (GM701) cells were kindly provided by Dr. M. King (Thomas Jefferson University) and cultured in Dulbecco's minimum essential medium (Invitrogen) supplemented with 10% heat-inactivated fetal bovine serum and antibiotics. Human prostate cancer cells, PC3 and LNCaP, were purchased from ATCC (Manassas, VA) and cultured in RPMI 1640 supplemented with 5 and 10% fetal bovine serum, respectively.

The primary antibodies used are listed in Table I. All secondary antibodies, *i.e.* goat, donkey, or sheep anti-mouse or rabbit or goat IgG conjugated to horseradish peroxidase, fluorescein isothiocyanate, or rhodamine, together with enhanced chemiluminescence (ECL) reagents were acquired from Amersham Biosciences. Biotinylated goat anti-rat or anti-rabbit antibodies were obtained from Jackson ImmunoResearch (West Grove, PA). Fluorogenic caspase substrates DEVD-AFC and LEHD-AFC, *Pan*-caspase inhibitor Z-VAD-fmk, caspase-3/7 inhibitor Z-DEVD-fmk, and recombinant caspase-3 were bought from Biomol (Plymouth Meeting, PA). Streptavidin conjugated to AlexaFluor 594 or 488 and mitochondrial dyes were purchased from Molecular Probes (Eugene, OR). All other chemicals were purchased from Sigma unless specified otherwise.

Subcellular Fractionation and Western Blotting—Mitochondria were prepared as described previously (30–32). Briefly, cells were treated with various chemicals, inhibitors, or vehicle (ethanol or Me_2SO) control. In some experiments, cells were pretreated with cyclosporin A (CsA), Z-VAD-fmk, or Z-DEVD-fmk before apoptosis induction. At the end of the treatment, cells were harvested with trypsin, washed twice in ice-cold PBS, and resuspended in 600 μl of homogenizing buffer (20 mM HEPES-KOH, pH 7.5, 10 mM KCl, 1.5 mM $MgCl_2$, 1 mM sodium EDTA, 1 mM sodium EGTA, and 1 mM dithiothreitol) containing 250 mM sucrose and a mixture of protease inhibitors (1 mM phenylmethylsulfonyl fluoride, 1% aprotinin, 1 mM leupeptin, 1 μg/ml pepstatin A, and 1 μg/ml chymostatin). After 30 min of incubation on ice, cells were homogenized in the same buffer using a glass Pyrex homogenizer (type A pestle, 140 strokes). Unbroken cells, large plasma membrane pieces, and nuclei were removed by centrifuging the homogenates at 500 × *g* for 5 min at 4 °C. The resulting supernatant was centrifuged at 10,000 × *g* for 20 min to obtain mitochondria. The remaining supernatant was again subjected to centrifugation at 100,000 × *g* for 1 h to obtain the cytosolic fraction (*i.e.* S100 fraction). Mitochondrial pellet was washed three times in homogenizing buffer and then solubilized in TNC buffer (10 mM Tris acetate, pH 8.0, 0.5% Nonidet P-40, 5 mM $CaCl_2$) containing protease inhibitors. Protein concentration was determined by Micro-BCA kit (Pierce).

For Western blotting, various amounts of mitochondrial or cytosolic proteins were loaded in each lane of a 15% SDS-polyacrylamide gel. After gel electrophoresis and protein transfer, the membrane was probed or reprobed, after stripping, with various primary and corresponding secondary antibodies. Western blotting was performed using ECL as described previously (30).

Characterization of Mitochondrial Preparation by Transmission Electron Microscopy—The mitochondrial fractions prepared from PC3 cells as described above were fixed for 30 min at 4 °C in 1% acrolein (v/v) in homogenizing buffer. At the end of fixation, the mitochondria were pelleted by centrifugation at 10,000 × *g* and then resuspended in homogenizing buffer containing 0.5% dimethyl sulfoxide (v/v). Mitochondria were pelleted and resuspended in the same buffer four times for 15 min each, post-fixed for 30 min in 1% osmium tetroxide at room temperature, washed in homogenizing buffer, dehydrated in graded ethanol (20, 40, 60, 80, 90, 95, and 100% 2 times), and then passed through propylene oxide, followed by infiltration and embedding in epoxy resin. Ultrathin (80–100-nm) sections were cut with a Reichert Ultracut E ultramicrotome, picked up on 200 mesh copper grids, and stained with 2% (w/v) aqueous uranyl acetate followed by lead citrate. Grids were examined and photographed in a Zeiss 10 C transmission electron microscopy at an accelerating voltage of 80 kV.

Preparation of Percoll Gradient-purified Mitochondria—PC3 cells (12×10^6) were treated with ethanol or BMD188 (40 μM) for 1 h and then harvested for homogenization and differential centrifugation as described above. The resulting 10,000 × *g* mitochondrial pellet was washed and then resuspended in an EDTA-free medium and layered on a Percoll gradient consisting of four layers of 10, 18, 30, and 70% (by volume) Percoll in 0.3 M mannitol and 5 mM MOPS, pH 7.2 (33). After centrifugation for 35 min at 13,500 × *g*, the purified mitochondria were separated from non-mitochondrial membranes and non-functional or-

ganelles and collected at the 30/70% interface and washed with 0.3 M mannitol, 5 mM MOPS, pH 7.2, containing 1 mg/ml bovine serum albumin to remove the Percoll.

PARP Cleavage—PARP cleavage assays were performed as described previously (30–32).

Quantification of Apoptotic Nuclei Using DAPI Staining—Cells were plated on glass coverslips (4×10^4 cells/18-mm^2 coverslip) the day before treatment. The next day, cells were treated with vehicle control (*i.e.* ethanol or Me_2SO) or various inducers. Thereafter, cells were incubated live with DAPI (0.5 μg/ml) for 10 min at 37 °C followed by washing. The percentage of cells exhibiting apoptotic nuclei, as judged by chromatin condensation or nuclear fragmentation, was assessed by fluorescence microscopy (34). An average of 600–700 cells was counted for each condition.

DEVDase and LEHDase Activity Measurement—Cells were washed twice in PBS and the whole cell lysate was made in the lysis buffer (50 mM HEPES, 1% Triton X-100, 0.1% CHAPS, 1 mM dithiothreitol, and 0.1 mM EDTA). For activity measurement, 30 or 100 μg whole cell lysate, mitochondria, or cytosol was added to a reaction mixture containing 10 or 30 μM fluorogenic peptide substrates, Ac-DEVD-AFC or Ac-LEHD-AFC, 50 mM HEPES, pH 7.4, 10% glycerol, 0.1% CHAPS, 100 mM NaCl, 1 mM EDTA, and 10 mM dithiothreitol, in a total volume of 1 ml and incubated at 37 °C for 1 h. Production of 7-amino-4-trifluoromethylcoumarin (AFC) was monitored in a spectrofluorimeter (Hitachi F-2000 fluorescence spectrophotometer) using excitation wavelength 400 nm and emission wavelength 505 nm. The fluorescent units were converted into nanomoles of AFC released per h per mg of protein using a standard curve. The results were generally presented as fold activation over the control (30). In some experiments, the DEVDase activity was continuously monitored over a period of 2 h.

Cell-free Caspase Activation in the Mitochondrial Fractions—Mitochondria and cytosol were prepared from treated or untreated PC3 cells as described above. Various amounts of freshly isolated, unlysed or lysed (using the TNC buffer) mitochondria were co-incubated with 100 μg of cytosol freshly prepared from untreated PC3 cells for 1 h at 37 °C. At the end, either 10 or 30 μM DEVD-AFC substrate was added to the mixture, which was further incubated for 1 h at 37 °C. Subsequently, the DEVDase activity in the co-incubates was measured.

Kinetic Study of Caspase Activation—Two sets of PC3 cells (10^7 each) were simultaneously treated with 40 μM BMD188 for 0, 30, 45, 60, 90, and 120 min. At the end, one set of cells was harvested for the preparation of whole cell lysate and the other set harvested for subcellular fractionation, as described above. Subsequently, the three preparations, *i.e.* whole cell lysate, cytosol, and mitochondria, all derived from 10^7 cells, were used to measure the caspase activity by incubating with 10 μM of the Ac-DEVD-AFC substrate, as detailed above.

Immunostaining of Caspases and Apaf-1—Cells grown on glass coverslips were treated for various time intervals. Fifteen min prior to the end of the treatment, cells were incubated live with DAPI to label apoptotic nuclei (30). Then cells were fixed in 4% paraformaldehyde for 10 min followed by permeabilization in 1% Triton X-100 for 10 min. After washing in PBS, cells were first blocked in 10% goat whole serum for 30 min at 37 °C and then probed with Apaf-1, caspase-9, or caspase-3 (all at 1:500) for 1 h at 37 °C. After washing in PBS, cells were incubated with biotinylated goat anti-rat or anti-rabbit IgG antibody (1:1000). Finally, cells were incubated with streptavidin-AlexaFluor 488 or 594 (1:500) for 1 h at 37 °C. After thorough washing, coverslips were mounted on slides using Vectashield mounting medium (Vector Laboratories, Inc., Burlingame, CA) and observed under an Olympus BX40 epifluorescence microscope. Images were captured with MagnaFire software and processed in Adobe Photoshop.

Proteinase K Digestion of Isolated Mitochondria—Freshly isolated mitochondria (100 μg) were incubated in the homogenizing buffer (without protease inhibitors) alone or in the presence of proteinase-K (0.1 μg/ml) only or proteinase K plus Triton X-100 (1% final concentration). After 10 min of incubation on ice, 2 μl of phenylmethylsulfonyl fluoride (100 μM) was added to terminate proteolysis followed by addition of 6× SDS-loading buffer. Samples were then boiled for 5 min and analyzed immediately by Western blotting (20).

Alkali Extraction of the Mitochondria—The mitochondrial pellet (100 μg) was suspended in 0.1 M Na_2CO_3, pH 12.0, and incubated on ice for 30 min. At the end of the incubation, the sample was centrifuged at 100,000 × *g* for 1 h. The resulting pellet was then lysed in the TNC buffer. Both supernatant and pellet were then subjected to Western blotting (35).

Cell-free Caspase Activation and Translocation Experiments—All cell-free reactions were performed in homogenizing buffer in a total volume of 100 μl. Freshly isolated cytosol and/or mitochondria were incubated at 37 °C for 2 h with addition of bovine cyt. c (50 μg/ml) (36, 37). At the end, samples containing co-incubated mitochondria were centrifuged at 10,000 × *g* for 20 min to obtain the mitochondrial pellet. The resulting pellet was washed twice and suspended in homogenizing buffer. For translocation studies, cyt. c-activated cytosol was further incubated with untreated mitochondria for 1 or 3 h at 37 °C followed by centrifugation (10,000 × *g*) for 20 min. Following two washes in homogenizing buffer, the mitochondrial pellet, together with the supernatant, was subjected to Western blotting. In separate sets of experiments, isolated cytosol or mitochondria from BMD188 (40 μM) treated or untreated cells were co-incubated in various combinations for 1 or 2 h at 4, 25, and 37 °C. After co-incubation, the pelleted mitochondria were washed twice with homogenizing buffer, and then equal amounts of proteins were separated followed by Western blotting. To determine whether the mitochondrially localized procaspases can *ever* be activated in the organelle, mitochondria were incubated in the homogenizing buffer for 2 h at 37 °C by addition of recombinant caspase-3 (1 μM) or caspase-9 (1 μM). At the end of the incubation, the mitochondria were pelleted, washed twice in homogenizing buffer, and resuspended in 100 μl of homogenizing buffer. The supernatant and pellet were then subjected to SDS-PAGE and Western blotting analysis.

RESULTS

Activated Mitochondria Possess Caspase Activity—Apoptosis induced by multiple stimuli is preceded by a rapid up-regulation and accumulation of cyt. c in the mitochondria (30). Because many procaspases are localized in the mitochondria (see Introduction), we reason that some of these mitochondrially localized procaspases, in particular procaspase-9 and procaspase-3, might become activated in the organelle in a cyt. c-dependent manner, analogous to apoptosome-mediated activation of procaspase-9 and -3 in the cytosol. To test this possibility, we used BMD188, a cyclic hydroxamate that activates MADAP in multiple cell types (30–32), to treat PC3 prostate epithelial cancer cells. Following treatment for various time intervals, whole cell lysate, and mitochondrial and cytosolic fractions were prepared from equal numbers of cells (*i.e.* 10^7 cells for each fraction), and the DEVDase activity, which measures caspase-3 and -7 activation, was determined. The quality of subcellular fractionation was monitored by Western blot analysis of known compartment-specific proteins: cytochrome *c* oxidase subunit II for mitochondria, lamin A/C for nuclei, and lactate dehydrogenase for cytosol. We did not detect any cross-contamination among different fractions (see Refs. 30 and 32, and data not shown). Electron microscopy analysis also revealed pure mitochondria in our preparations (not shown). As shown in Fig. 1*A*, 45 min post-BMD188 treatment of PC3 cells, about 4- and 2-fold DEVDase activity was observed in the whole cell lysate and mitochondria, respectively. Only marginal DEVDase activity was detected in the cytosol by this time (Fig. 1*A*). By 60–120 min, increased DEVDase activity was observed in the cytosol, but the corresponding mitochondrial DEVDase activity was still higher (Fig. 1*A*). As expected, the DEVDase activity was always the highest in the whole cell lysate (Fig. 1*A*).

Next, we further examined the DEVDase activity in the mitochondrial fractions using a cell-free system. Mitochondria and cytosol were isolated from 1.5-h BMD188-treated or untreated PC3 cells and used in DEVDase activity measurements. Untreated mitochondria, either lysed (with Nonidet P-40) or unlysed, had negligible caspase activity (Fig. 1*B*, *lanes 1* and *2*). Untreated cytosol consistently showed slightly higher basal level DEVDase activity (Fig. 1*B*, *lane 5*), which did not change when co-incubated with untreated mitochondria (Fig. 1*B*, *lanes 6* and *7*). When the mitochondria from BMD188-treated PC3 cells were co-incubated with untreated cytosol, significantly increased DEVDase activity was observed (Fig. 1*B*, *lanes 8* and *9*; note that higher DEVDase activities were observed in these experiments than in Fig. 1*A* because higher amounts (*i.e.* 100 μg) of protein and substrate (30 μM) were

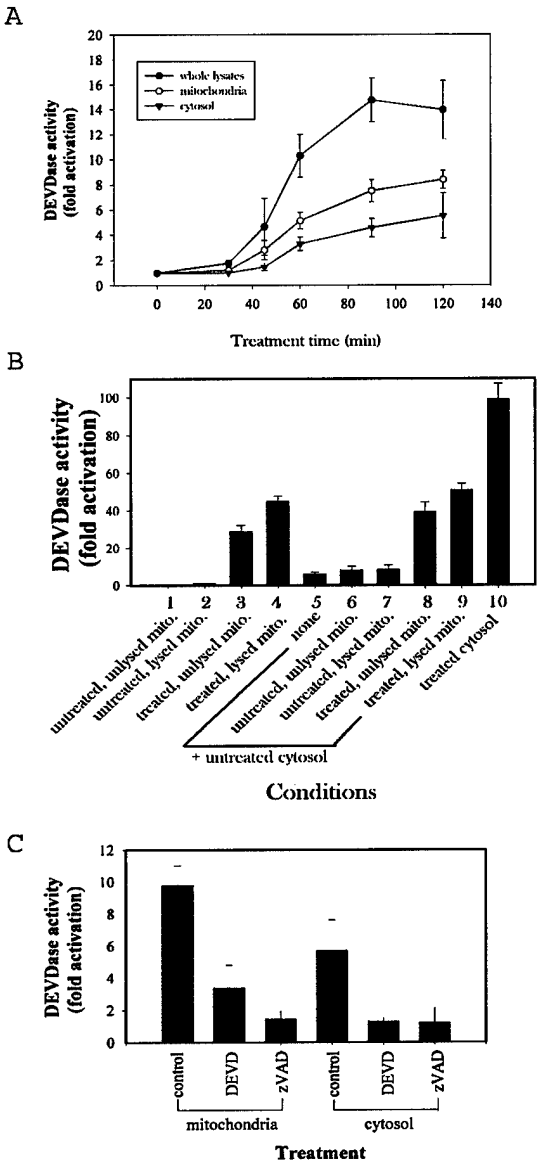

FIG. 1. **Activated mitochondria possess caspase activity.** *A*, mitochondria, cytosol, and whole cell lysate were prepared from equal numbers of PC3 cells (*i.e.* 10^7 cells for each fraction) treated with BMD188 (40 μM) for the indicated time intervals and used to measure DEVDase activity using 50 μg of protein and 10 μM Ac-DEVD-AFC substrate. The DEVDase activity was expressed as fold activation over the control, *i.e.* time 0. The data represent mean ± S.E. derived from three independent experiments. *B*, cell-free reconstitution experiment. One hundred μg of mitochondria (*mito*) was prepared from either control or BMD188-treated (40 μM; 90 min) PC3 cells. The mitochondria, either lysed (using Nonidet P-40) or unlysed, were either directly utilized in the DEVDase measurement (*lanes 1–4*) or first co-incubated with 100 μg of cytosol prepared from untreated PC3 cells (*lanes 6–9*) for 1 h at 37 °C before incubation with 30 μM DEVD-AFC substrate (1 h at 37 °C). *Lane 5* was the untreated cytosol alone. *Lane 10* was caspase-3 activity measured with 100 μg of whole cell lysate from the same batch of PC3 cells treated with BMD188. The data represent mean ± S.E. derived from 3 experiments. *C*, effects of caspase inhibitors on DEVDase activity. PC3 cells were pretreated with ethanol (vehicle control), Z-DEVD-fmk (50 μM), or Z-VAD-fmk (50 μM) for 1 h followed by BMD188 (40 μM; 2 h) treatment. Subsequently, mitochondrial and cytosolic fractions (50 μg each) were used for DEVDase activity assay by incubating with 10 μM Ac-DEVD-AFC. The data represent mean ± S.E. derived from five independent experiments.

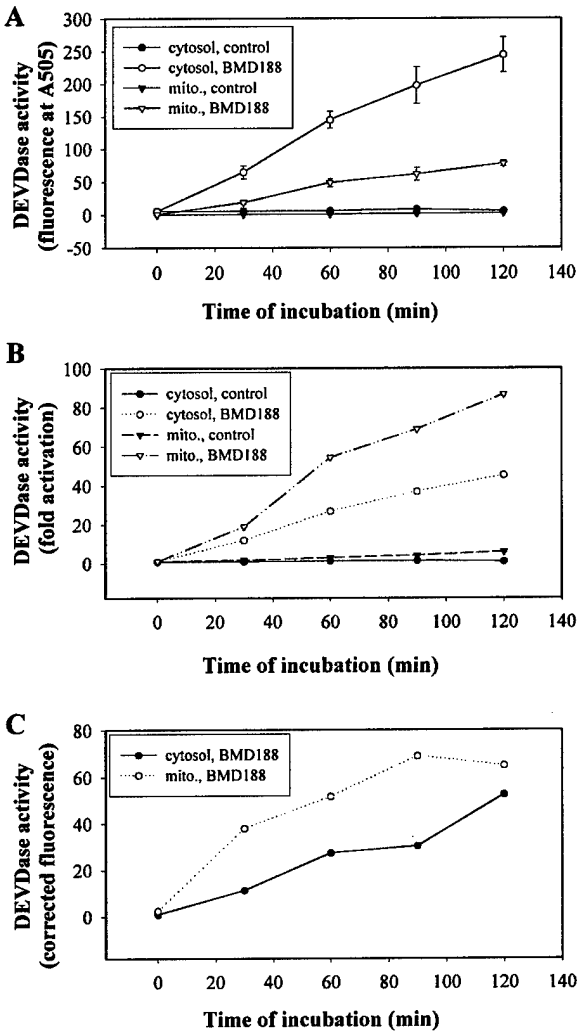

FIG. 2. **Caspase activation *in vitro*.** *A*, caspase activity expressed as the raw fluorescence unit as a result of Ac-DEVD-AFC hydrolysis. One hundred μg of cytosol or mitochondria (*mito*) from untreated (*control*) or BMD188-treated (40 μM; 90 min) PC3 cells was incubated with 30 μM Ac-DEVD-AFC substrate at 37 °C for 0 (*i.e.* immediate measurement following mixing), 30, 60, 90, and 120 min. The fluorescence measured at A_{505} was directly plotted as a function of time. Triplicate samples were run for each time point, and the data represent mean ± S.D. Note that the mitochondrial samples had lower background fluorescence levels (*i.e.* the values at time 0) than the cytosolic samples; the former was 0.4–0.9 and the latter was 5–7.5. *B*, caspase activity expressed as fold activation. The data obtained in *A* were plotted as fold activation that was derived by dividing the mean fluorescence value at each time point by the mean fluorescence value at time 0. Thus, the fold activation at time 0 was considered as 1. *C*, caspase activity expressed as corrected fluorescence, which was derived by dividing the mean fluorescence value at each time point in BMD188-treated mitochondria or cytosol by the mean fluorescence value at corresponding time point in control mitochondria or cytosol, respectively. Therefore, DEVDase activities at all time points in the control mitochondria and cytosol were 1 (not plotted).

used). Our initial interpretation was that cyt. c released from the BMD188-activated mitochondria caused caspase activation in the cytosol. Surprisingly, however, when the activated mitochondria were directly used in DEVDase activity measurement, in the absence of untreated cytosol, essentially similar levels of increased DEVDase activity were observed (Fig. 1*B*, compare *lanes 3* and *4 versus lanes 8* and *9*). In both cases, Nonidet P-40-lysed mitochondria gave rise to higher DEVDase activities (Fig. 1*B*, *lane 4 versus lane 3* and *lane 9 versus lane 8*). As expected, both Z-DEVD-fmk, a caspase-3/7-specific inhibitor, and Z-VAD-fmk, a *pan*-caspase inhibitor, inhibited the mitochondrial and cytosolic DEVDase activity (Fig. 1*C*), just as both inhibited the BMD188-induced apoptosis (30, 32). Collectively, the data in Fig. 1 suggest that the BMD188-activated mitochondria possess DEVDase activity, which most likely re-

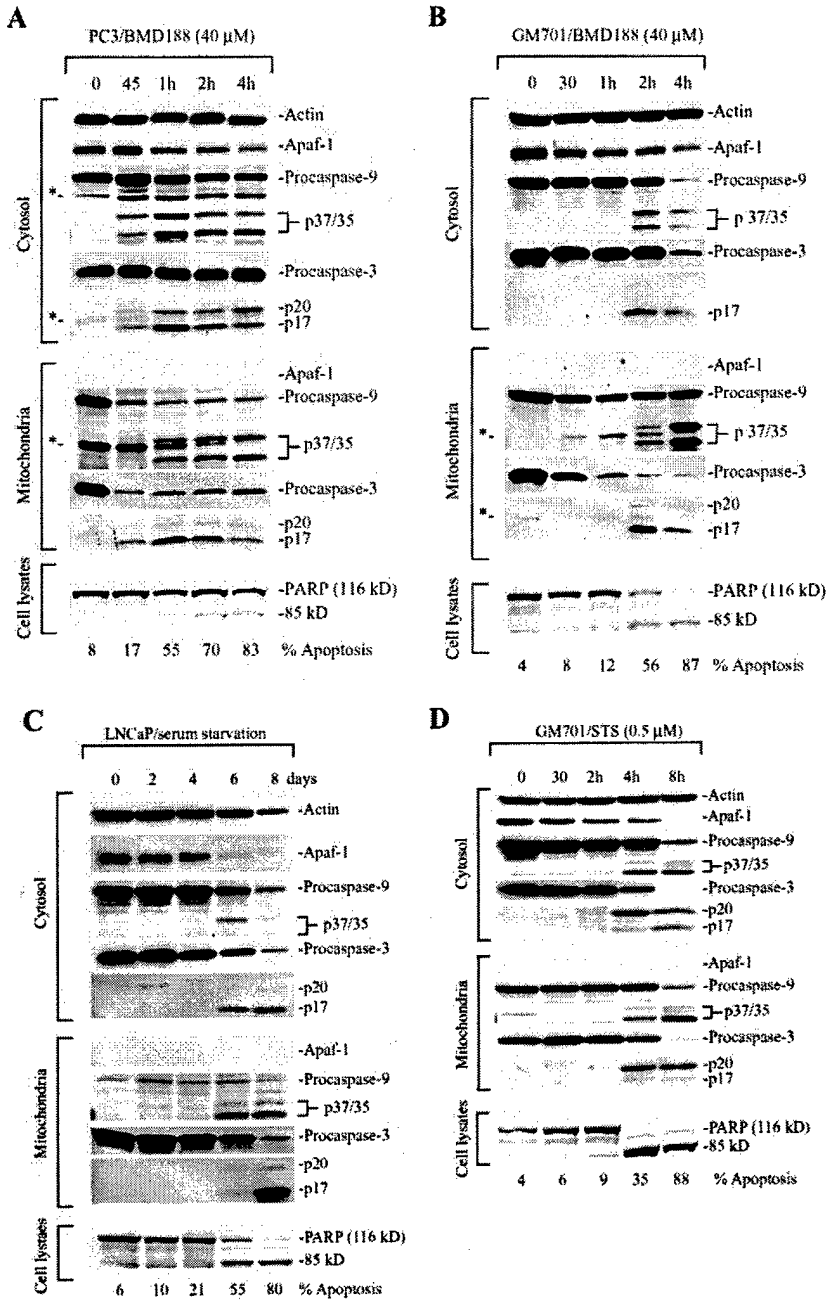

FIG. 3. **Proteolytic activation of procaspase-9 and -3 and redistribution of caspases and Apaf-1 during apoptosis.** Western blot analysis of the whole cell lysate, cytosolic and mitochondrial fractions from PC3 (*A*) or GM701 cells (*B*) treated with BMD188, LNCaP cells subjected to serum starvation (*C*), or GM701 cells treated with staurosporine (*STS*) (*D*). Thirty (cytosolic) or 60 (mitochondrial) μg of proteins was used in Western blotting for caspase-9, caspase-3, Apaf-1, and actin, as indicated. PARP cleavage and apoptosis were determined as described under "Materials and Methods." The *asterisks* on the *left* of *A* and *B* are novel or nonspecific bands detected by the antibodies against caspase-9 or caspase-3. All data are representative of at least three independent experiments.

side in the IMS as evidenced by the increased activities upon Nonidet P-40 lysis.

To characterize further the DEVDase activity associated with the BMD188-activated mitochondria, we purified mitochondria using the Percoll gradient and the corresponding cytosol from control or 1.5-h BMD188-treated PC3 cells and incubated them with DEVD-AFC substrate *in vitro* at 37 °C for a continuous period (*i.e.* from 0 to 120 min). The caspase activity was then plotted as either raw fluorescence, fold activation, or corrected fluorescence as a function of incubation time. As shown in Fig. 2, BMD188-activated mitochondria demonstrated a time-dependent increase in caspase activity. When expressed as raw fluorescence, the cytosol samples possessed higher fluorescence values than the corresponding mitochondrial samples at all time points (Fig. 2*A*). However, cytosol samples also possessed higher background (*i.e.* time 0) fluorescence values (see Fig. 2 legend). Therefore, when plotted as fold activation (Fig. 2*B*) or corrected fluorescence (Fig. 2*C*), the mitochondrial samples demonstrated higher DEVDase activities than did the corresponding cytosolic samples.

Similar DEVDase activity was also detected in the mitochondrial fractions in several other MADAP models (30) including PC3 cells treated with butyrate, GM701 cells treated with BMD188, LNCaP cells subjected to serum starvation, and MDA-MB-231 cells treated with etoposide (not shown).

Detection of Proteolytically Activated Caspase-9 and Caspase-3 in the Mitochondria during Apoptosis—In principle, the DEVDase activity in the activated mitochondria may result from either procaspases becoming activated in the mitochondria or activated caspases translocating to the organelle, or both. We explored these possibilities by focusing on the activation of procaspase-9 and -3, two pivotal caspases in the apoptosome pathway initiated by cyt. c and Apaf-1.

In PC3 cells, significant amounts of procaspase-9 and procaspase-3 were localized in the mitochondria (Fig. 3*A*). Procaspase-9 (~46 kDa) is activated mostly through auto-

activation via Apaf-1-mediated oligomerization, resulting in proteolytic cleavage at Asp^{315} to generate a 35-kDa fragment (p35) containing the caspase recruitment domain and the large subunit (38) and to expose the ATPF motif in the N terminus of the linker region to interact with XIAP and Smac/Diablo (39, 40). Partially activated caspase-9 activates caspase-3, which in turn can cleave procaspase 9 at Asp^{330} to generate a 37-kDa fragment (p37) (containing the caspase recruitment domain, large subunit, and the linker region) and ~10-kDa small subunit (38–41). In our experiments, we utilized an antibody that recognizes both the proform and the p37/p35 bands (Table I). As shown in Fig. 3*A*, 45 min post-BMD188 treatment, the mitochondrial procaspase-9 protein level was significantly reduced without the appearance of the p37/p35 bands, suggesting that, by this time point, the majority of the mitochondrial procaspase-9 was probably released from rather than activated in the organelle. Indeed, at 45 min, increased procaspase-9 was observed in both cytosol (Fig. 3*A*) and perinuclear area (see below). Also, the LEHDase assays did not detect caspase-9 activity (not shown).

In the cytosol, caspase-9 cleavage was observed at 45 min (Fig. 3*A*). By 1 h, the maximum level of caspase-9 cleavage products was observed in the cytosol (Fig. 3*A*). In the meantime, the p37/p35 bands began to appear in the mitochondria (Fig. 3*A*), suggesting that, in BMD188-treated PC3 cells, procaspase-9 became activated first in the cytosol and then the activated caspase-9 translocated to the mitochondria. In support, between 1 and 4 h, decreased amounts of activated caspase-9 were observed in the cytosol (Fig. 3*A*). At the same time, increasing levels of the p37/p35 products in the mitochondria were observed, whereas the mitochondrial procaspase-9 bands remained fairly constant (Fig. 3*A*). Interestingly, a prominent ~36-kDa protein band was detected by the anti-caspase-9 antibody only in the mitochondria, which began to decrease at 1 h and disappeared by 4 h after BMD188 treatment (Fig. 3*A*). Whether this band represents a caspase-9 isoform (42, 43) or just a nonspecific protein remains to be determined.

Procaspase-3 (~32 kDa) is generally first cleaved by caspase-8, caspase-9, caspase-10, or granzyme-B at Asp^{175} to generate the p12 small subunit and the ~p24 large subunit that still contains the pro-domain. Then the p24-p12 complex is further cleaved at Asp^{9}, possibly through its auto-catalytic activity, to generate p20, which could be further cleaved at Asp^{28} to produce the p17 fragment (41, 44, 45). Frequently, a p31 fragment can also be detected, resulting from the procaspase-3 removed of the first 9 amino acids in the pro-domain. Various experiments have demonstrated that the p20/p17/p12 bands represent catalytically active caspase-3 (44, 45). We utilized an antibody that recognizes both procaspase-3 and most cleavage products (Table I). In BMD188-treated PC3 cells, similar to caspase-9, the mitochondrial procaspase-3 was significantly reduced at 45 min (Fig. 3*A*). Different from caspase-9 by 45 min, the p20 and the p17 caspase-3 bands were detected simultaneously in the cytosol and mitochondria (Fig. 3*A*). By 1 h when significant amounts of caspase-3 activation occurred in both cytosol and mitochondria (Fig. 1 and Fig. 3*A*), PARP cleavage was observed, and 55% of the cells became apoptotic (Fig. 3*A*). Caspase-3 cleavage overall paralleled the DEVDase activity (Fig. 1). Of interest, the anti-caspase-3 antibody also detected an unknown ~19-kDa band in untreated cytosol and mitochondria, which decreased as apoptosis proceeded (Fig. 3*A*).

To determine whether appearance of the activated caspases in the mitochondrial fraction is cell type-specific, we treated GM701 fibroblasts with BMD188. As in BMD188-treated PC3 cells, the mitochondrial procaspase-9 and, in particular, procaspase-3 were decreased by 30 min (Fig. 3*B*). Whereas the maximum decrease of procaspase-9 was observed by 30 min, the procaspase-3 level continued to decrease until the end of the treatment, *i.e.* 4 h (Fig. 3*B*). Activated forms of caspase-9 and caspase-3 were simultaneously detected at 2 h post-BMD188 treatment when PARP was cleaved and 56% cells were apoptotic (Fig. 3*B*). At 2 h, the p37/p35 caspase-9 fragments were detected in the mitochondria without an obvious decrease in the intensity of the mitochondrial procaspase-9 band (Fig. 3*B*), suggesting that, as in the BMD188-treated PC3 cells, the mitochondrial activated caspase-9 resulted, most likely, from translocation from the cytosol. In support, 4 h post-treatment, most procaspase-9 became cleaved in the cytosol, but the p37/35 bands actually decreased compared with those at 2 h (Fig. 3*B*). In the meantime, the p37/p35 bands in the mitochondria significantly increased without a corresponding decrease of the proform (Fig. 3*B*), strongly suggesting that the activated caspase-9 in the cytosol had translocated to the mitochondria. Again, as observed in PC3 cells, caspase-3 activation was observed simultaneously in the cytosol and mitochondria (Fig. 3*B*). Although the mitochondrial procaspase-3 decreased at 30 min and further decreased at 1 h, no cleavage products were observed at these time points (Fig. 3*B*). The anti-caspase-9 and anti-caspase-3 antibodies again detected the ~36- and ~19-kDa bands, respectively, more obviously in the mitochondrial fractions (Fig. 3*B*). Accompanying the cleavages of procaspase-9 and procaspase-3, increased LEHDase (~2-fold increase) and DEVDase (up to 8-fold increase) activities were detected in both cytosolic and mitochondrial fractions (not shown).

In both PC3 epithelial cells and GM701 fibroblasts treated with BMD188, we observed an early decrease of procaspase-9 and/or -3 in the mitochondria without concomitant cleavage (Fig. 3, *A* and *B*), suggesting that the mitochondrial procaspases may have been released from the organelle into the cytosol or other subcellular compartments, as observed in other apoptosis models (17–19, 21, 22). We carried out an immunofluorescence experiment in GM701 (Fig. 4) and PC3 (not shown) cells to explore this possibility. Procaspase-9 and -3 were homogeneously distributed in GM701 cells (Fig. 4, *A* and *E*; note that the mitochondrial localization of these procaspases was not very obvious due to their overwhelming expression in the cytosol). By 30 min (not shown) or 1 h (Fig. 4, *B* and *F*) post-BMD188 treatment, there was a prominent increase of both caspase-9 and caspase-3 staining in the nuclear area in most of the cells. Since by 30 min to 1 h there was no caspase-9 or caspase-3 activation in BMD188-treated GM701 cells revealed either by Western blotting (Fig. 3*B*) or by activity assays (Ref. 30; data not shown), the increased staining in the nuclear area therefore most likely resulted from the procaspase, rather than the active caspase, translocation from the mitochondria. Another piece of supporting evidence for this conclusion was that all cells that showed perinuclear staining of caspases were healthy and alive (Fig. 4, *A–H*), and only ~10% of the cells were apoptotic at this time frame (Fig. 3*B*) (30), thus suggesting that the caspases had not been activated. The increased perinuclear staining of procaspases-9 or -3 generally was slightly larger than the DAPI staining (*e.g.* compare Fig. 4, *B* and *F versus D* and *H*), suggesting that the translocated procaspases were perhaps clustered outside the organelle.

To determine whether inducers other than BMD188 also can induce association of activated caspase-9 and -3 with the mitochondria, we subjected LNCaP cells to serum starvation, a MADAP model involving an early mitochondrial activation (30). As shown in Fig. 3*C*, activated caspase-9 and -3 were

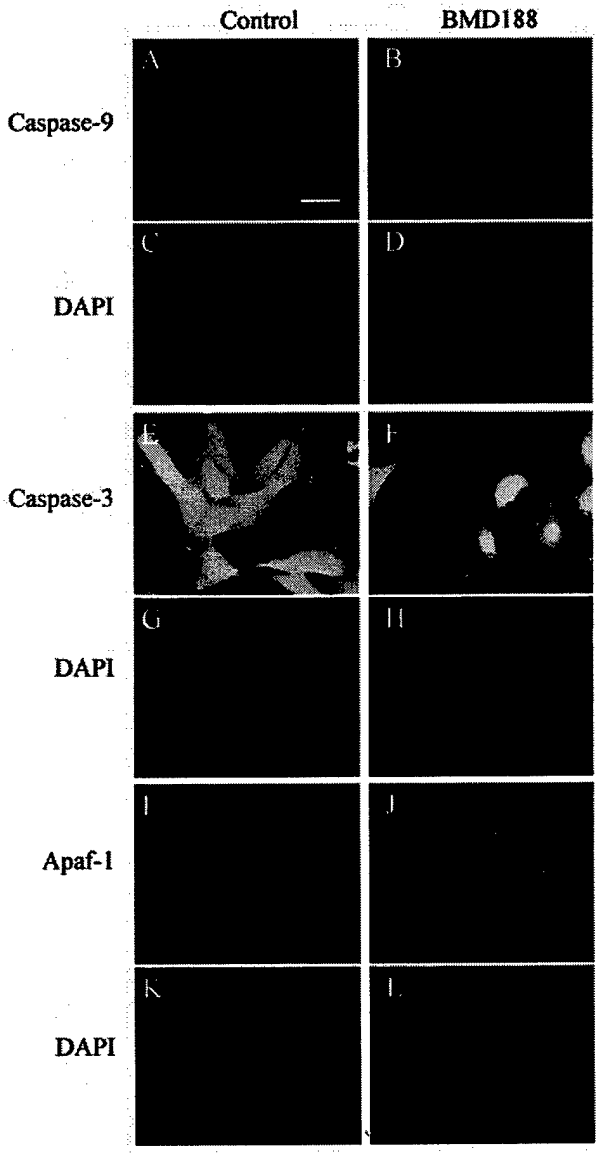

FIG. 4. **BMD188-induced translocation of procaspase-9, procaspase-3, and Apaf-1 to the perinuclear area.** GM701 cells treated with BMD188 (40 μM; 1 h) were processed for immunolabeling of caspase-9 (*A–D*), caspase-3 (*E–H*), or Apaf-1 (*I–L*). Nuclei were counterstained with DAPI. Microphotographs shown are representative of three independent experiments. *Bar*, 10 μm.

detected in the cytosol as well as in the mitochondria on day 6, when PARP was cleaved and 55% of the cells were apoptotic. In LNCaP cells there was only low levels of procaspase-9 in the mitochondria (Fig. 3*C*). When cytosolic procaspase-9 was cleaved on day 6, the p35 band was preferentially observed in the mitochondria, whereas the p37 band was most prominent in the cytosol (Fig. 3*C*). On day 8 when most cytosolic procaspase-9 was processed, essentially no p37/p35 bands were detected in the cytosol, whereas increased levels of both bands were seen in the mitochondria (Fig. 3*C*). These results once again suggest that the mitochondrial active caspase-9 most likely results from the translocation of the proteolytically activated caspase-9 in the cytosol. There was a slight decrease in the mitochondrial procaspase-9 in LNCaP cells starved for 8 days (Fig. 3*C*), raising the possibility that during late apoptosis the mitochondrial procaspase-9 might be activated *in situ*. Different from procaspase-9, LNCaP cells expressed abundant procaspase-3 in the mitochondria, which showed a time-dependent decrease, similar to cytosolic procaspase-3 (Fig. 3*C*). By day 6 when PARP was cleaved, decreased procaspase-3 and increased active p17 fragments were observed in both cytosol and mitochondria (Fig. 3*C*). By day 8 when most PARP was degraded, a further decrease of procaspase-3 and increase in the p20/p17 fragments were observed in both compartments. However, the increase of the p17 active caspase-3 in the mitochondria was much more prominent than that in the cytosol (Fig. 3*C*).

Similarly, in MDA-MB-231 breast cancer cells treated with etoposide, yet another MADAP model (30), we also observed activated caspase-9 and caspase-3 in the mitochondria (not shown).

To determine whether only MADAP inducers could cause association of active caspases with the mitochondria, we treated GM701 cells with staurosporine, which causes cell death independently of MRC functions and without mitochondrial activation (30, 32). As shown in Fig. 3*D*, although there was no early exodus of mitochondrially localized procaspase-9 or -3, activated forms of both caspases were detected in the mitochondria, simultaneously with their activation in the cytosol, PARP cleavage, and increased apoptosis.

The conclusions from the above experiments are as follows. 1) The presence of the activated caspase-9 and -3 seems to be a general phenomenon during apoptosis. 2) The mitochondrial caspase-9 activation generally appears either after the cytosolic caspase-9 activation (Fig. 3*A*) or concomitant with the cytosolic caspase-9 activation. In the latter case, the first appearance of the activated caspase-9 in the mitochondria is rarely accompanied by a decrease in the corresponding proform, whereas the first appearance of the activated caspase-9 in the cytosol is always accompanied by a decrease in procaspase-9 (Fig. 3, *B–D*). Late in apoptosis, however, the increased active caspase-9 levels in the mitochondria may (Fig. 3, *C* and *D*, the *last lanes*) or may not (Fig. 3, *A* and *B*, the *last lanes*) be accompanied by a decrease in the mitochondrial procaspase-9. These results suggest that the mitochondrial active caspase-9 may initially come from translocation from the cytosol but, late during apoptosis, the increased activated caspase-9 in the mitochondria may result from translocation and/or caspase-mediated activation in the organelle. 3) Activated caspase-3 is always detected simultaneously in the mitochondria and cytosol concomitant with the caspase-9 activation in the cytosol (Fig. 3, *A–D*), raising a similar possibility that the activated caspase-3 in the mitochondria may result from translocation and/or caspase-mediated activation in the organelle.

Apaf-1 Localizes Exclusively in the Cytosol and Translocates to the Perinuclear Area during Apoptosis—The second point mentioned above suggests that the initiator caspase, caspase-9, may not be activated in the organelle in a cyt. c/Apaf-1-dependent manner. Theoretically, if procaspase-9 were activated inside the mitochondria in an apoptosome-dependent manner, Apaf-1 should be expressed in the mitochondria. Western blot analysis indicated that, in all cells studied, Apaf-1 was expressed exclusively in the cytosol (Fig. 3 and data not shown), consistent with an earlier report (46). Upon apoptosis induction, Apaf-1 showed a rapid and time-dependent decrease (Fig. 3, *A–D*). Immunofluorescent labeling revealed that Apaf-1, much like the mitochondrial procaspase-9 and -3 (Fig. 4, *A–H*), translocated to the perinuclear area in GM701 (Fig. 4, *I–L*) or PC3 (not shown) cells treated with BMD188 or in serum-starved LNCaP cells (not shown). In multiple Western and immunolabeling experiments, we failed to observe translocation of Apaf-1 to the mitochondria upon apoptosis induction (Fig. 3 and 4; data not shown). These observations suggest that procaspase-9 is unlikely to be activated in the mitochondria in a cyt. c/Apaf-1-dependent manner.

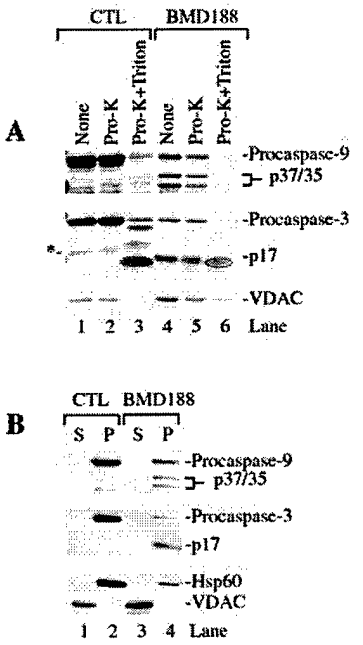

FIG. 5. **Active caspase-9 and caspase-3 are localized in the IMS of the mitochondria.** *A*, mitochondria prepared from GM701 cells either untreated (*lanes 1–3*) or treated with BMD188 (40 μM; 2 h; *lanes 4–6*) were subjected to proteinase K (*Pro-K*) digestion in the presence or absence of Triton X-100 as described under "Materials and Methods." *CTL*, control. At the end of digestion, samples were resolved by SDS-PAGE and immunoblotted for caspase-9, caspase-3, and VDAC. The *dot-circled bands* represent a degraded product of caspase-3 by proteinase K; and the *asterisk* indicates the unknown p19 band. *B*, mitochondria from control (*lanes 1* and *2*) and BMD188-treated (*lanes 3* and *4*) GM701 cells were subjected to alkali extraction as described under "Materials and Methods." At the end of treatment, the supernatant (*S*) and pellet (*P*) were collected by centrifugation and used in Western blotting for caspase-9 and -3, Hsp60, and VDAC. All data are representative of 2–3 independent experiments.

Active Caspases Are Located in the IMS of the Mitochondria—Next, we utilized the mitochondria from the BMD188-treated (3 h) or untreated GM701 cells to determine where the active caspases were located in the mitochondria, *i.e.* on the outer mitochondrial membrane (OMM) or in the IMS. When control mitochondria were treated with proteinase K alone, the procaspase-9 and procaspase-3 bands were detected (Fig. 5*A*, *lanes 1* and *2*). When the mitochondria were treated with proteinase K in the presence of Triton X-100 (to solubilize the organelle), procaspase-9 was completely degraded, whereas procaspase-3 was degraded into two specific fragments (Fig. 5*A*, *lane 3*). These results were consistent with these procaspases being located in the IMS (17–19, 21, 22). Likewise, when the BMD188-activated mitochondria were treated with proteinase K alone, the active caspase-9 (p37/p35) or caspase-3 (p17) bands were not significantly affected (Fig. 5*A*, *lane 5*). When these mitochondria were treated with proteinase K together with Triton X-100, both the pro- and active forms were degraded (Fig. 5*A*, *lane 6*; note that the bands marked by the *dotted circles* were a proteinase K degradation product rather than p17). These results suggest that the active caspase-9 and -3 were also present in the IMS. As an experimental control, voltage-dependent anion channel or VDAC, a protein mostly localized in the OMM with a small part of the molecule protruding to the cytosol (47, 48), was not digested by proteinase K treatment alone (Fig. 5*A*, *lane 2*) but mostly degraded after solubilization with Triton X-100 (Fig. 5*A*, *lanes 3* and *6*). Note that proteinase K treatment alone appeared to have partially digested both caspase-9 and caspase-3 as well as VDAC in the BMD188-treated mitochondria (Fig. 5*A*; compare *lanes 5 versus 4*), which was consistent with the observations that the 3-h BMD188-activated mitochondria had significant mitochondrial membrane permeabilization or MMP (30) thus allowing partial access of proteinase K to the IMS.

In another set of experiments, we utilized a different strategy to confirm the IMS localization of the activated caspase-9 and caspase-3 in the mitochondria. Specifically, we adopted an alkali extraction protocol to strip the proteins localized either peripheral or integral to the OMM, depending on the harshness of the extraction conditions. As shown in Fig. 5*B*, under our experimental conditions, VDAC, an OMM protein, was extracted from the mitochondria but Hsp60, a mitochondrial matrix protein, was not. Under the same conditions, both pro- and the activated forms of caspase-9 and caspase-3 remained in the mitochondrial pellet (Fig. 5*B*), thus confirming that the activated caspases were localized in the IMS. Note that in both experiments BMD188 treatment resulted in an up-regulation of VDAC (Fig. 5*A*, *lane 4 versus lane 1*; Fig. 5*B*, *lane 3 versus lane 1*), consistent with our previous observations that MADAP inducers such as BMD188 systematically up-regulate MRC proteins as well as mitochondrially localized non-MRC proteins (30).

Association of Active Caspases with the Mitochondria Is Inhibited by CsA—In the following experiments, we addressed how the activated caspase-9 and -3 might end up in the IMS of the mitochondria. First, we utilized the BMD188-treated PC3 cells to assess the relationship between mitochondrial protein release, caspase activation, and caspase association with the mitochondria. Western blotting using a monoclonal anti-cyt. c antibody that specifically recognizes holo-cyt. c (30) revealed significant release of holo-cyt. c from the mitochondria as early as 5 min post-treatment (Fig. 6). By 15 min cyt. c release reached the peak level (Fig. 6). By 2 h, cyt. c accumulation in the cytosol decreased (Fig. 6) probably due to extensive cell death by this time (Fig. 3*A*) leading to cyt. c leak into the culture medium (30, 49). Note that this antibody somehow did not react well with the holo-cyt. c in the mitochondrial fraction in certain cell types (Fig. 6 and data not shown). Surprisingly, the 60-kDa mitochondrial matrix protein Hsp60 was also rapidly released; the release was observed as early as 5 min and peaked at ~30 min (Fig. 6). The release of both cyt. c and Hsp60 occurred before the activated caspase-9 and -3 appeared in the mitochondria at ~1 h (Fig. 6). The release of both cyt. c and Hsp60 was inhibited (*i.e.* delayed) by CsA, an inhibitor of MMP (48), but not by Z-VAD, a general caspase inhibitor (Fig. 6). Interestingly, CsA also appeared to decrease the levels of active caspase-9 and caspase-3 specifically in the mitochondria, especially at 1 h post-treatment (Fig. 6). By contrast, Z-VAD inhibited activation of caspase-9 and, more prominently, of caspase-3, leading to significantly reduced levels in both cytosol and mitochondria (Fig. 6). Together, these results suggest that 1) perturbation of the mitochondrial integrity, as evidenced by cyt. c and Hsp60 release, occurs prior to caspase activation and their association with the mitochondria; 2) a CsA-inhibitable mechanism(s) is involved in the initial mitochondrial protein release; and 3) a similar CsA-inhibitable mechanism(s) might also be involved in the later association of the activated caspases in the mitochondria.

Mitochondrially Localized Active Caspases Result Mostly from Translocation and Partly from in Situ Activation—Next, we performed several sets of cell-free experiments to further address how the active caspases in the mitochondria may have originated. In the first set (Fig. 7, *A* and *B*, *lanes 1–4*), mitochondria or cytosol prepared from untreated GM701 cells were activated with cyt. c. As shown in Fig. 7*A* (*lane 4*), cyt. c caused complete proteolysis of procasapse-9 in the cytosol generating

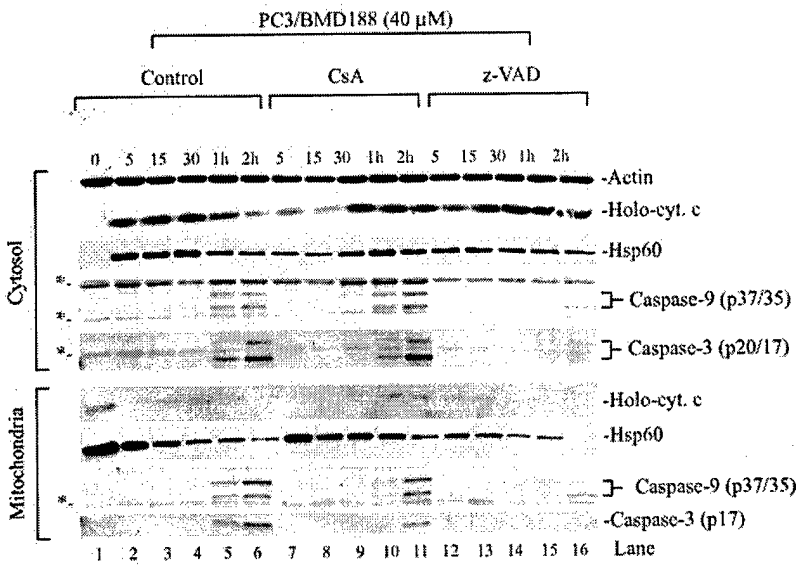

FIG. 6. **CsA inhibits both initial mitochondrial protein release and later caspase association with the mitochondria.** PC3 cells were pretreated with vehicle (*control*), CsA (10 μM), or Z-VAD-fmk (50 μM) for 1 h followed by BMD188 (40 μM) treatment in the presence of these inhibitors for the times indicated. At the end of the treatment, cells were harvested for subcellular fractionation. Twenty five μg of cytosolic or mitochondrial proteins were used in Western blotting of holo-cyt. c, Hsp60, caspase-9, or caspase-3. The *asterisks* on the *left* indicate unknown caspase-9 or -3 bands. Data are representative of 2–3 independent experiments.

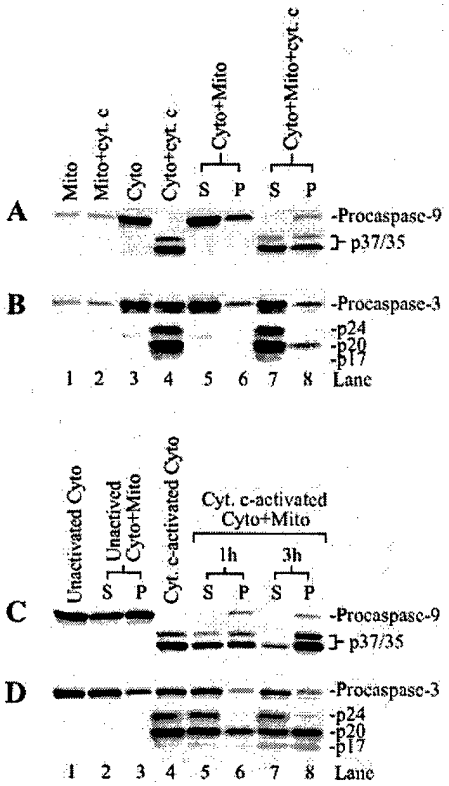

FIG. 7. **Cell-free activation and translocation of caspase-9 and caspase-3.** Mitochondria and cytosol were prepared from untreated GM701 cells. Caspase activation and translocation to mitochondria were assessed by Western blotting. *A* and *B*, cell-free activation of caspase-9 (*A*) or caspase-3 (*B*) initiated by cyt. c. Freshly prepared mitochondria (25 μg) or cytosol (40 μg) was individually incubated with none or bovine heart cyt. c at 37 °C for 2 h (*lanes 1–4*). In a parallel experiment, cytosol (*Cyto*) and mitochondria (*Mito*) were co-incubated with none or cyt. c (*lanes 5–8*). At the end of the incubation, mitochondria were pelleted, and cytosolic and mitochondrial samples were separated and probed for caspase-9 (*A*) or caspase-3 (*B*) (*lanes 5–8*). *C* and *D*, time course of caspase activation and translocation. Cyt. c-activated (*lanes 4–8*) (2 h at 37 °C) cytosol (40 μg) was co-incubated with fresh mitochondria (40 μg) at 37 °C for 1 or 3 h. After incubation, mitochondrial pellet (*P*) and supernatant (*S*) were subjected to Western blotting for caspase-9 (*C*) or caspase-3 (*D*). As controls, unactivated cytosol (*lane 1*), and the supernatant and the pellet obtained from co-incubated unactivated cytosol and unactivated mitochondria (*lanes 2* and *3*, respectively), were also run on the gel. Data are representative of at least 3 independent experiments.

prominent p37/p35 bands. Similarly, stimulation of the cytosol with cyt. c activated caspase-3 to generate the p24/p20/p17 bands (Fig. 7*B*, *lane 4*). In contrast to cytosolic procaspases, neither the mitochondrial procaspase-9 nor the mitochondrial procaspase-3 was proteolytically activated by cyt. c (Fig. 7, *A* and *B*, *lanes 2*), confirming that there is no Apaf-1 in the mitochondria.

In the second set of cell-free experiments (Fig. 7, *A* and *B*, *lanes 5–8*), we first combined the cytosol and the mitochondria (*i.e. Cyto + Mito*) and then activated the mixture with cyt. c. At the end, the mitochondrial pellets were separated from the cytosol, and caspase activation was assessed by Western blotting. As shown in Fig. 7, *A* and *B* (*lanes 5* and *6*), simple co-incubation of the cytosol with the mitochondria did not result in procaspase-9 or procaspase-3 activation. However, stimulation with cyt. c resulted in complete procaspase-9 activation (Fig. 7*A*, *lane 7*), just as stimulating cytosol alone with cyt. c. Significantly, nearly equal amounts of the cleaved p37/p35 bands were now detected in the mitochondrial pellet (Fig. 7*A*, *lane 8*), and both the cytosolic and the mitochondrial p37/p35 bands were roughly half those when cytosol alone was activated with cytochrome *c* (Fig. 7*A*, compare *lanes 7* and *8 versus lane 4*). These results suggest that ~50% of the cyt. c-activated caspase-9 in the cytosol translocated to the mitochondria. Likewise, cyt. c alone activated procaspase-3 in the cytosol and the mitochondria to generate the p24 and p20 bands and a small amount of p17 (Fig. 7*B*, *lane 7*). Surprisingly, only the active p20 fragment translocated to the mitochondria (Fig. 7*B*, *lane 8*).

Next, we ran a time course experiment in which we first made cyt. c-activated cytosol and then co-incubated it with the untreated mitochondria for 1 or 3 h. As shown in Fig. 7*C* (*lanes 1–3*), no caspase-9 or caspase-3 activation was observed in unactivated cytosol or unactivated cytosol + mitochondria mix. However, the cytosolic procaspase-9 was again completely activated by cyt. c (Fig. 7*C*, *lane 4*). Co-incubation of the cyt. c-activated cytosol with the untreated mitochondria for 1 h led ~50% of the p37/p35 bands to translocate to the mitochondria (Fig. 7*C*, *lanes 4–6*). Co-incubation for 3 h rendered all of the p37 band and most of the p35 band to translocate to the mitochondria (Fig. 7*C*, *lanes 7* and *8 versus lanes 5* and *6*). In the meantime, there was a decrease in the mitochondrial procaspase-9 band (Fig. 7*C*, compare *lane 8 versus lane 6*), suggesting that procaspase-9 may also have been activated in the mitochondria. Similarly, co-incubation of the cyt. c-activated

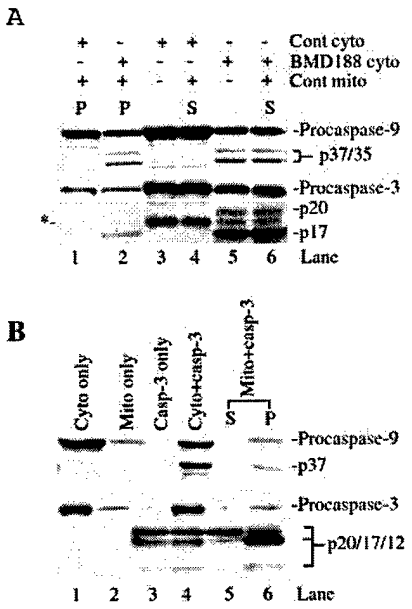

FIG. 8. **Activation of the mitochondrial procaspases in the organelle.** *A*, cell-free recombination experiments to show that the active caspases in the BMD188-actived cytosols may activate the mitochondrially localized procaspases. Cytosol (*cyto*) and mitochondria (*mito*) were isolated from control or BMD188-treated GM701 cells. Control or treated cytosol (30 μg) was then co-incubated with control mitochondria (40 μg) for 1 h at 37 °C. At the end of incubation, cytosol (*S*) and mitochondria (*P*) were separated by centrifugation followed by Western blotting for caspase-9, and -3. The *asterisk* indicates the unknown p19 band. *B*, recombinant active caspase-3 can activate the mitochondrially localized procaspase-9 and procaspase-3. Cytosol (40 μg; *lane 1*) and mitochondria (30 μg; *lane 2*), freshly prepared from untreated GM701 cells, were incubated with recombinant active caspase-3 (*lanes 4–6*, respectively). *S* and *P* refer to the supernatant and mitochondrial pellet, respectively, at the end of the incubation. As a control, an aliquot (5 ng) of the recombinant caspase-3 was also run on the same gel (*lane 3*). Data are representative of 3 independent experiments.

cytosol with the mitochondria for 1 h resulted in specific translocation of the p20 active caspase-3 band to the mitochondria with a concomitant decrease in the cytosolic p20 (Fig. 7*D*, *lanes 4–6*). There was also a decrease in the mitochondrial procaspase-3 (Fig. 7*D*, compare *lane 6 versus lane 3*). Co-incubation for 3 h resulted in the accumulation of more p20 band as well as the p17 and p24 bands in the mitochondria (Fig. 7*C*, *lanes 7* and *8 versus lanes 5* and *6*), without a further decrease in the mitochondrial procaspase-3 (Fig. 7*D*, *lane 8 versus lane 6*).

Mitochondrial Procaspases Can Be Activated in the Organelle—The above cell-free reconstitution experiments have established that the mitochondrial active caspase-9 and -3 result mostly from translocation. Some evidence suggests that the mitochondrial procaspases may *also* become activated by translocated active caspases (see above). Therefore, we performed several additional cell-free experiments to address further this possibility. First, we performed a cell-free recombination experiment in which the freshly isolated mitochondria were co-incubated with either untreated or BMD188-treated GM701 cell cytosol and then separated the mitochondrial pellet from the cytosol. The rationale is that the BMD188-activated caspases in the cytosol may directly activate the mitochondrially localized procaspases, or translocate to the mitochondria, or both. As shown in Fig. 8*A*, the BMD188-treated cytosol had active caspase-9 (p37/p35) and caspase-3 (p20/p17) (*lane 5*), whereas the control cytosol had neither (*lane 3*). Correspondingly, the control cytosol had more procaspases than the BMD188-activated cytosol (Fig. 8*A*, compare *lane 3 versus lane 5*). After co-incubation for 1 h, nearly identical amounts of both procaspase-9 or -3 and their activated forms were recovered from the supernatant (Fig. 8*A*, compare *lane 6 versus 5*). Nevertheless, activated forms of both caspase-9 and caspase-3 were identified in the mitochondrial pellets concomitant with a decrease in the corresponding procaspases in the mitochondria (Fig. 8*A*, compare *lane 2 versus lane 1*). When the co-incubation was extended to 2 h, a further decrease in the mitochondrial procaspases was observed (not shown). These results suggest that, in this cell-free system, small amounts of the activated caspases in the cytosol may have permeabilized the OMM (48, 49), gained access to and subsequently activated the mitochondrially localized procaspase-9 and -3 in the organelle.

To explore further this possibility, we directly incubated the intact mitochondria with recombinant active caspase-3 to see whether the mitochondrially localized procaspase-9 or -3 can *ever* be activated in the organelle. As shown in Fig. 8*B*, unactivated cytosol (*lane 1*) and mitochondria (*lane 2*) showed only procaspase-9 and procaspase-3 bands. The recombinant caspase-3 showed p20, p17, and p12 bands (Fig. 8*B*, *lane 3*). Co-incubation of the cytosol with active caspase-3 generated, as expected, the p37 active caspase-9, resulting from procaspase 9 cleavage at Asp^{330} by caspase-3 (40). Similarly, co-incubation of the mitochondria with active caspase-3 also generated the p37 active caspase-9 concomitant with a decrease of procaspase-9, both of which were detected exclusively in the mitochondrial pellet (Fig. 8*B*, compare *lane 6* with *lane 2*). These results suggest that exogenously added active caspase-3 entered the mitochondria and activated the procaspase-9 in the organelle. Surprisingly, co-incubation of the cytosol with active caspase-3 did not lead to obvious caspase-3 activation in the cytosol (Fig. 8*B*, compare *lane 4* with *lane 3*). When the mitochondria were incubated with the active caspase-3, most p12 was recovered from the mitochondrial pellet (Fig. 8*B*, *lane 6 versus 3*), and little p17 was recovered from the supernatant (Fig. 8*B*, *lane 5 versus lane 3*), whereas slightly more p20 was recovered from the supernatant (Fig. 8*B*, *lane 5 versus lane 3*), suggesting that most of the exogenously supplied p17/p12 (but not p20) caspase-3 translocated to the mitochondria. However, there was a prominent increase in the level of p17 in the mitochondrial pellet concomitant with decreased procaspase-3 as well as p20 (Fig. 8*B*, *lane 6 versus lanes 2* and *3*). Since the p17 fragment comes mainly from caspase-3-mediated autocatalysis (44, 45), these results, together, suggest the following: 1) the p17/12 caspase-3 enters the mitochondria to activate the procaspase-9 and -3 in the organelle, and 2) the activated mitochondrial caspase-9 (*i.e.* the p37) may further activate the mitochondrial procaspase-3, which autocleaves more procaspase-3 to generate more p17.

DISCUSSION

The current study focuses on the mitochondria-associated active caspase-9 and caspase-3. The multifaceted results allow us to present a model (Fig. 9) to explain their location, origin, relationship with the cytosolic counterparts, and potential biological functions. In response to apoptotic stimulation, several mitochondrial proteins such as the IMS protein cyt. c and the matrix protein Hsp60 are released, involving CsA-sensitive MMP. In certain apoptotic systems, the mitochondrial procaspases are similarly released into the cytosol, some of which translocate to the perinuclear area. In a similar fashion, Apaf-1, which is located exclusively in the cytosol, also translocates to the perinuclear region (Fig. 9). The released cyt. c triggers apoptosome formation in the cytosol leading to caspase-9 and, subsequently, caspase-3 activation. The activated caspase-9 and -3 rapidly translocate back to the mitochondria where they may further activate residual or other

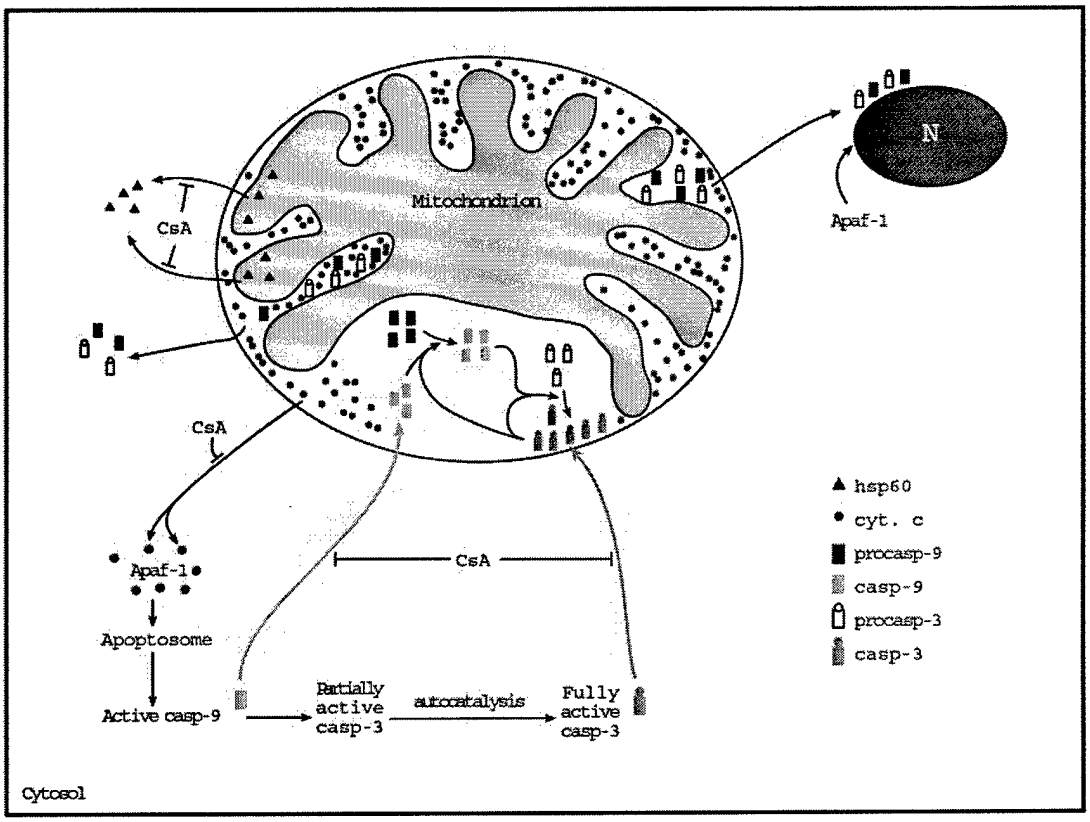

FIG. 9. **A hypothetical model illustrating the dynamic movements of various apoptosis-related molecules in different subcellular compartments during apoptosis.** *Casp.*, caspase. See text for detailed discussion.

resident procaspases in the organelle, degrade mitochondrial proteins, disintegrate mitochondria, and help drive the apoptotic process to completion.

Active Caspases in the Mitochondria: Unlikely Involvement of Apaf-1 in the Activation of Procaspase-9 in the Organelle—A multitude of studies have demonstrated the presence of pro- and activated caspases in the mitochondria (14, 17–19, 21, 27, 28, 50), although this phenomenon has been challenged recently (51). The reason for this discrepancy remains unclear, but the negative results may likely result from cell type-specific variations, different antibodies used, insufficient protein loading, and utilization of digitonin-permeabilized mitochondria (51). Our well controlled experiments using mitochondria prepared by either Percoll gradient purification (Fig. 2) or differential centrifugation (the rest) demonstrate the presence of procaspases in unstimulated mitochondria and, more importantly, of activated caspases in apoptosis-stimulated mitochondria. Like their procaspase counterparts, the activated caspase-9 and -3 are localized in the IMS of the mitochondria (Fig. 5).

Our recent observation (30) that a wide diversity of apoptotic inducers cause an early up-regulation and accumulation of cyt. c in the mitochondria raises the following intriguing question. Could this increased mitochondrial cyt. c lead to procaspase-9 activation right in the organelle analogous to apoptosome-mediated procaspase-9 activation in the cytosol? Several pieces of evidence make our initial hypothesis unlikely. First, in all our apoptotic models the initial appearance of the activated caspase-9 in the mitochondria occurs either following or concomitant with the caspase-9 activation in the cytosol without proteolytic degradation of the mitochondrial procaspase-9 (Fig. 3). These observations suggest that caspase-9 activation is initiated in the cytosol. Second, Apaf-1, the key adaptor molecule in apoptosome-mediated caspase-9 activation, is exclusively expressed in the cytosol, consistent with the observations of other investigators (46), and is never found in the mitochondria. Third, even after apoptotic stimulation, no association of Apaf-1 with the mitochondrial fractions is observed (Fig. 3, *A–D*). Finally, cell-free reconstitution experiments demonstrate that cyt. c does not directly activate the mitochondrial procaspase-9 although it completely activates the cytosolic procaspase-9 (Fig. 7*A*), thus confirming the lack of Apaf-1 in the mitochondria. These observations make it clear that procaspase-9 cannot be activated inside the mitochondria in an Apaf-1/apoptosome-dependent manner.

Interestingly, in all the apoptotic models studied here, cytosolic Apaf-1 rapidly translocates to the perinuclear area, similar to recent findings (52) in different mammalian cells. Remarkably, the Apaf-1 homologue in *Caenorhabditis elegans*, CED-4, also translocates to the nuclear membrane during apoptosis (53). What could be the functions of this translocation? One clue is that, in addition to Apaf-1, cyt. c (52), procaspase-9 and -3 (this study), and many other caspases (22–24, 26, 28, 29) also become associated with the nucleus during apoptosis. It is possible that these molecules move together to assemble functional apoptosomes to induce caspase activation in or around the nucleus in order to disassemble the nuclear cytoplasmic barrier (54) and catalyze the systematic degradation of the nucleus.

Active Caspases in the Mitochondria Are Derived Mostly from the Translocation—If the Apaf-1-containing apoptosome is not involved, then how is the mitochondrial active caspase-9 brought about? Although Apaf-1-independent mechanisms recently emerged (11–13) could be involved, the most plausible explanation is that the active caspase-9 in the mitochondria comes from translocation from the cytosol. Supporting evidence comes from PC3 or GM701 cells treated with BMD188 in which increasing levels of the activated caspase-9 are seen in the mitochondria in the absence of corresponding decreases in the

mitochondrial procaspase-9 levels (Fig. 3, *A* and *B*). Instead, the cytosolic procaspase-9 continuously decreases without a corresponding increase in the active caspase-9 (Fig. 3, *A* and *B*). More importantly, in PC3 cells the cytosolic caspase-9 activation occurs prior to the mitochondrial caspase-9 activation (Fig. 3*A*). Cell-free reconstitution experiments also provide clear-cut evidence that the cytosolically activated caspase-9 can translocate to the mitochondria. Translocation seems to be a temperature- and energy-dependent process; translocation is decreased at room temperature and stopped at 4 °C.[2]

The mitochondria-associated active caspase-3 generally appears at the same time when the cytosolic caspase-3 becomes activated (Fig. 3, *A–D*), but at least in some cases, an early translocation of the activated cytosolic caspase-3 to the mitochondria can be suggested. For example, in BMD188-treated PC3 cells, the mitochondrial caspase-3 activation is observed at 45 min post-treatment (Figs. 1, 2, and 3*A*). However, the active mitochondrial caspase-9 is not observed by this time (Fig. 3*A*), suggesting that the active caspase-3 in the mitochondria probably comes from translocation from the cytosol. In addition, increasing amounts of both active caspase-3 (*i.e.* the p20 fragment) as well as the procaspase-3 are observed in the mitochondria (Fig. 3*A*). Finally, cell-free reconstitution experiments show that the cytosolically activated caspase-3 can indeed translocate to the mitochondria (Fig. 7).

How may activated caspases translocate to the IMS of the mitochondria? It is still unclear how various procaspases, which generally lack an identifiable mitochondria-targeting sequence (51), get into the IMS. Evidence presented here suggests that a CsA-inhibitable mechanism(s) seems to be responsible, at least partially, for both the early release of the mitochondrial proteins such as cyt. c and Hsp60 as well as for the later translocation of the activated caspases back to the mitochondria. CsA, which has been shown to inhibit apoptosis in multiple model systems, is generally thought to block apoptosis by inhibiting MMP (48, 49). CsA has been shown recently (55) to also inhibit the remodeling of the mitochondrial cristae and consequently inhibit cyt. c release. How mitochondrial proteins are released from the mitochondria is still controversial, but it seems to involve different types of channels consisting of proapoptotic Bcl-2 proteins such as Bax and Bak and some resident mitochondrial proteins such as VDAC (reviewed in Refs. 48 and 49). Consistent with our earlier data (30), CsA inhibits the early release of both cyt. c and Hsp60 (Fig. 6), thus suggesting the potential involvement of MMP in this process. Interestingly, CsA also appears to inhibit the later translocation of active caspases as it specifically reduces their levels in the mitochondria (Fig. 6). These results suggest that translocation of the activated caspases back to the mitochondria might use a CsA-sensitive mechanism(s) similar to those utilized for the initial mitochondrial protein release. It is unclear how the activated cytosolic caspase-9, most of which is thought to remain bound to the apoptosome (38–40), gets to the mitochondria. The supramolecular openings formed by Bid, Bax, and the mitochondrial membrane lipids can release molecules of 2,000 kDa (56), which should be sufficient to "entertain" the 700-kDa to 1.4-MDa apoptosome. However, Apaf-1 is never detected in the mitochondria. It is possible that some activated caspase-9, especially those activated by caspase-3, may not be apoptosome-bound and thus be free to translocate to the mitochondria.

Recent evidence (6–10) suggests that, in some apoptotic systems, caspase-2 activation precedes or may even be required for the compromise of the mitochondrial integrity such as cyt. c release. Our data suggest that, in our systems, caspase activation occurs after the disruption of the mitochondrial integrity and function (30) (Fig. 6 of this study). More importantly, Z-VAD does not affect the initial release of the mitochondrial proteins (Fig. 6). Since Z-VAD inhibits caspase activation, as expected, but the activated caspase-9 and -3 are still observed in the mitochondria, the reduced levels of the mitochondria-associated active caspases (Fig. 6) mostly likely are caused by the overall inhibition of caspase activation rather than inhibition of translocation.

Active Caspases in the Mitochondria May Also Derive Partly from the Caspase-mediated Activation in the Organelle—Conceptually, translocated active caspases may subsequently activate the mitochondrial procaspases in the organelle. Several pieces of evidence support this possibility. First, late during apoptosis most mitochondrial procaspase-9 (Fig. 3*D*) and procaspase-3 (Fig. 3, *B–D*) becomes completely proteolyzed. Second, cell-free reconstitution experiments suggest that the mitochondrial procaspase-9 and -3 may become proteolytically activated in the organelle (Fig. 7, *C* and *D*). Third, cell-free recombination experiments also suggest direct procaspase activation in the mitochondria (Fig. 8*A*). Finally, both mitochondrial procaspase-9 and -3 can be activated by recombinant active caspase-3 (Fig. 8*B*). Various cell-free experiments using intact mitochondria (Figs. 7 and 8) suggest that a small amount of activated caspases may permeabilize the OMM (47, 48), enter the IMS, and activate the mitochondrially localized procaspases. Under continuous apoptotic stimulation presumably the MMP persists, thus allowing the access of the cytosolically activated caspases to the IMS without the obvious need for caspase-mediated permeabilization, which explains why CsA but not Z-VAD inhibits caspase translocation to the mitochondria (Fig. 6).

The Potential Biological Functions of the Mitochondrially Localized Active Caspases—Multiple pieces of evidence suggest that the active caspases in the mitochondria may play a role in apoptosis. First, significant amounts of activated caspase-9 and -3 are accumulated in the mitochondria, especially late during apoptosis (Fig. 3, *A–D*). In support, significant caspase activities are detected in the mitochondria (Figs. 1 and 2; and data not shown). Second, in the reconstitution experiments, activated caspases preferentially translocate to the mitochondria (Fig. 7). Third, the preferential association of the active caspase-3 with the mitochondria seems to be essential for the complete activation of caspase-9.[2] Finally, the cytosolic procaspase-3 does not seem to be efficiently activated by exogenous active caspase-3 in the absence of the mitochondria (Fig. 8*B*).

Presumably, the activated caspase-9 and -3 in the mitochondria can play the following functions. First, they may further activate residual or other resident procaspases in the organelle (Fig. 9). Thus the expression of the active caspases in the mitochondria establishes a positive feedback amplification mechanism. Second, they may degrade some mitochondrial proteins. It is interesting to note that compared with the known caspase substrates in the cytosol and other organelles, few distinct mitochondrial substrates have been identified. Recently, caspase-9 is shown to be able to degrade certain cellular components other than caspases (57). Therefore, it is possible that active caspase-3 as well as caspase-9 in the mitochondria may specifically degrade some mitochondrial substrates such as the MRC protein complexes. Third, the mitochondrial active caspase-9 and -3 may further disintegrate mitochondrial integrity and function such as facilitating MMP, cyt. c release, and generation of reactive oxygen species (58). Together these functions help drive the apoptotic process to completion.

[2] D. Chandra and D. G. Tang, unpublished observations.

Acknowledgments—We thank M. King for providing GM701.2-8C cells; Biomide Corp. for BMD188; X. Wang for antibody against Smac; A. Ellis for help with EM; and members of the Tang laboratory for helpful discussions. We also thank S. Bratton for helpful discussions and critically reading the manuscript.

REFERENCES

1. Horvitz, H. R. (1999) *Cancer Res.* **59,** S1701–S1706
2. Salvesen, G. S., and Dixit, V. M. (1997) *Cell* **91,** 443–446
3. Thornberry, N. A., and Lazebnik, Y. (1998) *Science* **281,** 1312–1316
4. Wang, X. (2001) *Genes Dev.* **15,** 2922–2933
5. Ashkenazi, A., and Dixit, V. M. (1998) *Science* **281,** 1305–1308
6. Guo, Y., Srinivasula, S. M., Druilhe, A., Fernandes-Alnemri, T., and Alnemri, E. S. (2002) *J. Biol. Chem.* **277,** 13430–13437
7. Paroni, G., Henderson, C., Schneider, C., and Brancolini, C. (2002) *J. Biol. Chem.* **277,** 15147–15161
8. Robertson, J. D., Enoksson, M., Suomela, M., Zhivotovsky, B., and Orrenius, S. (2002) *J. Biol. Chem.* **277,** 29803–29809
9. Lassus, P., Opitz-Araya, X., and Lazebnik, Y. (2002) *Science* **297,** 1352–1354
10. Read, S. H., Baliga, B. C., Ekert, P. G., Vaux, D. L., and Kumar, S. (2002) *J. Cell Biol.* **159,** 739–745
11. Marsden, V. S., O'Connor, L., O'Reilly, L., Silke, J., Metcalf, D., Ekert, P. G., Huang, D. C. S., Cecconi, F., Kuida, K., Tomaselli, K. J., Roy, S., Nicholson, D. W., Vaux, D., Bouillet, P., Adams, J. M., and Strasser, A. (2002) *Nature* **419,** 634–637
12. Rao, R. V., Castro-Obregon, S., Frankowski, H., Schuler, M., Stoka, V., del Rio, G., Bredsen, D. E., and Ellerby, H. M. (2002) *J. Biol. Chem.* **277,** 21836–21842
13. Morishima, N., Nakanishi, K., Takenouchi, H., Shibata, T., and Yasuhiko, Y. (2002) *J. Biol. Chem.* **277,** 34287–34294
14. Zhivotovsky, B., Samali, A., Gahm, A., and Orrenius, S. (1999) *Cell Death Differ.* **6,** 644–651
15. Mancini, M., Machamer C. E., Roy, S., Nicholson, D. W., Thornberry, N. A. Casciola-Rosen, L. A., and Rosen, A. (2000) *J. Cell Biol.* **149,** 603–612
16. Nakagawa, T., Zhu, H., Morishima, N., Li, E., Xu, J., Yankner, B. A., and Yuan, J. (2000) *Nature* **403,** 98–103
17. Susin, S. A., Lorenzo, H. K., Zamzami, N., Marzo, I., Brenner, C., Larochette, N., Prevost, M. C., Alzari, P. M., and Kroemer, G. (1999) *J. Exp. Med.* **189,** 381–394
18. Mancini, M., Nicholson, D. W., Roy, S., Thornberry, N. A., Peterson, E. P., Casiola-Rosen, L. A., and Rosen, A. (1998) *J. Cell Biol.* **140,** 1485–1495
19. Samali, A., Zhivotovsky, B., Jones, D. P., and Orrenius, S. (1998) *FEBS Lett.* **431,** 167–169
20. Quin, Z. H., Wang, Y., Kikly, K. K., Sapp, E., Kegel, K. B., Aronin, N., and DiFiglia, M. (2001) *J. Biol. Chem.* **276,** 8079–8086
21. Krajewski, S., Krajewska, M., Ellerby, L. M., Welsh, K., Xie, Z. H., Deveraux, Q. L., Salvesen, G. S., Bredesen, D. E., Rosenthal, R. E., Fiskum, G., and Reed, J. C. (1999) *Proc. Natl. Acad. Sci. U. S. A.* **96,** 5752–5757
22. Nakagawara, A., Nakamura, Y., Ikeda, H., Hiwasa, T., Kuida, K., Su, M. S., Zhao, H., Cnaan, A., and Sakiyama, S. (1997) *Cancer Res.* **57,** 4578–4584
23. Mao, P.-L., Jiang, Y., Wee, B. Y., and Porter, A. G. (1998) *J. Biol. Chem.* **273,** 23621–23624
24. Fujita, E., Kouroku, Y., Jimbo, A., Isoai, A., Maruyama, K., and Momoi, T. (2002) *Cell Death Differ.* **9,** 1108–1114
25. Chandler, J. M., Cohen, G. M., and MacFarlane, M. (1998) *J. Biol. Chem.* **273,** 10815–10818
26. Colussi, P. A., Harvey, N. L., and Kumar, S. (1998) *J. Biol. Chem.* **273,** 24535–24542
27. Costantini, P., Bruey, J.-M., Castedo, M., Metivier, D., Loeffler, M., Susin, S. A., Ravagnan, L., Zamzami, N., Garrido, C., and Kroemer, G. (2002) *Cell Death Differ.* **9,** 82–88
28. Krajewska, M., Wang, H.-G., Krajewski, S., Zapata, J. M., Shabaik, A., Gascoyne, R., and Reed, J. C. (1997) *Cancer Res.* **57,** 1605–1613
29. Martins, L. M., Kottke, T., Mesner, P. W., Basi, G. S., Sinha, S., Frigon, N., Jr., Tatar, E., Tung, J. S., Brynt, K., Takahashi, A., Svingen, P. A., Madden, B. J., McCormick, D. J., Earnshaw, W. C., and Kaufmann, S. H. (1997) *J. Biol. Chem.* **272,** 7421–7430
30. Chandra, D., Liu, J.-W., and Tang, D. G. (2002) *J. Biol. Chem.* **277,** 50842–50854
31. Tang, D. G., Li, L., Zhu, Z., and Joshi, B. (1998) *Biochem. Biophys. Res. Commun.* **242,** 380–384
32. Joshi, B., Li, L., Taffe, B. G., Zhu, Z., Wahl, S., Tian, H., Ben-Josef, E., Taylor, J. D., Porter, A. T., and Tang, D. G. (1999) *Cancer Res.* **59,** 4343–4355
33. Petit, P. X., O'Connor, J. E., Grunwald, D., and Brown, S. C. (1990) *Eur. J. Biochem.* **194,** 389–397
34. Tang D. G., Li, L., Chopra, D. P., and Porter, A. T. (1998) *Cancer Res.* **58,** 3466–3479
35. Antonsson, A., Montessuit, S., Sanchez, B., and Martinous, J.-C. (2001) *J. Biol. Chem.* **276,** 11615–11623
36. Slee, E. A., Harte, M. T., Kluck, R. M., Wolf, B. B., Casiano, C. A., Newmeyer, D. D., Wang, H. G., Reed, J. C., Nicholson, D. W., Alnemri, E. S., Green, D. R., and Martin, S. J. (1999) *J. Cell Biol.* **144,** 281–292
37. Bratton, S. B., Walker, G., Roberts, D. L., Cain, K., and Cohen, G. M. (2001) *Cell Death Differ.* **8,** 425–433
38. Srinivasula, S. M., Ahmad, M., Fernandez-Alnemri, T., and Alnemri, E. S. (1998) *Mol. Cell* **1,** 949–957
39. Srinivasula, S. M., Hedge, R., Saleh, A., Dhatta, P., Shiozaki, E., Chai, J., Lee, R. A., Robbins, P. D., Fernandez-Alnemri, T., Shi, Y., and Alnemri, E. S. (2001) *Nature* **410,** 112–116
40. Bratton, S. B., Walker, G., Srinivasula, S. M., Sun, X. M., Butterworth, M., Alnemri, E. S., and Cohen, G. M. (2001) *EMBO J.* **20,** 998–1009
41. Budihardjo, I., Oliver, H., Lutter, M., Luo, W., and Wang, X. (1999) *Annu. Rev. Cell Dev. Biol.* **15,** 269–290
42. Chalfant, C. E., Rathman, K., Pinkerman, R. L., Wood, R. E., Obeid, L. M., Ogretmen, B., and Hannun, Y. A. (2002) *J. Biol. Chem.* **277,** 12587–12595
43. Angelastro, J. M., Moon, N. Y., Liu, D. X., Yang, A.-S., Greene, L. A., and Franke, T. F. (2001) *J. Biol. Chem.* **276,** 12190–12200
44. Li, S., Zhao, Y., He, X., Kim, T.-H., Kuharsky, D. K., Rabinowich, H., Chen, J., Du, C., and Yin, X.-M. (2002) *J. Biol. Chem.* **277,** 26912–26920
45. Deng, Y., Lin, Y., and Wu, X. (2002) *Genes Dev.* **16,** 33–45
46. Hausmann, G., O'Reilly, L. A., van Driel, R., Beaumont, J. G., Strasser, A., Adams, J. M., and Huang, D. C. (2000) *J. Cell Biol.* **149,** 623–634
47. Debatin, K. M., Poncet, D., and Kroemer, G. (2002) *Oncogene* **21,** 8786–8803
48. van Loo, G., Saelens, X., van Gurp, M., MacFarlane, M., Martin, S. J., and Vandennabeele, P. (2002) *Cell Death Differ.* **9,** 1031–1042
49. Jemmerson, R., LaPlante, B., and Treeful, A. (2002) *Cell Death Differ.* **9,** 538–548
50. Krebs, J. F., Armstrong, R. C., Srinivasan, A., Aja, T., Wong, A. M., Aboy, A., Sayers, R., Pham, B., Vu, T., Hoang, K., Karanewsky, D. S., Leist, C., Schmitz, A., Wu, J. C., Tomaselli, K. J., and Fritz, L. C. (1999) *J. Cell Biol.* **144,** 915–926
51. van Loo, G., Saelens, X., Matthijssens, F., Schotte, P., Beyaert, R., Declercq, W., and Vandenabeele, P. (2002) *Cell Death Differ.* **9,** 1207–1211
52. Ruiz-Vela, A., Gonzalez, G., de Buitrago, G., and Martinez-A, C. (2002) *FEBS Lett.* **517,** 133–138
53. Chen, F., Hersh, B. M., Conradt, B., Zhou, Z., Riemer, D., Gruenbaum, Y., and Horvitz, H. R. (2000) *Science* **287,** 1485–1489
54. Faleiro, L., and Lazebnik, Y. (2000) *J. Cell Biol.* **151,** 951–960
55. Scorrano, L., Ashiya, M., Buttle, K., Weiler, S., Oakes, S. A., Mannella, C. A., and Korsmeyer, S. J. (2002) *Dev. Cell* **2,** 55–67
56. Kuwana, T., Mackey, M. R., Perkins, G., Ellisman, M. H., Latterich, M., Schneiter, R., Green, D. R., and Newmeyer, D. D. (2002) *Cell* **111,** 331–342
57. Nakanishi, K., Maruyama, M., Shibata, T., and Morishima, N. (2001) *J. Biol. Chem.* **276,** 41237–41244
58. Ricci, J.-E., Gottlieb, R. A., and Green, D. R. (2003) *J. Cell Biol.* **160,** 65–75

THE JOURNAL OF BIOLOGICAL CHEMISTRY
Vol. 278, No. 27, Issue of July 4, pp. 25091–25100, 2003
Printed in U.S.A.

Subcellular Localization and Tumor-suppressive Functions of 15-Lipoxygenase 2 (15-LOX2) and Its Splice Variants*

Received for publication, February 24, 2003, and in revised form, April 11, 2003
Published, JBC Papers in Press, April 18, 2003, DOI 10.1074/jbc.M301920200

Bobby Bhatia‡§, Carlos J. Maldonado‡¶, Shaohua Tang‡, Dhyan Chandra‡‖, Russell D. Klein‡, Dharam Chopra, Scott B. Shappell‡‡, Peiying Yang§§, Robert A. Newman§§¶¶, and Dean G. Tang‡‖‖**

*From the ‡Department of Carcinogenesis, the University of Texas M. D. Anderson Cancer Center, Science Park Research Division, Smithville, Texas 78957, the **Institute of Chemical Toxicology, Wayne State University, Detroit, Michigan 48226, the ‡‡Department of Pathology, Vanderbilt University School of Medicine, Nashville, Tennessee 37221, and the §§Department of Experimental Therapeutics, University of Texas M. D. Anderson Cancer Center, Houston, Texas 77030*

15-Lipoxygenase 2 (15-LOX2), the most abundant arachidonate (AA)-metabolizing enzyme expressed in adult human prostate, is a negative cell-cycle regulator in normal human prostate epithelial cells. Here we study the subcellular distribution of 15-LOX2 and report its tumor-suppressive functions. Immunocytochemistry and biochemical fractionation reveal that 15-LOX2 is expressed at multiple subcellular locations, including cytoplasm, cytoskeleton, cell-cell border, and nucleus. Surprisingly, the three splice variants of 15-LOX2 we previously cloned, *i.e.* 15-LOX2sv-a/b/c, are mostly excluded from the nucleus. A potential bi-partite nuclear localization signal (NLS), ^{203}RKGLWRSLNEMKRIFNFRR^{221}, is identified in the N terminus of 15-LOX2, which is retained in all splice variants. Site-directed mutagenesis reveals that this putative NLS is only partially involved in the nuclear import of 15-LOX2. To elucidate the relationship between nuclear localization, enzymatic activity, and tumor suppressive functions, we established PCa cell clones stably expressing 15-LOX2 or 15-LOX2sv-b. The 15-LOX2 clones express 15-LOX2 in the nuclei and possess robust enzymatic activity, whereas 15-LOX2sv-b clones show neither nuclear protein localization nor AA-metabolizing activity. To our surprise, both 15-LOX2- and 15-LOX2sv-b-stable clones proliferate much slower *in vitro* when compared with control clones. More importantly, when orthotopically implanted in nude mouse prostate, both 15-LOX2 and 15-LOX2sv-b suppress PC3 tumor growth *in vivo*. Together, these results suggest that both 15-LOX2 and 15-LOX2sv-b suppress prostate tumor development, and the tumor-suppressive functions apparently do not necessarily depend on AA-metabolizing activity and nuclear localization.

15-Lipoxygenase 2 (15-LOX2)[1] is a recently cloned lipoxygenase that shows the highest homology (~80% amino acid identity) to murine 8-LOX, with ~40% identity to human 5-LOX, 12-LOX, or 15-LOX1 (1). It has at least three splice variants (termed 15-LOX2sv-a/b/c) (2, 3) and metabolizes preferentially arachidonic acid (AA) to 15(*S*)-hydroxyeicosatetraenoic acid (15(*S*)-HETE) (1). 15-LOX2 shows an interesting tissue expression pattern, *i.e.* mainly in prostate, lung, skin, and cornea (1–3). This tissue-restricted expression pattern suggests that 15-LOX2 may play a role in the normal development and its abnormal expression/function may contribute to tumorigenesis in these organs. Indeed, work by Shappell *et al.* (4–6) indicates that 15-LOX2 mRNA, protein expression, and enzymatic activity are decreased in high grade prostate intraepithelial neoplasia (PIN) and prostate cancer (PCa), and the expression levels of 15-LOX2 are inversely correlated with the pathological grade (Gleason scores) of the patients. We recently reported that 15-LOX2 is a negative cell-cycle regulator in normal human prostate (NHP) epithelial cells (3). These observations (3–6) together raise the possibility that 15-LOX2 may represent an endogenous prostate tumor suppressor, and its down-regulation may contribute to PCa development. Here we provide experimental data in support of this possibility as restoration of 15-LOX2 expression inhibits PCa cell proliferation *in vitro* and tumor development *in vivo*. We further show that the tumor-suppressive functions of 15-LOX2 do not necessarily depend on the AA-metabolizing activity and nuclear localization as 15-LOX2sv-b, a splice variant that does not metabolize AA and is mostly excluded from nucleus, demonstrates similar inhibitory effect on PCa development.

MATERIALS AND METHODS

Cells and Reagents—Six primary NHP cell strains, NHP1–NHP6, were prepared from six different donors. NHP1, NHP3, NHP4, and NHP6 cells were obtained from Clonetics (Walkersville, MD), and NHP2 and NHP5 cells were generated as previously described (7–9). These cells were cultured in serum-free, PrEBM medium (Clonetics)

* This work was supported in part by NCI, National Institute of Health (NIH) Grant CA-90297, Burroughs-Wellcome Fund Award BWF-1122, Department of Defense Grant DAMD17-03-1-0137, NIEHS, NIH Cancer Center Grant ES07784, and University of Texas M. D. Anderson Cancer Center Institutional fund (to D. G. T). The costs of publication of this article were defrayed in part by the payment of page charges. This article must therefore be hereby marked "*advertisement*" in accordance with 18 U.S.C. Section 1734 solely to indicate this fact.

§ A student in the Graduate School of Biomedical Sciences program.

¶ Supported by NIH Post-doctoral Training Grant T32 CA09480-16.

‖ Supported by Department of Defense Postdoctoral Traineeship Award DAMD17-02-1-0083.

¶¶ Supported by NCI, NIH Cancer Center Support Grant CA16672.

‖‖ To whom correspondence should be addressed: Dept. of Carcinogenesis, the University of Texas M. D. Anderson Cancer Center, Science Park Research Division, Park Rd. 1C, Smithville, TX 78957. Tel.: 512-237-9575; Fax: 512-237-2475; E-mail: dtang@sprd1.mdacc.tmc.edu.

[1] The abbreviations used are: 15-LOX2, 15-lipoxygenase 2; 15-LOX2sv-a/b/c, 15-lipoxygenase 2 splice variant a, b, or c; AA, arachidonic acid; CAP, cytoskeleton-associated proteins; Cox-II, cytochrome oxidase subunit II; CSK, cytoskeleton; LDH, lactate dehydrogenase; NHP, normal human prostate epithelial cells; PCa, prostate cancer; NLS, nuclear localization signal; PPAR-γ, peroxisome proliferator-activated receptor-γ; WCL, whole cell lysate; DAPI, 4′,6-diamidino-2-phenylindole; 15(*S*)-HETE, 15(*S*)-hydroxyeicosatetraenoic acid; FBS, fetal bovine serum; GFP, green fluorescent protein; HM, heavy membrane; LM, light membrane; MES, 4-morpholineethanesulfonic acid; hrGFP, humanized *Renilla* GFP; IRES, internal ribosomal entry site; UT, untransfected; UG, urogenital; RT, reverse transcription; ER, endoplasmic reticulum; pCMV, cytomegalovirus promoter.

supplemented with insulin, epidermal growth factor, hydrocortisone, bovine pituitary extract, and cholera toxin, and used during passages 2–6 (3). PCa cell lines, *i.e.* PPC-1, PC3, and LNCaP, were cultured in RPMI 1640 supplemented with 10% heat-inactivated fetal bovine serum (FBS) and antibiotics. HEK 293 cells were purchased from ATCC and cultured in Dulbecco's modified Eagle's medium supplemented with 5% FBS and antibiotics.

Rabbit polyclonal anti-15-LOX2 antibody was described before (4). Rabbit polyclonal anti-E-cadherin and goat polyclonal anti-lamin A antibodies were obtained from Santa Cruz Biotechnology Inc. (Santa Cruz, CA). Monoclonal anti-human vinculin (clone hVIN-1) was bought from Sigma (St. Louis, MO). Goat anti-lactate dehydrogenase (LDH) antibody was purchased from Chemicon (Chemicon International, Inc., Temecula, CA). Monoclonal anti-actin and anti-cytochrome *c* oxidase subunit II (Cox-II) antibodies were purchased from ICN (Indianapolis, IN) and BD Pharmingen (San Diego, CA), respectively. A monoclonal anti-BrdUrd (5-bromo-2′-deoxyuridine) antibody and a rabbit polyclonal anti-Bap31 antibody were kindly provided by Drs. M. Raff and G. Shore, respectively. Anti-GFP (green fluorescent protein) antibodies were obtained from Clontech (Palo Alto, CA). All secondary antibodies (goat anti-mouse or -rabbit IgG or rabbit anti-goat IgG conjugated to horseradish peroxidase, fluorescein isothiocyanate, or Rhodamine) were acquired from Amersham Biosciences (Piscataway, NJ). Liposome FuGENE 6 was bought from Roche Applied Science (Indianapolis, IN). All other chemicals were bought from Sigma unless specified otherwise.

Immunohistochemistry of 15-LOX2 Expression in Tissue Sections—Paraffin-embedded sections of normal prostate tissues and PCa were blocked for endogenous peroxidase activity with 3% H_2O_2 in water for 10 min. Antigen retrieval was done by incubating the slides with 10 mM citrate buffer (pH 6.0) for 10 min in a microwave oven. Slides were then blocked for nonspecific binding in 10% goat whole serum (30 min) followed by incubation in anti-15-LOX2 antibody (30 min, room temperature). Slides were finally incubated with goat anti-rabbit IgG conjugated to horseradish peroxidase followed by substrate (dimethyl amino azobenzene) incubation.

Immunofluorescence Detection of 15-LOX2 Expression in Cultured NHP Cells—The basic procedure was as described previously (3). For double labeling of 15-LOX2 and E-cadherin or 15-LOX2 and vinculin, cells were first labeled for 15-LOX2 followed by goat anti-rabbit IgG conjugated to fluorescein isothiocyanate. After post-blocking in 15% goat whole serum, cells were incubated with antibodies against E-cadherin or vinculin followed by secondary antibody conjugated to Rhodamine.

Western Blotting and Subcellular Fractionation—Whole cell lysate (WCL) was prepared in TNC buffer (10 mM Tris acetate, pH 8.0, 0.5% Nonidet P-40, and 5 mM $CaCl_2$) or complete radioimmune precipitation assay (RIPA) buffer (50 mM Tris-HCl, pH 7.5, 150 mM NaCl, 1% Nonidet P-40, 0.5% sodium deoxycholate, 0.5% Triton X-100, 10 mM EDTA) containing protease inhibitor mixture. The WCL prepared in TNC generally contains much lower nuclear, cytoskeletal, or cytoskeleton (CSK)-associated organelles (such as mitochondria) or proteins. Protein concentrations were determined by MicroBCA kit (Pierce, Rockford, IL). Samples containing same amounts of proteins were loaded on 15% SDS-PAGE and Western blotting performed using enhanced chemiluminescence (ECL).

Subcellular fractionation was carried out in log-phase NHP6 cells as previously described (10–13) with slight modifications. Briefly, heavy membrane (HM) and light membrane (LM) fractions and cytosol were prepared using homogenization combined with differential centrifugation. Nuclei were prepared using the NUCLEI EZ PREP kit (Sigma). To prepare CSK and CSK-associated proteins (CAP) (10), NHP6 cells were first lysed in TNC buffer by scraping. The Nonidet P-40-insoluble pellet was extracted (10 min, 3×) on ice with high salt, Triton-containing CSK extraction buffer (600 mM KCl, 1.0 mM $MgCl_2$, 50 mM MES, pH 7.6, 10 μg/ml DNase, 10 μg/ml RNase, 1% Triton X-100, and protease mixture). The Triton-resistant residue was designated as CSK, and the Triton-soluble portions from each extraction were pooled and proteins precipitated with an equal volume of ice-cold acetone (10). The resultant protein pellet was designated CAP (10). 50–100 μg of each subcellular fraction was used in Western blotting for 15-LOX2. Then the same membrane was stripped and reprobed for various marker proteins as detailed in the text.

Establishing Stable PCa Cell Lines Expressing 15-LOX2 or 15-LOX2sv-b—15-LOX2 or 15-LOX2 splice variant cDNAs (3) were subcloned into pIRES-hrGFP (Stratagene, La Jolla, CA), in which the target gene (*i.e.* 15-LOX2 or 15-LOXsv-a/b/c) is driven by pCMV and hrGFP (humanized *Renilla* green fluorescent protein) is transcribed from an internal ribosomal entry site (IRES). The resultant vectors were designated p15-LOX2-hrGFP, p15-LOX2sv-a-hrGFP, p15-LOX2sv-b-hrGFP, and p15-LOX2sv-c-hrGFP, respectively. These vectors, along with pIRES-hrGFP empty vector, were first transiently transfected into 293 cells to characterize their expressions. To establish stable clones, PC3 or LNCaP cells were co-transfected with pIRES-hrGFP, p15-LOX2-hrGFP, or p15-LOX2sv-b-hrGFP and pCMV-neo (Invitrogen) as a selectable marker. 48 h after transfection, G418 was added to the medium (800 μg/ml for LNCaP and 1 mg/ml for PC3 cells, respectively). Two weeks later, antibiotic-resistant PC3 cells were harvested and plated at clonal density (*i.e.* 50–100 cells/10-cm dish) and individual GFP-positive clones were selected, under an inverted fluorescence microscope, using a cloning ring. For LNCaP cells, stable clones were established by first enriching GFP-positive cells using fluorescence-activate cell sorting, followed by a limiting dilution method in 96-well culture plates. Two to four stable clones of each cell type were propagated and characterized by both Western blotting and immunofluorescence microscopy.

Determination of 15-HETE Production in Stably Transfected PCa Cells by Liquid Chromatography and Tandem Mass Spectrometry—Untransfected LNCaP or PC3 cells, or these cells stably transfected with pIRES-hrGFP, p15-LOX2-hrGFP, or p15-LOX2sv-b-hrGFP, were used to measure 15(*S*)-HETE production as previously detailed (3).

Effect of 15-LOX2 Expression on PCa Cell Proliferation—Untransfected PC3 cells or stable PC3 cell transfectants (passage 8) were plated, in quadruplicate, in 24-well flat-bottom culture plates at 5000 cells/well. The cells were cultured in RPMI medium containing 1, 2, or 5% FBS. In some conditions, AA at 1–25 μM was added in the culture medium. 72 h after plating, the numbers of dead and live cells in each well were determined by harvesting both floating and adherent cells and counting using the trypan dye exclusion assays (9). The results were expressed as a percentage of the control, and the experiment was repeated three times.

Effect of 15-LOX2 Expression on PCa Development in Vivo—Surgical orthotopic implantation was carried out to assess the effect of restoration of 15-LOX2 expression on PCa development *in vivo*. The basic procedure was previously described (14). Briefly, animals were anesthetized by intraperitoneal injection of Nembutal Mix (10 μl/g of body weight). Four groups of PC3 cells, *i.e.* untransfected (UT) or cells transfected with pIRES-hrGFP (GFP), p15-LOX2-hrGFP (15-LOX2), or p15-LOX2sv-b-hrGFP (15-LOX2sv-b), all at passage 8, were orthotopically injected into athymic NCr-nu (The Jackson Laboratory, Bar Harbor, ME) nude mouse prostate (2×10^6 in 25 μl of RPMI/prostate). Tumor development was monitored 2 weeks after surgical implantation. About 2 months (*i.e.* 63 days) after implantation, the experiment was terminated, animals were sacrificed, and primary tumors together with the urogenital (UG) organs except bladder were dissected out. Tumor weights (with UG organs) were determined, and prostates from all four groups were used in H-E staining and immunohistochemical analysis.

Nuclear Localization of 15-LOX2 and Its Splice Variants—PC3 or LNCaP cells grown on glass coverslips were either untransfected or transiently transfected with various vectors using FuGENE 6 (3). Cells were fixed 48 h after transfection and then processed for 15-LOX2 staining (3). The distribution of 15-LOX2 in the transfected (*i.e.* GFP^+) cells was observed under a fluorescence microscope. In some cases, stable transfectants of PC3 and LNCaP cells were used in similar studies. In other experiments, cells were used in subcellular fractionation.

Site-specific Mutagenesis of 15-LOX2 and Nuclear Localization Studies—Site-specific mutagenesis was performed to change the 15-LOX2 R203K204, K214R215, and R220R221 to A203S204, R214S215, and A220S221, respectively, using the QuikChange site-specific mutagenesis system (Stratagene) and p15-LOX2-hrGFP as template. A triple mutant was also made. The successfully mutated sequences were confirmed by restriction digestion and sequencing analysis. These 15-LOX2 mutants, along with 15-LOX2 and 15-LOX2sv-a/b expression constructs, were transiently transfected into PC3 cells, and, 48 h later, cells were processed for 15-LOX2 staining.

RT-PCR Analysis of the mRNA Levels 15-LOX2 and Its Splice Variants and Mutants—Log-phase LNCaP cells were transfected with pIRES-hrGFP, p15-LOX2-hrGFP, p15-LOX2sv-a-hrGFP, p15-LOX2sv-b-hrGFP, p15-LOX2sv-c-hrGFP, or four NLS mutants mentioned above. 48 h after transfection, cells were selected by adding G418 (800 μg/ml). Ten days later, these G418-selected LNCaP cells, together with untransfected PC3 cells or PC3 stable clones, were harvested for RT-PCR analysis. Total RNA was isolated with the RNeasy Mini kit (Qiagen), and 0.6 μg of the total RNA was used in RT-PCR analysis using the MasterAmp One-Step RT-PCR kit (Epicenter, Madison, WI). Primers C (5′-ACTACCTCCCAAAGAACTTCCCC-3′, forward) and D (5′-

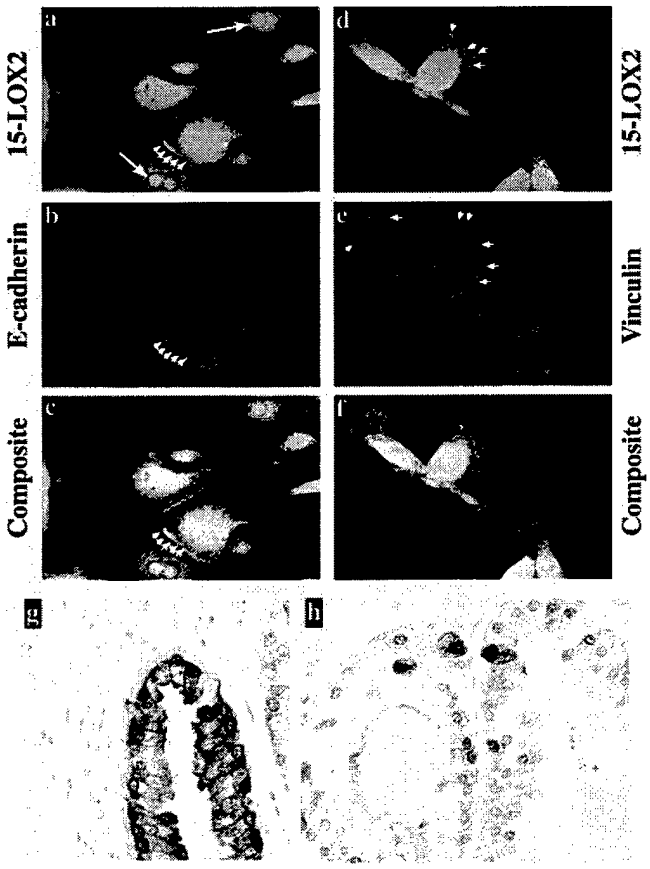

FIG. 1. **Immunofluorescent and immunohistochemical analysis of 15-LOX2 expression in NHP cells *in vitro* and benign prostate epithelial cells *in vivo*.** *a–f*, NHP2 (P5) grown on glass coverslips were double-labeled with 15-LOX2 and E-cadherin (*a* and *b*, respectively) or with 15-LOX2 and vinculin (*d* and *e*, respectively). *c* and *f* are composite images. *Small arrows* indicate the cell-cell border localization of 15-LOX2, whereas the *large arrows* are the nuclear localization. Note the colocalization of 15-LOX2 with E-cadherin (*a–c*) but not with vinculin (*d–f*). *g* and *h*, prostate tissue sections of normal (*g*) or PIN (*h*) glands stained for 15-LOX2 (*brown*). Note clear staining at the cell-cell border as well as in the nuclei in addition to cytoplasmic staining in both images. Original magnifications, ×400 for *a–f* and ×100 for *g* and *h*.

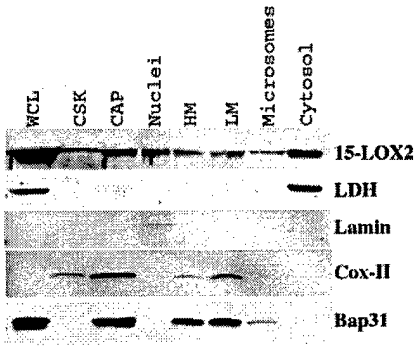

FIG. 2. **Analysis of 15-LOX2 expression by subcellular fractionation.** NHP 6 (P5) cells were fractionated into CSK, CAP, nuclei, HM, LM, microsomes, and cytosol, as detailed under "Materials and Methods." WCL (prepared in TNC buffer) was used as control. Proteins from each fraction (50 μg for CSK and microsomes and 100 μg for all other fractions) were separated on 15% SDS-PAGE and transferred to nitrocellulose membrane. The blot was probed for 15-LOX2 and then for various marker proteins as indicated (see text). *Cox-II*, cytochrome *c* oxidase subunit II; *LDH*, lactate dehydrogenase.

TTCAATGCCGATGCCTGTG-3′, reverse) were used to amplify 15-LOX2 as previously described (3). This pair of primers amplifies 15-LOX2 and 15-LOX2sv-c as a 546-bp band and 15-LOX2sv-a and 15-LOX2sv-b as a 459-bp band (3). RT-PCR of glyceraldehyde-3-phosphate dehydrogenase was used as a control (3). Plasmids (1 ng) were used as positive controls.

Statistical Analysis—Student's *t* test was used to determine the statistical differences between various experimental groups with $p < 0.05$ considered significantly different.

RESULTS

15-LOX2 Is Expressed in the Nucleus and Other Subcellular Locations—15-LOX2 is a negative cell-cycle regulator in NHP cells (3). In an attempt to understand its molecular mechanisms of action, we studied its subcellular expression in cultured primary NHP cells as well as in benign prostate epithelial cells *in vivo*. As observed previously (3), 15-LOX2 was primarily expressed in the cytoplasm. However, significant amounts of 15-LOX2 were also localized at the cell-cell borders (Fig. 1*a*, *small arrows*) as well as in the nuclei (Fig. 1*a*, *large arrows*). The 15-LOX2 distributed at the cell-cell borders partially co-localized with the adhesion molecule E-cadherin (Fig. 1, *a–c*). In some cells, 15-LOX2 was also observed as discrete dots or clusters at the cell periphery (Fig. 1*d*, *arrows*) resembling cell-matrix interaction sites called focal adhesions (15). Double staining of 15-LOX2 and vinculin, a protein marker for focal adhesions (15), however, did not reveal any co-localization (Fig. 1, *d–f*). *In vivo*, 15-LOX2 was also expressed in the cytoplasm, cell-cell borders, as well as in the nuclei (Fig. 1*g*). Note that, as previously reported (4), 15-LOX2 was specifically expressed in the glandular prostate epithelial cells *in vivo* but not in basal cells or other cell types including stromal cells (Fig. 1*g*). Also, as noted previously (5), 15-LOX2 staining was reduced in the precursor lesion PIN (prostate intraepithelial neoplasia), and most cells in these lesions homogeneously lost the 15-LOX2 staining (Fig. 1*h*). However, prominent cell membrane and cell-cell border staining, and, in particular, nuclear staining was still evident in some 15-LOX2-positive cells (Fig. 1*h*).

To confirm the subcellular distribution pattern of 15-LOX2 biochemically, we carried out a fractionation analysis (10–13). NHP6 cells were fractionated into CSK, CAP, nuclei, HM (the 1000 × *g* pellet containing mainly large mitochondria, plasma membrane sheets, and small amounts of other organelles (13, 16)), LM (the 10,000 × *g* pellet containing mainly smaller mitochondria and some lysosomes and peroxisomes (13, 16)), microsomes (*i.e.* the 100,000 × *g* pellet containing ER, Golgi, endosomes, and membrane skeleton (12, 16)), and cytosol (*i.e.* the 100,000 × *g* supernatant (13)). WCL was used as a control. As shown in Fig. 2, consistent with the immunostaining data (Fig. 1), 15-LOX2 was primarily detected in the cytosol, but significant amounts of 15-LOX2 were also detected in the nuclei and CAP. Lower yet easily detectable levels of 15-LOX2 were also observed in all other fractions, including CSK, HM, LM, and microsomes (Fig. 2). As expected, the highest amount of 15-LOX2 was detected in WCL. The purity of each fraction was confirmed by specific markers. For instance, lactate dehydrogenase (LDH), a cytosolic marker (16), was detected only in the cytosol (Fig. 2), suggesting that there was no contamination of all other subcellular fractions by the cytosol. Similarly, lamin A, a nuclear intermediate filament, was detected only in the nuclei. Cytochrome *c* oxidase subunit II (Cox-II), a mitochondrial inner membrane respiratory complex protein, was detected, as expected, most prominently in CAP and also in CSK (Fig. 2), because most mitochondria normally are associated with microtubules and some other cytoskeletal elements (17). Cox-II was also detected, expectedly, in the HM and LM fractions (Fig. 2), which normally are enriched with the mitochondria (11, 13). Note that no lamin A or Cox-II was detected in WCL, probably due to the low levels of nuclei and mitochondria

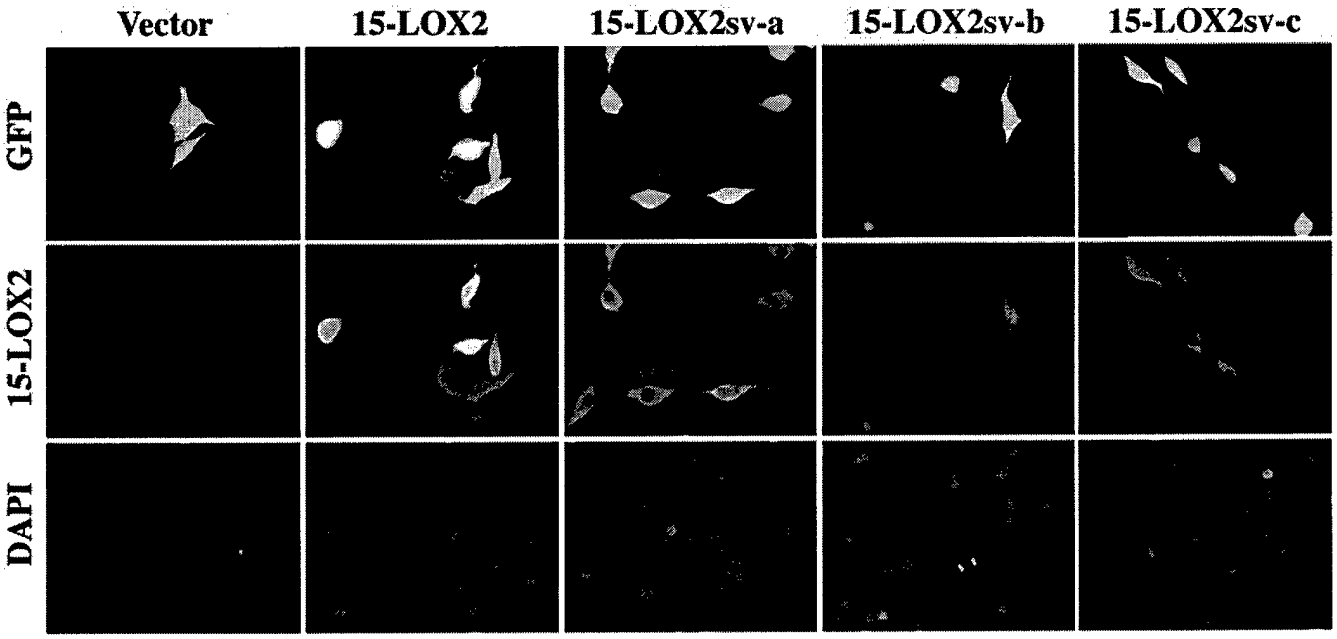

FIG. 3. **Lack of nuclear localization of 15-LOX2 splice variants.** LNCaP cells were transiently transfected with the vector (*pIRES-hrGFP*), p15-LOX2-IRES-hrGFP (*15-LOX2*), p15-LOX2sv-a-IRES-hrGFP (*15-LOX2sv-a*), p15-LOX2sv-b-IRES-hrGFP (*15-LOX2sv-b*), or p15-LOX2sv-c-IRES-hrGFP (*15-LOX2sv-c*). 48 h post transfection, cells were processed for 15-LOX2 immunostaining and nuclei were counterstained by 4′,6-diamidino-2-phenylindole (*DAPI*). Shown are the representative microphotographs of GFP, 15-LOX2, and DAPI images from three independent experiments with comparable results. Over several thousands of cells analyzed, 15-LOX2 splice variants were clearly excluded from the nucleus in the majority (>95%) of the cells, although the strong transgene expression in some cells tended to mask their non-nuclear expression pattern. Original magnifications, ×200.

in the WCL prepared using the TNC buffer (see "Materials and Methods"). Finally, Bap31, an integral ER membrane protein (18), was detected in CAP, HM, LM, microsomes, and WCL, but not in the cytosol, nuclei, or CSK (Fig. 2).

Collectively, data in Figs. 1 and 2 indicate that, in addition to its predominant expression in the cytosol, 15-LOX2 is also expressed at multiple other subcellular locations, including nuclei, cell-cell borders, CSK, and membrane fractions.

None of the Three 15-LOX2 Splice Variants Is Localized to the Nucleus—The nuclear localization of 15-LOX2 is particularly interesting, because it suggests that the molecule may play a distinct signaling function in the nucleus. Therefore, our subsequent studies focused on the nuclear localization of 15-LOX2 and its relationship with the enzymatic and functional activities. We previously cloned three 15-LOX2 splice variants termed 15-LOX2sv-a/b/c (3). These splice variants have spliced out some critical amino acid residues important for the AA-metabolizing enzymatic activities (2, 3). To determine whether these splice variants are also localized in the nucleus, we transiently transfected various expression plasmids into LNCaP cells, which do not express readily detectable levels of 15-LOX2. As shown in Fig. 3, although 15-LOX2 was distributed throughout the cells, including the nucleus as confirmed by subcellular fractionation (not shown), all three splice variants were mostly excluded from the nucleus. Identical results were observed in stably transfected LNCaP (Fig. 4, *a–d*) or PC3 cells (Fig. 4, *e–h*). It should be pointed out that the obvious lack of nuclear staining of 15-LOX2 splice variants was not due to overall reduced protein expression, because comparable levels of 15-LOX2 and its splice variants were observed in multiple experiments of either transiently (*e.g.* Fig. 3) or stably (*e.g.* Fig. 4) transfected PCa cells. A typical example is shown in Fig. 4, in which LNCaP cells stably transfected with 15-LOX2 or 15-LOX2sv-b (Fig. 4, *b* and *d*) or PC3 cells stably transfected with 15-LOX2 or 15-LOX2sv-b (Fig. 4, *f* and *h*) showed very similar levels of protein expression (also see Figs. 5 and 7*b* and the discussion below).

A Putative Nuclear Localization Signal in 15-LOX2 Is Insufficient for Its Nuclear Targeting—Transport between the nucleus and the cytoplasm occurs through the nuclear pore complex on the nuclear envelope, and proteins can enter the nucleus either by diffusion or by signal-mediated transport (19). Generally, only proteins with masses <40 kDa are able to enter the nucleus by passive diffusion (19). Signal-mediated nuclear transport requires energy, optimal temperature, a NLS, and soluble transport machinery (19). Two of the best characterized NLSs are the SV40 large T NLS (often called the classic monopartite NLS), which is composed of a stretch of basic amino acids, and the nucleoplasmin bipartite NLS, which is composed of two basic stretches or clusters separated by 9–12 amino acid residues (19, 20). Recent studies have also revealed other potential NLS (*e.g.* glycine-rich sequences) that do not conform to these two motifs (19, 20).

Because a significant portion of 15-LOX2 is localized in the nucleus, we reason that there may exist one or more specific NLSs in the molecule responsible for its nuclear targeting. Therefore, we looked for a potential NLS in 15-LOX2 by searching an available data base (cubic.bioc.columbia.edu/predictNLS (20)) and by using tools such as PROSITE and MotifScan. We did not find any credible stretch of basic amino acids that would correspond to the monopartite NLS. However, we did uncover a potential bipartite NLS, ^{203}RKGLWRSLNEMKRIFNFRR^{221}, which is located at the N terminus of 15-LOX2. To determine whether this putative NLS plays a role in the nuclear import of 15-LOX2, we used site-specific mutagenesis to mutate the three di-basic amino acid sequences. As shown in Fig. 5, 15-LOX2 transfected into PC3 cells was localized throughout the cells, including nuclear area (*a–c*), whereas both 15-LOX2sv-a and 15-LOX2sv-b were mostly excluded from nuclei (*d–i*). Compared with 15-LOX2-transfected PC3 cells, cells transfected with the 15-LOX2 mutants, *i.e.* 15-LOX2RK/AS (Fig. 5, *j–l*), 15-LOX2KR/RS (Fig. 5, *m–o*), 15-LOX2RR/AS (Fig. 5, *p–r*), or triple mutant (not shown), showed partially reduced nuclear staining. Most cells transfected with the 15-LOX2 mutants

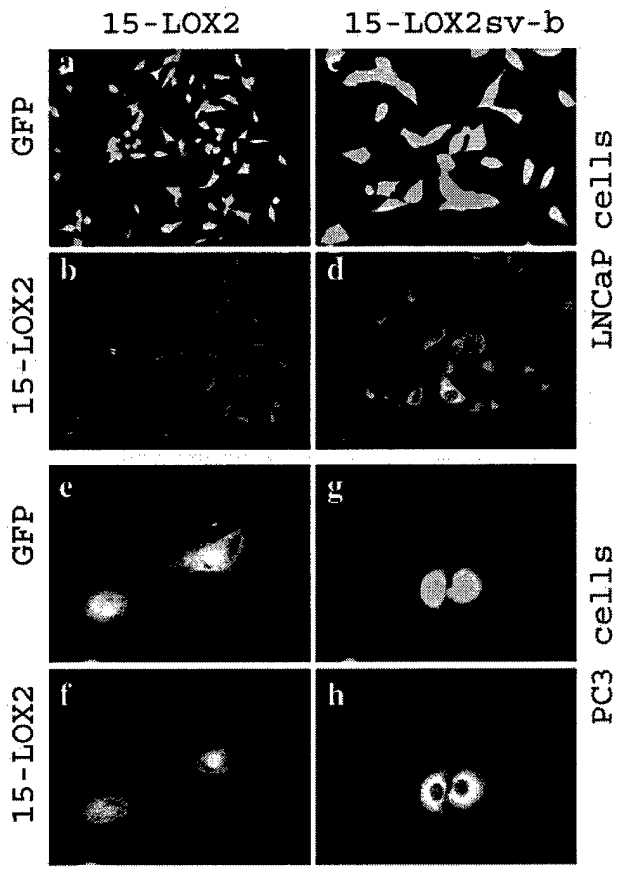

FIG. 4. **Nuclear exclusion of 15-LOXsv-b and similar protein levels of 15-LOX2 and 15-LOX2sv-b in stably transfected PCa cells.** *a–d*, a clone (clone 1) of LNCaP cells stably transfected with p15-LOX2-hrGFP (*a* and *b*) or p15-LOX2sv-b-hrGFP (*c* and *d*) was plated on glass coverslips and processed for immunofluorescent staining using the rabbit polyclonal anti-15-LOX2 antibody (3). Shown are the representative images of GFP (*a* and *c*) and 15-LOX2 (*b*) or 15-LOX2sv-b (*d*). Note that images in *c* and *d* were enlarged to show the non-nuclear expression pattern of 15-LOX2sv-b. Original magnifications: *a* and *b*, ×200; *c* and *d*, ×400. *e–h*, a clone (clone 1) of PC3 cells stably transfected with p15-LOX2-hrGFP (*e* and *f*) or p15-LOX2sv-b-hrGFP (*g* and *h*) was processed for immunofluorescent staining. Shown are the representative images of GFP (*e* and *g*) and 15-LOX2 (*f*) or 15-LOX2sv-b (*h*). Original magnifications: ×400. Untransfected LNCaP or PC3 cells, or LNCaP or PC3 cells stably transfected with pIRES-hrGFP, showed no 15-LOX2 staining (not shown; also see Fig. 3 and Ref. 3). Note that 15-LOXsv-b is mostly excluded from the nucleus in both LNCaP (*d*) and PC3 (*h*) cells and that similar protein levels of 15-LOX2 and 15-LOX2sv-b were observed in stably transfected PCa cells (compare *d versus b* or *h versus f*).

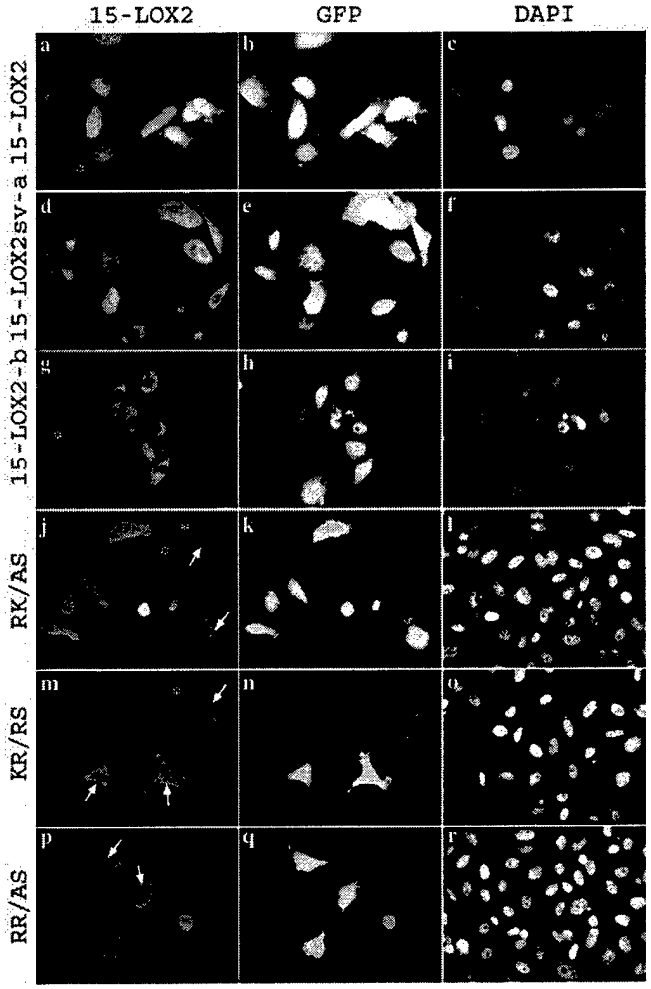

FIG. 5. **Partial involvement of the putative NLS (^{203}RKGLWRSLNEMKRIFNFRR^{221}) in the import of 15-LOX2 to the nucleus.** The *underlined* RK, KR, and RR sequences were mutated individually or in combination as described under "Materials and Methods." The respective expression plasmids, along with 15-LOX2, 15-LOX2sv-a, or 15-LOX2sv-b vectors, were transfected into PC3 cells. Shown are the representative microphotographs of 15-LOX2 (*a*, *d*, *g*, *j*, *m*, and *p*), GFP (*b*, *e*, *h*, *k*, *n*, and *q*), and DAPI (*c*, *f*, *i*, *l*, *o*, and *r*) images. Note that 15-LOX2sv-a (*d*) and 15-LOX2sv-b (*g*) were excluded from the nucleus in most cells, whereas 15-LOX2 was expressed throughout the cell, including the nuclear area (*a*). The RK/AS (*j*), KR/RS (*m*), and RR/AS (*p*) mutants and the triple mutant (not shown) showed reduced nuclear staining (*arrows*). Asterisks in *a*, *d*, *g*, *j*, and *m* illustrate several transfected 15-LOX2-positive cells that are only weakly positive or negative for GFP, probably because GFP was translated downstream of 15-LOX2 through IRES. The images are representative of the results from two independent experiments. Original magnifications: ×200.

showed a nuclear staining intensity between those of 15-LOX2 and 15-LOX2sv-a/b (*e.g.* Fig. 5, *j*, *m*, and *p*; *arrows*). These observations suggest that the Arg^{203}–Arg^{221} NLS is only partially involved in the nuclear import of 15-LOX2.

Similar to the 15-LOX2 splice variants transfected into PCa cells (Figs. 3 and 4), the 15-LOX2 NLS mutants transfected into PC3 cells also showed levels of protein expression comparable to that of 15-LOX2 on immunofluorescence staining (Fig. 5). Because the transient transfection efficiency varied greatly with different expression constructs and the efficiency (1–10%) generally did not allow us to quantify the protein levels by Western blotting, we adopted a different approach to analyze the mRNA levels of 15-LOX2 and its variants or NLS mutants transfected into PCa cells. For this purpose, LNCaP cells were first transiently transfected with various expression constructs followed by selection with G418 for 10 days. At the end of the selection, the majority of G418-resistant cells were GFP-positive, and these enriched cells were then used in RT-PCR analysis using a pair of primers that could pick up 15-LOX2 and all its three splice variants (3). As shown in Fig. 6, untransfected LNCaP cells and LNCaP cells transfected with pIRES-hrGFP did not express 15-LOX2 or any splice variant, consistent with previous observations (3) as well as with protein data (*e.g.* Fig. 3). In contrast, LNCaP cells transfected with 15-LOX2 or its splice variants or NLS mutants showed overall similar mRNA levels (Fig. 6; data not shown for 15-LOX2sv-c and the NLS triple mutant). In fact, we consistently observed slightly higher mRNA levels for most 15-LOX2 splice variants or mutants (Fig. 6). These results are consistent with our immunofluorescence data that show similar protein levels of 15-LOX2 and its variants or NLS mutants transfected into the PCa cells.

Restoration of 15-LOX2 Expression Inhibits PCa Cell Proliferation in Vitro and Prostate Tumor Development in Vivo: 15-LOX2sv-b Also Demonstrates Significant Inhibitory Effect—

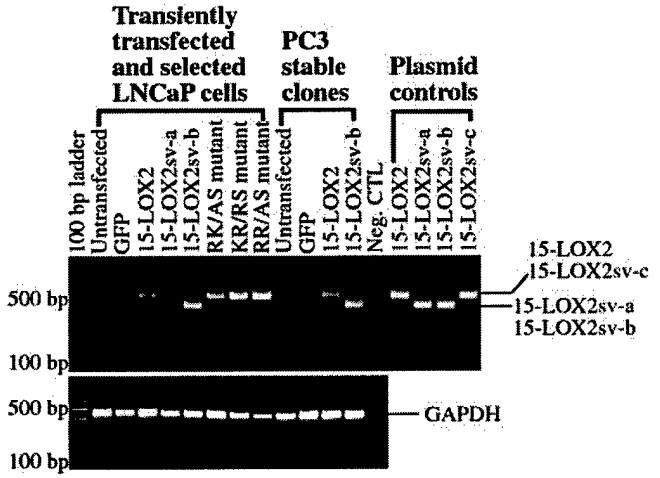

FIG. 6. **Similar levels of mRNA expression of 15-LOX2 and its splice variants or NLS mutants transfected into PCa cells.** LNCaP cells were transiently transfected with various expression constructs, selected for using G418, and then used for RNA extraction and RT-PCR analysis, as detailed under "Materials and Methods." PC3 stable clones were also analyzed for mRNA expression. The RT-PCR was performed using C-D primers, which amplify 15-LOX2 and 15-LOX2sv-c as a 546-bp band and 15-LOX2sv-a and 15-LOX2sv-b as a 459-bp band (3). RT-PCR of glyceraldehyde-3-phosphate dehydrogenase was used as a control (3). The respective plasmids (the *last four lanes*; 1 ng each) were used as positive controls.

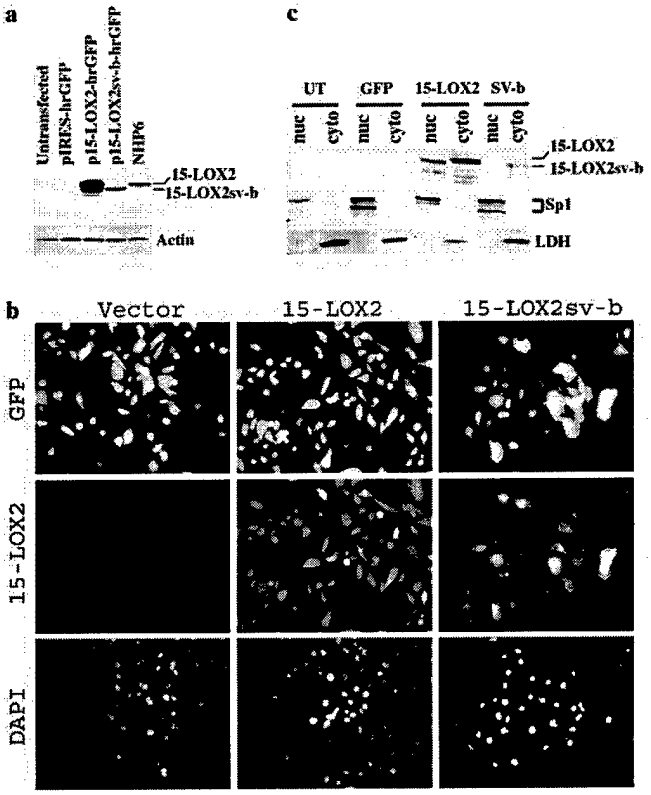

FIG. 7. **Establishment of stable PC3 cell clones expressing 15-LOX2 or 15-LOX2sv-b.** *a*, Western blotting of 15-LOX2 and 15-LOX2sv-b in a stable clone of PC3 cells (passage 6) using 30 μg of whole cell lysate. The 15-LOX2 and 15-LOX2sv-b protein bands were indicated on the *right*. NHP6 (passage 5) cells were used as a positive control. *b*, the same clone of PC3 cells (as shown in *a*) stably transfected with pIRES-hrGFP (*Vector*), p15-LOX2-IRES-hrGFP (*15-LOX2*), or p15-LOX2svb-IRES-hrGFP (*15-LOX2sv-b*), respectively, were stained for 15-LOX2 and nuclei (*DAPI*). Original magnifications, ×200. *c*, nuclear localization of 15-LOX2 but not 15-LOX2sv-b in stably transfected PC3 cells. Subcellular fractionation was carried out as described under "Materials and Methods," and 60 μg of nuclear (*nuc*) or cytosolic (*cyto*) proteins/lane was separated on a 15% SDS-PAGE. After transfer, the membrane was probed for 15-LOX2, stripped, and then reprobed for Sp1 proteins (as a nuclear marker; the *upper bands* being the phosphorylated Sp1) or LDH. Note that several *lower bands* were consistently detected in both cytosolic and nuclear fractions from the cells transfected with 15-LOX2, which might be degradation products.

Most PCa cells demonstrate reduced or lost expression of 15-LOX2 (3–6), suggesting that 15-LOX2 may represent an endogenous prostate tumor suppressor. To directly test this hypothesis, we started by attempting to establish PCa cell lines (PPC-1 and LNCaP) stably expressing 15-LOX2 using the pCMS expression constructs (3), in which 15-LOX2 or its splice variants are driven by the CMV promoter, whereas the EGFP module is driven by the SV40 promoter. Multiple experiments indicated that, although we could initially establish stable clones expressing both 15-LOX2 (or splice variants) and GFP, expression of 15-LOX2 or its splice variants was preferentially lost starting from passage 3 (not shown). These results are consistent with the concept that 15-LOX2, and perhaps its splice variants as well, are inhibitory to PCa cells.

We then made expression constructs in the pIRES-hrGFP vector, in which the transcription of both 15-LOX2 (or splice variants) and hrGFP is controlled by the same CMV promoter and translation of hrGFP is initiated from an internal ribosomal entry site (IRES). When transiently transfected into 293 (not shown) or PCa cells (Figs. 3–6), the expected protein products were detected by immunofluorescence and/or Western blotting. We then used these constructs and established stable PC3 and LNCaP clones expressing 15-LOX2 or 15-LOX2sv-b. Of the several hundred GFP^+ clones transfected with 15-LOX2 or 15-LOX2sv-b that we screened, only ~1% of the cells could be made into long term stable clones. By contrast, ~60% of GFP^+ cells transfected with hrGFP alone could become stable clones. These observations are also consistent with the 15-LOX2 being inhibitory to PCa cells.

Shown in Fig. 7*a* is one clone of PC3 cells expressing 15-LOX2, 15-LOX2sv-b, or GFP alone. Nearly all cells in the clone were GFP-positive but only the cells stably transfected with 15-LOX2 or 15-LOX2sv-b were double positive for 15-LOX2 and GFP (Fig. 7*b*). Again, 15-LOX2 was expressed in the whole cell, including the nucleus, but 15-LOX2sv-b was mostly excluded from the nucleus as revealed by both immunolabeling (Fig. 7*b*) and subcellular fractionation (Fig. 7*c*). Similar results were observed with several other PC3 cells clones as well as with stable LNCaP clones (not shown). Note that in both Western blotting (Fig. 7*a*) and subcellular fractionation (Fig. 7*c*), we observed lower protein levels of 15-LOX2sv-b than 15-LOX2. Similar differences were also observed in transiently transfected 293 cells (3) as well as in other stable clones of PC3 and LNCaP cells (not shown). This difference was unlikely due to differential protein expression as we consistently observed, on immunofluorescence microscopy, very similar protein levels of 15-LOX2 and its splice variants or NLS mutants (Figs. 3–5 and 7*b*). More importantly, we observed similar levels of 15-LOX2 and 15-LOX2sv-b mRNA in the stably transfected PC3 cells (Fig. 6). These observations, together, suggest that the polyclonal anti-15-LOX2 antibody preferentially recognizes 15-LOX2 and does not recognize its splice variants well on Western blotting (*e.g.* Fig. 7, *a* and *c*), although it recognizes equally well the undenatured proteins of 15-LOX2 and its variants or NLS mutants in immunofluorescent staining (*e.g.* Figs. 3–5, and 7*b*). This conclusion is also supported by our multiple experiments with transiently transfected 293 cells as well as with other PCa stable clones (3; data not shown). We are currently developing 15-LOX2 isoform-specific antibodies to directly address this issue.

As expected, untransfected PC3 and LNCaP cells, as well as

TABLE I
15(S)-HETE production in stably transfected PCa cells

15(S)-HETE production was measured in lysates from log-phase cells, in the presence of exogenous AA (100 μM; 37 °C × 10 min) using LC/MS/MS analysis as previously described (3). Data were obtained from two separate experiments and the values are mean ± S.D derived from two to three samples with each cell type.

Cells	15(S)-HETE level
	ng/10⁶ cells
PC3	
Untransfected	0.63 ± 0.18
GFP	1.33 ± 0.15
15-LOX2	27.95 ± 3.16[a]
15-LOX2sv-b	1.77 ± 0.23
LNCaP	
Untransfected	0.85 ± 0.02
GFP	0.73 ± 0.05
15-LOX2	13.42 ± 0.25[a]
15-LOX2[b]	0.024 ± 0.002
15-LOX2sv-b	0.84 ± 0.06

[a] $p < 0.001$ (Student t test).
[b] 15(S)-HETE measurement in the absence of exogenous AA.

PC3 and LNCaP cells, transfected with GFP vector alone produced little 15(S)-HETE (Table I), because they do not express appreciable 15-LOX2 (3). By contrast, cells transfected with 15-LOX2 produced a significant amount of 15(S)-HETE (Table I). In contrast to 15-LOX2-transfected cells, cells transfected with 15-LOX2sv-b, in which two exons have been spliced out (3), produced little 15(S)-HETE (Table I). These measurements were done in the presence of added substrate, AA. In the absence of exogenous AA, the 15-LOX2-transfected LNCaP stable clones produced no 15(S)-HETE (Table I), suggesting that there was very little free AA in the cells under the normal culture conditions. Collectively, these data suggest that the 15-LOX2 in the stably transfected PCa cells is enzymatically active (*i.e.* capable of metabolizing AA), whereas the 15-LOX2sv-b is not.

To assess the effect of 15-LOX2 re-expression on PCa development, we first performed a cell proliferation assay using the stable clones. Consistent with our previous transient transfection experiments (3), PC3 cells stably expressing 15-LOX2 expression proliferated slower than either untransfected cells or the vector-transfected cells (Fig. 8*a*). Surprisingly, PC3 cells stably expressing 15-LOX2sv-b, which does not possess AA-metabolizing activity and is mostly excluded from the nucleus (see above), also showed slower cell proliferation (Fig. 8*a*). The inhibitory effect of 15-LOX2 and 15-LOX2sv-b was observed in either 1% or 5% FBS (Fig. 8*a*). As previously observed (3), re-expression of 15-LOX2 or 15-LOX2sv-b by itself did not affect apoptosis in the transfected cells, which were all healthy (*e.g.* Figs. 3–6, and 7*b*). However, in the presence of exogenous AA, the 15-LOX2 stable clones, but not 15-LOX2sv-b clones, showed a significant increase in apoptosis (not shown). For example, in the presence of 5 μM AA (72 h), only 14% of the PC3 cells stably transfected with 15-LOX2 were alive, compared with 88%, 70%, and 65% survivability in untransfected and PC3 cells stably transfected with GFP or 15-LOX2sv-b, respectively. These results, consistent with previous observations that high doses of 15(S)-HETE induce cell death in PCa cells (3, 21), suggest that the exogenously added AA is metabolized by transfected 15-LOX2 but not 15-LOX2sv-b to produce 15(S)-HETE, which in turn induces cell death.

Next, we carried out an orthotopic tumor implantation experiment in which PC3 cells stably expressing 15-LOX2 or 15-LOX2sv-b or the vector alone were injected into the mouse prostate. The experiment was terminated 63 days post tumor cell inoculation. As shown in Fig. 8 (*b* and *c*), the PC3 tumors

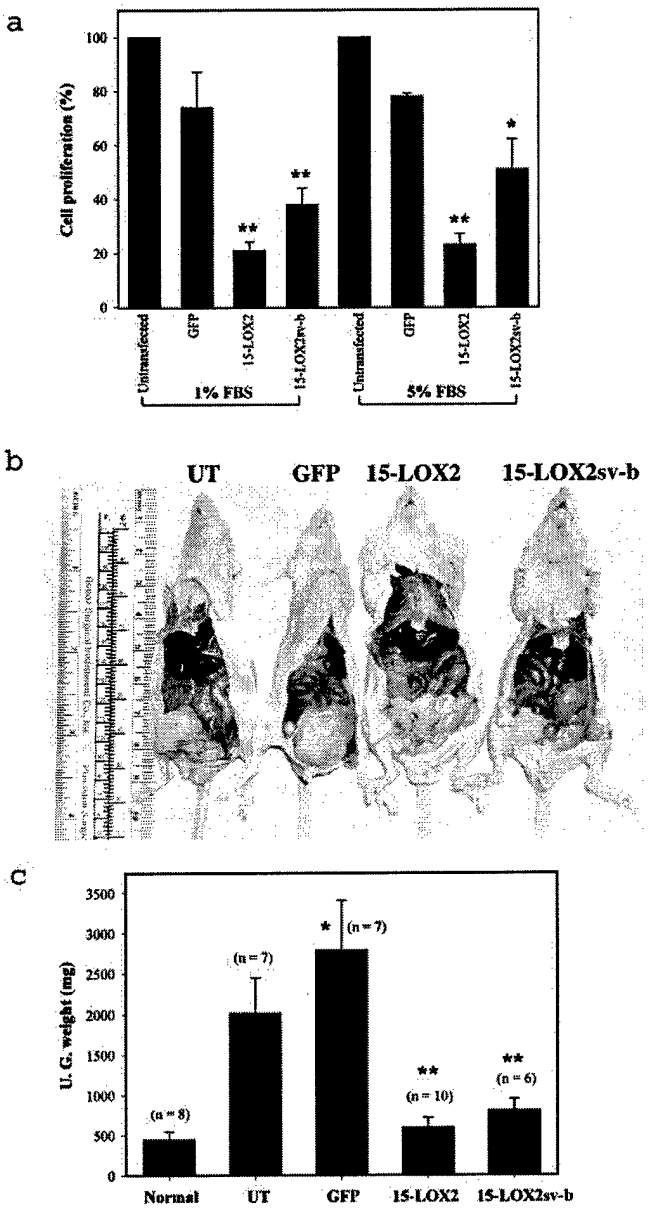

FIG. 8. **Inhibition of PC3 cell proliferation *in vitro* (*a*) and tumor development *in vivo* (*b* and *c*) by restoration of 15-LOX2 expression.** In *a*, proliferation of untransfected PC3 cells 72 h after plating was used as the baseline and considered 100%. Proliferation of PC3 cells stably transfected with pIRES-hrGFP (*GFP*), p15-LOX2-IRES-hrGFP (*15-LOX2*), or p15-LOX2sv-b-IRES-hrGFP (*15-LOX2sv-b*) was presented as percent proliferation of the untransfected PC3 cells. The *bars* represent the mean ± S.D. derived from three independent experiments. *, $p < 0.01$; **, $p < 0.001$. Note that the GFP-transfected stable PC3 cells also proliferated slightly slower (statistically insignificant) than the untransfected controls, as previously observed (3). In *b*, large solid tumors can be easily seen in the UT (untransfected) and GFP groups, whereas the 15-LOX2 and 15-LOX2sv-b groups showed minimal tumor burden. In *c*, the UG (urogenital) weights in the UT and GFP groups are significantly higher ($p < 0.001$) than the uninjected prostates (normal). For unknown reasons, tumors in the GFP group are larger than those in the UT group (*, $p < 0.05$; also see *b*). In contrast, tumors in both the 15-LOX2 and 15-LOX2sv-b groups are significantly (**, $p < 0.001$) smaller than tumors in either the UT or GFP group. The numbers (n) of animals in each group are indicated in the *parentheses*.

bearing 15-LOX2 were significantly smaller than the tumors bearing empty vector (*i.e.* GFP), suggesting that 15-LOX2 re-expression suppresses orthotopically implanted prostate tumor growth *in vivo*. Surprisingly and in support of the *in vitro* data (Fig. 8*a*), the PC3 tumors stably expressing 15-LOX2sv-b were

also significantly smaller than the control tumors (Fig. 8, *b* and *c*). These results together indicate that restored expression of 15-LOX2 inhibits PCa cell proliferation *in vitro* and tumor development *in vivo* by functioning as a negative cell-cycle regulator. Like 15-LOX2, 15-LOX2sv-b also exhibits inhibitory effects.

DISCUSSION

The present study has made the following novel findings: 1) 15-LOX2 is expressed at multiple subcellular locations, including the cell-cell border and nucleus in addition to cytosol; 2) none of the three 15-LOX2 splice variants is expressed in the nucleus; 3) a putative NLS found in the N terminus of 15-LOX2 is partially involved in its nuclear targeting; 4) stable restoration of 15-LOX2 expression in PCa cells inhibits their proliferation *in vitro* and tumor development *in vivo*; and 5) 15-LOX2sv-b, which does not possess the AA-metabolizing activity and is mostly excluded from the nucleus, demonstrates similar inhibitory effects when overexpressed.

Localization of 15-LOX2 at the Cell-Cell Borders—A portion of 15-LOX2 is concentrated at the cell-cell borders in NHP cells *in vitro* as well as in prostate epithelial cells *in vivo* (Fig. 1). Located at the cell-cell borders are cell junctions, including occluding, anchoring, and communicating junctions (22). The anchoring junctions at the cell-cell borders mainly have two types: adherens junctions and desmosomes, both of which hold cells together and are formed by transmembrane adhesion proteins that belong to the cadherin family (22, 23). In adherens junctions, the cytoplasmic tails of cadherins (mainly E-cadherin) bind to anchor proteins (catenins, α-actinin, and vinculin) that tie them to actin filaments (22, 23). In desmosomes, the cytoplasmic tails of cadherins (desmoglein and desmocollin) bind to anchor proteins (plakoglobin and desmoplakin) that tie them to intermediate filaments keratins (22, 23). Interestingly, 15-LOX2 expressed at the cell-cell borders co-localizes with E-cadherin (Fig. 1), the major cadherin molecule expressed in epithelial cells. Western blotting analysis suggests that the 15-LOX2 expression pattern in multiple NHP strains and PCa cell lines coincides with that of a novel E-cadherin splice isoform: both are abundantly expressed in all primary strains and both are lost in all PCa cell lines examined (3).[2] Subcellular fractionation studies indicate that a significant portion of 15-LOX2 localizes to the CAP as well as the cytoskeleton and membrane fractions (Fig. 2). Together, these observations suggest that some 15-LOX2 molecules are probably associated with the E-cadherin-based adherens junctional structures that help maintain the prostate epithelial integrity. A provocative piece of evidence that supports this possibility is that both 15-LOX2 and E-cadherin are down-regulated or lost in PCa cells, and, in both cases, the loss of 15-LOX2 or E-cadherin expression is inversely correlated with grades and stages of the disease (4, 5, 24, 25).

Several other mammalian LOXs have also been shown to be localized in non-cytosolic compartments and interact with some of their constituents. For example, 5-LOX has been reported to bind actin and α-actinin (26). Platelet-type 12-LOX has been shown to be distributed in the membrane fractions (27) and may interact with some cytoskeletal proteins such as keratin and lamin (28). Finally, 15-LOX1 is well known to interact with, oxidize, and degrade intracellular organelle (*e.g.* ER and mitochondria) membranes (29, 30). These observations together suggest that LOX in general and 15-LOX2 in particular are localized at multiple subcellular microdomains and may participate in distinct cellular processes.

Nuclear Localization of 15-LOX2—Another particularly interesting subcellular localization of 15-LOX2 is in the nucleus. Conceptually, this might provide an explanation to a conundrum we briefly touched upon before (3): how may 15-LOX2 inhibit cell-cycle progression? The main 15-LOX2 metabolite, 15(*S*)-HETE, has been shown to be a ligand for peroxisome proliferator-activated receptor γ or PPARγ (21, 31, 32), which has recently been shown to mediate cell-cycle arrest in a diverse array of cell types by suppressing cyclin D1 expression (33–35). Therefore, it is possible that 15-LOX2 may affect cell-cycle arrest in NHP cells (3) by activating PPARγ. However, the concentration of 15(*S*)-HETE required to activate PPARγ is generally $\geq$30 μM (21, 31, 32), which may be difficult to attain intracellularly. Therefore, the nuclear localization of 15-LOX2 may allow the generation of sufficient concentrations of the 15(*S*)-HETE ligand in the proximity of PPARγ to achieve activation of the receptor.

How is 15-LOX2 imported to the nucleus? A database search allowed us to identify a potential bipartite NLS at the N terminus of 15-LOX2. Site-specific mutagenesis studies reveal that this sequence is only partially involved in the nuclear import of 15-LOX2, because its mutations do not completely eliminate the nuclear expression of the molecule. This result is not surprising because many of these putative NLSs are not the sole determinants of or may even not be involved at all in protein nuclear import (36). The relevant example is 5-LOX, which translocates to the nucleus upon cell stimulation. Several groups identified a typical bipartite NLS (^{638}RKNLEAIVSVIAERNKKK^{655}) that appears to be sufficient for 5-LOX nuclear localization (37–40), whereas another group found that the nuclear import of 5-LOX is probably mediated by a non-conventional signal located in the N-terminal β-barrel domain (41, 42). However, a recent study (43), using more rigorous structural and functional criteria, convincingly demonstrated that neither of these two sequences functions as the true NLS for 5-LOX. It turns out that most of the site-specific mutations (*e.g.* R651Q) carried out in these regions that eliminate the 5-LOX nuclear localization also abrogate the enzymatic activity of the protein, which seems to be important for the nuclear import (43). Instead, a previously unrecognized basic region, ^{518}RGRKSSGFPKSVK^{530} located on a random coil of the catalytic domain, appears to function as the authentic NLS, because this sequence is sufficient to drive GFP to the nucleus and mutations of the underlined basic amino acids significantly diminish the nuclear import of 5-LOX without affecting the enzymatic activity (43). A homology search did not identify related sequence(s) in 15-LOX2. Therefore, it is still unclear how 15-LOX2 is imported into the nucleus. Perhaps the Arg^{203}–Arg^{221} NLS in 15-LOX2 cooperates with some other sequences or motifs to import the molecule to the nucleus.

Consistent with the notion that the Arg^{203}–Arg^{221} NLS is not the sole determinant of the 15-LOX2 nuclear localization, the three 15-LOX2 splice variants, which all retain this NLS, are mostly excluded from the nucleus. Because these splice variants do not share conserved regions in the sequences divergent from the parental 15-LOX2 (3), it is unlikely that their inability to go into the nucleus is due to deletion of an NLS in these variant-unique regions. The nuclear exclusion of these 15-LOX2 splice variants is also unlikely due to an overall reduced protein expression, because we have consistently observed similar mRNA (Fig. 6) as well as comparable protein expression levels (Figs. 3–5, and 7*b*) of 15-LOX2 and its variants or NLS mutants. It is possible that changes in protein folding or conformation somehow mask the responsible NLS and preclude these splice variants from interacting with importins, proteins required for nuclear import (19), and thus prevent their import. In support of this possibility, we have consistently noticed that

[2] B. Bhatia and S. Tang, unpublished observations.

the anti-15-LOX2 antibody does not recognize well the denatured 15-LOX2 splice variants on Western blotting (Fig. 7, *a* and *c*; data not shown), suggesting that 15-LOX2 splice variants probably adopt different conformations from 15-LOX2. Alternatively, the reduced or lost enzymatic activity (*i.e.* to metabolize AA to produce 15(*S*)-HETE) renders these variants cytoplasmic, because it has been previously demonstrated that mutations that eliminate the 5-LOX enzymatic activity also abolish its nuclear import (see discussion above). Indeed, compared with 15-LOX2, 15-LOX2sv-a has decreased specificity and activity (2), whereas 15-LOX2sv-b is inactive (Table I). 15-LOX2sv-c is also predicted to be enzymatically dead, because this splice variant lacks the C-terminal isoleucine, which is conserved in all known LOXs and is required for the coordination of catalytic iron (44). Yet another possibility is that 15-LOX2, upon entering the nucleus, is retained in the organelle by physically interacting with one or more other proteins. The 15-LOX2 splice variants, on the other hand, due to structural changes, cannot be retained in the nucleus, although they might be able to be imported. We are currently exploring these possibilities.

15-LOX2sv-b Also Inhibits PCa Cell Proliferation and Tumor Development in Vivo—15-LOX2 is a negative cell-cycle regulator (3) and its expression is down-regulated or lost in PCa cells (3–6), suggesting that it may represent an endogenous prostate tumor suppressor. To lend direct support to this possibility, stable re-expression of 15-LOX2 in PCa cells inhibits their proliferation *in vitro* as well as tumor growth *in vivo*. Surprisingly, 15-LOX2sv-b, a splice variant that does not localize in the nucleus and does not possess AA-metabolizing enzymatic activity, also inhibits PCa cell proliferation and tumor growth. This observation is slightly different from our previous transient transfection experiments in which we found apparent but statistically insignificant inhibitory effect of 15-LOX2sv-b on PCa cell proliferation (3). A likely explanation for this discrepancy is that the inhibitory effect of 15-LOX2sv-b is manifested more slowly than that of 15-LOX2 so that by 48 h after transfection only a small inhibitory effect was observed for 15-LOX2sv-b (3). Therefore, the inhibitory effect of 15-LOX2sv-b is fully manifested in the stable clones (this study). Another possibility is that, in previous transient transfection experiments, we used the pCMS expression constructs in which 15-LOX2sv-b and GFP were driven by separate promoters (3). As pointed out under "Results," in some cells transfected with the pCMS expression constructs the 15-LOX2sv-b (and 15-LOX2) expression is preferentially lost, which may lead to an underestimation of their inhibitory effect on PCa cell proliferation. On the other hand, a tumor-suppressive function of 15-LOX2sv-b is consistent with our previous findings that the mRNA and protein levels of 15-LOX2 splice variants are also reduced in multiple PCa cells (3). The precise biological roles of 15-LOX2 as well as various 15-LOX2 splice variants, the latter of which are also expressed *in vivo*,[3] in maintaining physiological prostate homeostasis and in PCa development remain to be clarified. Nevertheless, the results presented in this study raise the possibility that 15-LOX2 may possess biological activities independent of AA-metabolizing activity and independent of its nuclear localization. How 15-LOX2 inhibits PCa cell proliferation without resorting to AA metabolism is currently unclear. One possibility is that 15-LOX2 as well as its splice variants might directly catalyze the oxidation and degradation of biomembranes, analogous to 15-LOX1 (29, 30).

Together, the data presented herein suggest at least two signaling pathways that could conceptually mediate the biological functions of 15-LOX2 (Fig. 9). Under physiological, unstimulated conditions, 15-LOX2 as well as its splice variants may inhibit cell proliferation through as-yet-unknown mechanisms independent of the nuclear localization and enzymatic activity (*i.e.* AA metabolism). Furthermore, localization of 15-LOX2 to the cell-cell borders and its association with the cytoskeleton may help maintain the differentiated phenotype of prostate glands. Under stimulated conditions, AA will be mobilized resulting in increased 15(*S*)-HETE production in the cells, especially in the nucleus, which may lead to PPARγ-dependent cell-cycle arrest. This model explains why PCa cells suppress the expression of both 15-LOX2 and its enzymatically inactive splice variants (3). The model also predicts that restoration of 15-LOX2 or its splice variant expression should suppress PCa development, a prediction borne out by orthotopic tumor implantation analysis (Fig. 8).

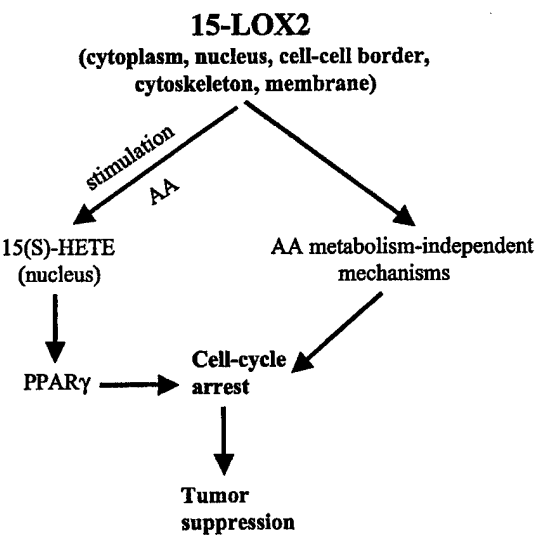

FIG. 9. **A hypothetical model of the mechanisms of action of 15-LOX2.** See text for details.

Acknowledgments—We gratefully acknowledge M. Raff for anti-bromodeoxyuridine antibody, G. Shore for anti-Bap31 antibody, and the Histology Core for help with immunohistochemistry.

REFERENCES

1. Brash, A. R., Boeglin, W. E., and Chang, M. S. (1997) *Proc. Natl. Acad. Sci. U. S. A.* **94,** 6148–6152
2. Kilty, I., Alison, L., and Vickers, P. J. (1999) *Eur. J. Biochem.* **266,** 83–93
3. Tang, S., Bhatia, B., Maldonado, C., Yang, P., Newman, R. A., Liu, J., Chandra, D., Traag, J., Klein, R. D., Fischer, S. M., Chopra, D., Shen, J., Zhau, H., Chung, L. W. K., and Tang, D. G. (2002) *J. Biol. Chem.* **277,** 16189–16201
4. Shappell, S. B., Boeglin, W. E., Olson, S. J., Kasper, S., and Brash, A. R. (1999) *Am. J. Pathol.* **155,** 235–245
5. Jack, G. S., Brash, A. R., Olson, S. J., Manning, S., Coffey, C. S., Smith, J. A., Jr., and Shappell, S. B. (2000) *Hum. Pathol.* **31,** 1146–1154
6. Shappell, S. B., Manning, S., Boeglin, W. E., Guan, Y. F., Roberts, R. L., Davis, L., Olson, S. J., Jack, G. S., Coffey, C. S., Wheeler, T. M., Breyer, M. D., Brash, A. R. (2001) *Neoplasia* **3,** 287–303
7. Chopra, D. P., Grignon, D. J., Joiakim, A., Mathieu, P. A., Mohamed, A., Sakr, W. A., Powell, I. J., and Sarkar, F. H. (1996) *J. Cell. Physiol.* **169,** 269–280
8. Chopra, D. P., Sarkar, F. H., Grignon, D. J., Sakr, W. A., Mohamed, A., and Waghray, A. (1997) *Cancer Res.* **57,** 3688–3692
9. Tang, D. G., Li, L., Chopra, D., and Porter, A. T. (1998) *Cancer Res.* **58,** 3466–3479
10. Tang, D. G., Timar, J., Grossi, I. M., Renaud, C., Kimler, V., Diglio, C. A., Taylor, J. D., Honn, K. V. (1993) *Exp. Cell Res.* **207,** 361–375
11. Joshi, B., Li, L., Taffe, B. G., Zhu, Z., Ben-Josef, B., Taylor, J. D., Porter, A. T., and Tang, D. G. (1999) *Cancer Res.* **59,** 4343–4355
12. Liu, J.-W., Chandra, D., Tang, S.-H., Chopra, D., and Tang, D. G. (2002) *Cancer Res.* **62,** 2976–2981
13. Chandra, D., Liu, J.-W., and Tang, D. G. (2002) *J. Biol. Chem.* **277,** 50842–50854
14. Li, L., Zhu, Z., Joshi, B., Zhang, C., Johnson, C. R., Marnett, L. J., Honn, K. V., Crissman, J. D., Porter, A. T., and Tang, D. G. (1999) *Anticancer Res.* **19,** 61–70
15. Tang, D. G., Chen, Y., Diglio, C. A., and Honn, K. V. (1993) *J. Cell Biol.* **121,** 689–704

[3] S. B. Shappell, unpublished observations.

16. Evans, W. H. (1992) in *Preparative Centrifugation: A Practical Approach* (Rickwood, D., ed) pp. 233–270, The IRL Press, Oxford, UK
17. Scheffler, I. E. (1999) *Mitochondria*, Wiley-Liss, New York, pp. 26–33
18. Breckenridge, D. G., Nguyen, M., Kuppig, S., Reth, M., and Shore, G. C. (2002) *Proc. Natl. Acad. Sci. U. S. A.* **99,** 4331–4336
19. Kaffman, A., and O'Shea, E. (1999) *Annu. Rev. Cell Dev. Biol.* **15,** 291–339
20. Cokol, M., Nair, R., and Rost, B. (2000) *EMBO Rep.* **1,** 411–415
21. Shappell, S. B., Gupta, R. A., Manning, S., Whitehead, R., Boeglin, W. E., Schneider, C., Case, T., Price, J., Jack, G. S., Wheeler, T. M., Matusik, R. J., Brash, A. R., and DuBois, R. N. (2001) *Cancer Res.* **61,** 497–503
22. Alberts, B., Johnson, A., Lewis, J., Raff, M., Roberts, K., and Walter, P. (2002) *Molecular Biology of the Cell*, 4th Ed., pp. 1065–1090, Garland Science, Taylor & Francis Group, New York
23. Takeichi, M. (1991) *Science* **251,** 1451–1455
24. Umbas, R., Schalken, J. A., Aalders, T. W., Karthaus, H. F., Schaafsman, H. E., Debruyne, F. M., and Isaacs, W. B. (1992) *Cancer Res.* **52,** 5104–5109
25. Bussemakers, M. J., Van Bokhoven, A., Tomita, K., Jansen, C. F., and Schalken, J. A. (2000) *Int. J. Cancer* **85,** 446–450
26. Lepley, R. A., and Fitzpatrick, F. A. (1984) *J. Biol. Chem.* **269,** 24163–24168
27. Timar, J., Raso, E., Dome, B., Li, L., Grignon, D., Nie, D., Honn, K. V., and Hagmann, W. (2000) *Int. J. Cancer* **87,** 37–43
28. Tang, K., Finley, R. L., Jr., Nie, D., and Honn, K. V. (2000) *Biochemistry* **39,** 3185–3191
29. Kuhn, H., and Borngraber, S. (1999) *Adv. Exp. Med. Biol.* **447,** 5–28
30. Walther, M., Anton, M., Wiedmann, M., Fletterick, R., and Kuhn, H. (2002) *J. Biol. Chem.* **277,** 27360–27366
31. Kersten, S., Desvergne, B., and Wahli, W. (2000) *Nature* **405,** 421–424
32. Huang, J. T., Welch, J. S., Ricote, M., Binder, C. J., Wilson, T. M., Kelly, C., Witztum, J. L., Funk, C. D., Conrad, D., and Glass, C. K. (1999) *Nature* **400,** 378–382
33. Wang, C., Fu, M., D'Amico, M., Albanese, C., Zhou, J.-N., Brownlee, M., Lisanti, M. P., Chatterjee, V. K. K., Lazar, M. A., and Pestell, R. G. (2001) *Mol. Cell. Biol.* **21,** 3057–3070
34. Wakino, S., Kintscher, U., Kim, S., Yin, F., Hsueh, W. A., and Law, R. E. (2000) *J. Biol. Chem.* **275,** 22435–22441
35. Kitamura, S., Miyazaki, Y., Hiraoka, S., Nagasawa, Y., Toyota, M., Takakra, R., Kiyohara, T., Shinomura, Y., and Matsuzawa, Y. (2001) *Int. J. Cancer* **94,** 335–342
36. Dingwall, C., and Laskey, R. A. (1991) *Trends Biochem. Sci.* **16,** 478–481
37. Lepley, R. A., and Fitzpatrick, F. A. (1998) *Arch. Biochem. Biophys.* **356,** 71–76
38. Healy, A. M., Peters-Golden, M., Yao, J. P., and Brock, T. G. (1999) *J. Biol. Chem.* **274,** 29812–29818
39. Hanaka, H., Shimizu, T., and Izumi, T. (2002) *Biochem. J.* **361,** 505–514
40. Christmas, P., Fox, J. W., Ursino, S. R., and Soberman, R. J. (1999) *J. Biol. Chem.* **274,** 25594–25598
41. Chen, X. S., Zhang, Y.-Y., and Funk, C. D. (1998) *J. Biol. Chem.* **273,** 31237–31244
42. Chen, X.-S., and Funk, C. D. (2001) *J. Biol. Chem.* **276,** 811–818
43. Jones, S. M., Luo, M., Healy, A. M., Peters-Golden, M., and Brock, T. G. (2002) *J. Biol. Chem.* **277,** 38550–38556
44. Brash, A. R. (1999) *J. Biol. Chem.* **274,** 23679–23682